CHALMERS
UNIVERSITY OF TECHNOLOGY

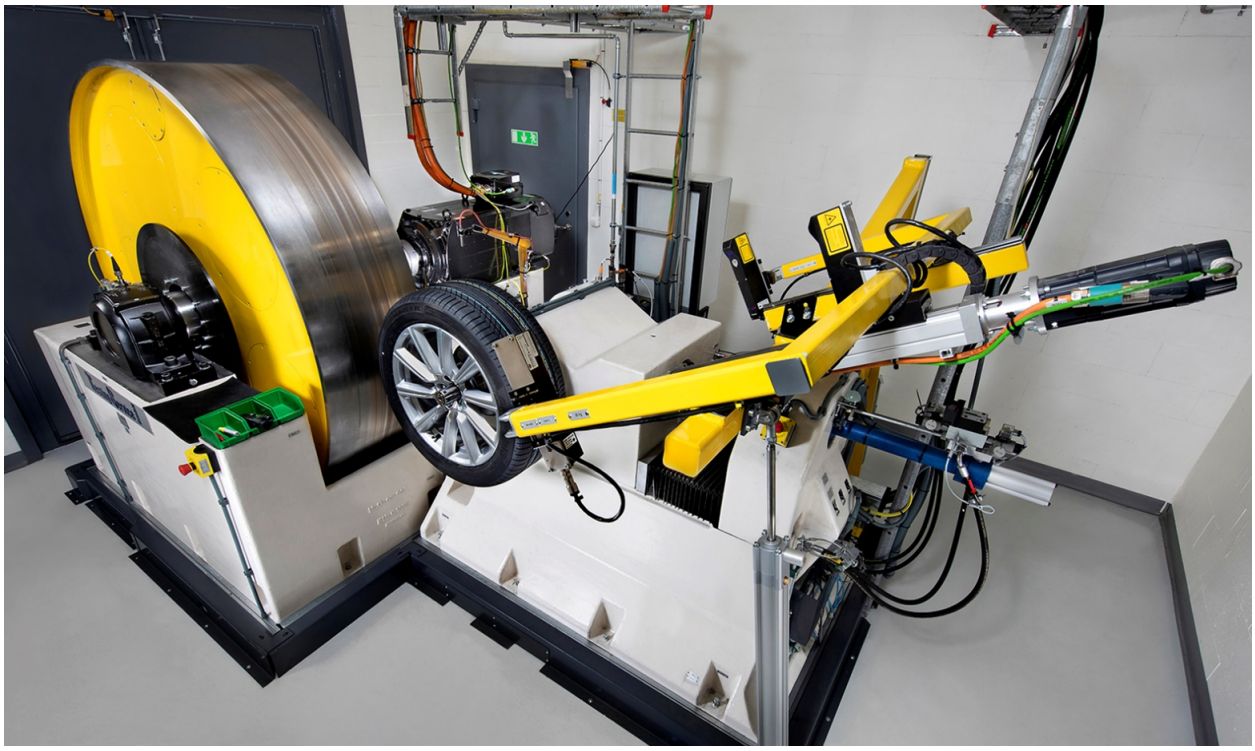

Tire Warmup Relation to Rolling Resistance

Understanding how rolling resistance affects and is affected by tire temperature in realistic driving scenarios

Master's thesis for MSc in Mobility Engineering

Abhishek Amit Kolekar

Vivekanandan Madhuravasal Narasimhan

DEPARTMENT OF MECHANICS AND MARITIME SCIENCES

CHALMERS UNIVERSITY OF TECHNOLOGY

Gothenburg, Sweden 2024

www.chalmers.se

Master's thesis 2024

Tire Warmup Relation to Rolling Resistance

Understanding how rolling resistance affects and is affected by tire temperature in realistic driving scenarios

Abhishek Amit Kolekar

Vivekanandan Madhuravasal Narasimhan

In Collaboration with Volvo Car Corporation

CHALMERS
UNIVERSITY OF TECHNOLOGY

Department of Mechanics and Maritime Sciences
Division of Vehicle Engineering and Autonomous Systems
Chalmers University of Technology
Gothenburg, Sweden 2024

Tire Warmup Relation to Rolling Resistance
Understanding how rolling resistance affects and is affected by tire temperature in realistic driving scenarios

Examiner: Bengt J H Jacobson, Chalmers University of Technology

Supervisors: Teddy Hobeika, Volvo Car Corporation
Johan Lindquist Holmberg, Volvo Car Corporation
Carl Emvin, Chalmers University of Technology

Master's Thesis 2024
Department of Mechanics and Maritime Sciences
Division Of Vehicle Engineering and Autonomous Systems
Chalmers University of Technology
SE-412 96 Gothenburg
Telephone +46 31 772 1000

Cover: Rolling Resistance measurement rig at PV16, Volvo Car Corporation

Typeset in LaTeX
Printed by Chalmers Reproservice
Gothenburg, Sweden 2024

Tire Warmup Relation to Rolling Resistance
Understanding how rolling resistance affects and is affected by tire temperature in realistic driving scenarios
Abhishek Amit Kolekar
Vivekanandan Madhuravasal Narasimhan
Department Of Mechanics and Maritime Sciences
Division Of Vehicle Engineering and Autonomous Systems
Chalmers University of Technology

Abstract

The automotive sector is committed to advancing energy efficiency by providing customers with sustainable transportation solutions. With the increasing adoption of electric vehicles with high powertrain efficiency but limited range, reducing other forms of losses, such as rolling resistance, is important. Rolling Resistance (RR) typically contributes around 25% of the energy loss in Electric Vehicles (EVs) [1]. The current measurement of the tire's rolling resistance is obtained at steady state, which rarely occurs in real-world driving conditions that involve frequent starts and stops, preventing the tire from reaching a steady state equilibrium.

This thesis focuses on the effect of warmup on the rolling resistance of tires differing only by their aspect ratios, focusing on measuring and calculating rolling resistance under realistic conditions. The variation of the tire temperature and rolling resistance is measured during both the warmup (transient) and the steady state on the tire test rig by varying the inflation pressure, speed, and normal load for different tires. The rolling resistance showed a negative correlation with the inflation pressure, a positive correlation with the speed, and no correlation to the load.

Using the data obtained in the warmup region, a rolling resistance model is created that uses temperature and speed as inputs to calculate the instantaneous rolling resistance. A thermal tire model is also developed that can predict the internal temperature of the tire based on the rolling resistance and speed. Using drive cycle tests, the models were validated, and it was observed that the rolling resistance of the tires varied dramatically through the cycle and rarely matched the ISO standard rolling resistance value. Depending on the tire, it was found that the transient rolling resistance was 25-30% higher before reaching a steady state value.

Data from the drive cycle test was used to calculate the rolling energy loss using both the ISO standard rolling resistance coefficient & the rolling resistance model developed. It was found that the rolling energy loss can vary from 6 to 22% between the two approaches, which provides a better understanding of the transient behavior of rolling resistance with respect to a complex drive cycle. This enables better insights into the contribution of rolling resistance to the overall energy loss, and the tire selection process can be made more effective.

Keywords: rolling resistance, tire warmup, modeling, transient rolling energy loss.

Preface

In this research work, the influence of tire temperature on rolling resistance was captured in an empirical model, which can be further used to analyze rolling energy loss. A semi-physical thermal model was also developed to predict the evolution of tire temperature in a drive cycle. The thesis work was carried out between January and June 2024 under the supervision of Professor Bengt J H Jacobson and Carl Emvin from the Division of Vehicle Engineering and Autonomous Systems at Chalmers University of Technology, and Teddy Hobeika from the Vehicle Energy Efficiency Team at Volvo Car Corporation (VCC).

Acknowledgement

We extend our deepest gratitude to our supervisors, for the path we chose to tread was interesting, albeit full of resistance, but they were always supportive and helped us keep the progress rolling. We would also like to thank Johan Lindquist Holmberg and Roger Andren at VCC for their insights and support throughout the research work. We are also grateful to the Vehicle Energy Efficiency Team at VCC for their support and input and the coffee that kept us going.

Abhishek Amit Kolekar
Vivekanandan Madhuravasal Narasimhan
Gothenburg, Sweden, June 2024

List of Acronyms

Below is the list of acronyms that have been used throughout this thesis listed in alphabetical order:

RR	Rolling Resistance
RRf	Rolling Resistance Force (N)
RRc	Rolling Resistance Coefficient (N/kN)
ICE	Internal Combustion Engine
EV(s)	Electric Vehicle(s)
T (in graphs and figures)	Temperature (°C)
A40/A50/A60	Aspect ratio 40/50/60

Nomenclature

Below is the nomenclature of parameters and variables that have been used throughout this thesis.

Parameters

A_0	Linear Fitted Parameters for RR Model (-)
A_1	Linear Fitted Parameters for RR Model $(1/m/s)$
B_0	Exponential Fitted Parameters for RR Model $(1/^{\circ}\mathrm{C})$
B_1	Exponential Fitted Parameters for RR Model $(1/^{\circ}\mathrm{C} \cdot (m/s))$
α	Fitted Exponent for Pressure Dependence Factor (-)
β	Fitted Exponent for Load Compensation Factor (-)
k	Empirically Fitted Conductive Heat Transfer Coefficient between tire and road $(W/m^2 \cdot^{\circ} C)$
f	Empirically Fitted Convective Heat Transfer Coefficient (speed factor) between tire and ambient Air $(W/m^2 \cdot^{\circ} C \cdot m/s)$
c	Empirically Fitted Convective Heat Transfer Coefficient (constant) between tire and ambient Air $(W/m^2 \cdot^{\circ} C)$
H_{gas}	Convective Heat Transfer Coefficient between tire to inflation gas $(W/^{\circ}C)$
$C_{p,gas}$	Specific Heat Capacity of inflation gas $(J/kg/^{\circ}C)$
$C_{p,tire}$	Specific Heat Capacity of tire $(J/kg/^{\circ}C)$
A_{cp}	Area of contact patch of tire (m^2)
A_{tire}	Surface area of entire tire except the contact patch (m^2)

Variables

P	Measured Inflation Pressure (kPa)
F_z	Normal Load (N)

v_x	Longitudinal Velocity of Tire/Vehicle (m/s)
T	Tire Temperature (°C)
$RRf(v_x, T)$	RRf as a function of velocity and temperature (N/kN)
$RRc(v_x, T)$	RRc as a function of velocity and temperature (N/kN)
T_{gas}	Temperature of inflation gas (°C)
T_{amb}	Temperature of ambient air (°C)
T_{road}	Temperature of road/roller (°C)
P_{gas}	Modeled inflation pressure (kPa)
m_{gas}	Mass of Inflation Gas (kg)
m_{tire}	Mass of Tire Rubber (kg)
$\dot{Q}_{IHG}$	Heat generation due to rolling resistance (W)
$\dot{Q}_{tire \to amb}$	Heat loss to ambient air (W)
$\dot{Q}_{tire \to road}$	Heat loss to road (W)
$\dot{Q}_{tire \to gas}$	Heat loss to inflation gas (W)
E	Energy Loss (J or Wh)

Contents

List of Figures

List of Tables

1
Introduction

1.1 Background

In the ISO 28580:2009 standard [2], the rolling resistance of tires is defined as the energy consumed by the tire per unit distance traveled. The measurement of rolling resistance is done after steady-state equilibrium is attained by the tire. The measurements are done on a test rig with a rolling steel drum that drives the test tire. The test tire is mounted on a torque measurement hub. The ISO standard simplifies the rolling resistance measurement by treating it as a constant parameter within a controlled environment—fixed speed, temperature, and measurement after thermal equilibrium is attained. While a standardized testing method allows different tires to be compared, it does not provide an accurate interpretation of what the rolling resistance is under real operating conditions.

Everyday driving, characterized by frequent stops and changes in speed, prevents the tire from reaching a thermal steady state. Previous studies show that the rolling resistance is up to 30-40% higher [3], [4] in the warmup phase as compared to the steady state rolling resistance, especially for shorter travel distances. The rolling resistance contributes to a large part of driving resistance in Electric Vehicles (EVs) as the electric drivetrains have much higher efficiencies than the internal combustion engine counterparts, and a large part of energy loss in deceleration can be recovered by regenerative braking in EVs. Furthermore, the distinctive features of tires, including tread patterns, load ratings, sizes, and compounds, introduce additional variations in their behavior.

1.2 Problem Motivating the Project and Envisioned Solution

The aim is to understand, model, and simulate temperature evolution within the tire under transient conditions, considering a spectrum of tires, and establish correlations with changes in rolling resistance, considering various factors such as inflation pressure, normal load, and speed. A better model of the tire and the thermal dependence of rolling resistance will improve the range estimation and help to reduce the contribution of rolling resistance to the overall driving resistance by picking the best tire considering the use case.

The flowchart in Figure 1.1 shows a holistic overview of the three phases followed within the testing phases later described in Figure 3.1. The experimentation phase involved gathering data by running tests to identify the impact of varying parameters on rolling resistance. This was followed by the analysis of the tests obtained by post-processing the data and visualizing the results. Automation of the test analysis helped to streamline the process of obtaining results that was used to understand certain phenomena. In the discussion phase, the test results were further analysed to see if the proposed tests explained the phenomenon in question and discuss the next steps.

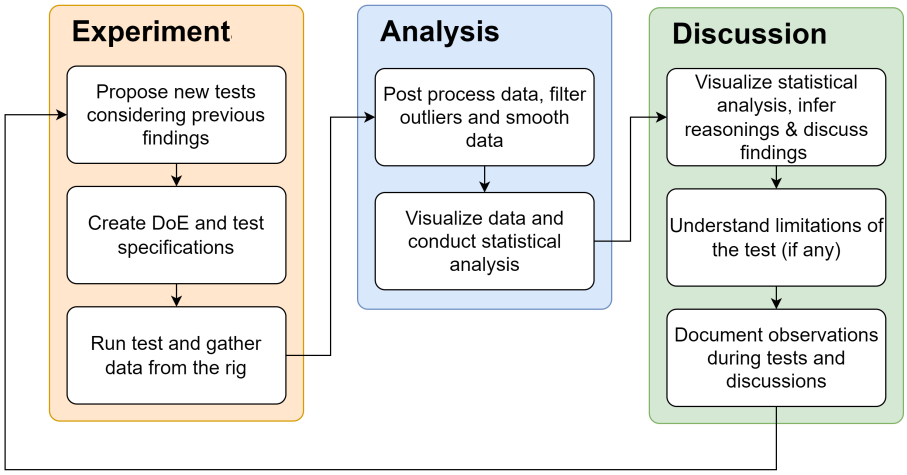

Figure 1.1: Thesis phases

1.3 Research Questions

The following questions guide the research work in this thesis.

1. What are the different factors that affect rolling resistance? What are their contributions?
2. Can the temperature dependence of the rolling resistance of the tire be formulated? Additionally, can mathematical or physical models be developed to capture the temperature and rolling resistance of the tire?
3. Can the energy loss due to rolling resistance be quantified in a drive cycle?
4. Does the behaviour remain the same even with realistic driving?

1.4 Objectives & Deliverables

The objectives and deliverables of the thesis are as follows:

- Establishing baseline values, deciding new tests, and creating workflows to analyze new data.
- Processing and visualizing collected data to draw logical conclusions and establish correlations between changes in operating conditions, rolling resistance, and temperature.
- Formulating empirical relationships between temperature changes and rolling resistance. Proposing a dynamic model and the numerical parameters of this model.
- Conducting drive cycle tests to understand and verify the transient behavior of temperature and rolling resistance under realistic driving conditions.

1.5 Stakeholders

The following table lists the project stakeholders.

Table 1.1: Thesis Stakeholders

Name	Organization	Role
Abhishek Amit Kolekar	Chalmers	Student
Vivekanandan Madhuravasal Narasimhan	Chalmers	Student
Bengt J H Jacobson	Chalmers	Examiner
Teddy Hobeika	VCC	Industrial Supervisor
Johan Lindquist Holmberg	VCC	Industrial Supervisor
Carl Emvin	Chalmers	Academic Supervisor

1.6 Limitations

- Only free rolling tires are tested in the drum testing rig. The model developed does not include the effect of driving manoeuvres (braking, acceleration, turning) and wheel orientation (camber, toe) on the rolling resistance or temperature of the tire.
- Effect of road undulations and surface texture are not tested.
- Only tires designed for cars are tested. The tires represent only a small window of the physical variation in tires available.

2
Literature Review and Theory

2.1 Literature Review

This sections lists literature that was reviewed and important to the thesis work.

2.1.1 Review article by Ydrefors et al [5]

The review article titled "Rolling resistance and its relation to operating conditions: A literature review" provides a detailed overview of the literature and previous works in the field of rolling resistance and factors that affect the rolling resistance. It starts with the historical work on rolling resistance, the explanation of rolling resistance, the measurement of rolling resistance, and the different factors affecting it. The compensation methods and equations for each of the factors are also listed along with each factor. The article also details the different measurement techniques used to quantify the rolling resistance of tires and their corresponding advantages and disadvantages. It also highlights the importance of measuring the rolling resistance under non-steady state behavior. The article concludes that the current testing method of tires, while detailed, lacks an overall generalization that would allow the comparison of different testing methods. It also concludes that while the effect of different operating conditions is known, there is still some knowledge gap in the effect of road surface properties and curvature. It also highlights the lack of information on the effect of temperature outside the testing standards.

2.1.2 Journal article by Hyttinen et al [6]

The journal article titled "Truck tyre transient rolling resistance and temperature at varying vehicle velocities - Measurements and simulations" talks about rolling resistance measurement in a wind tunnel and on-road tests and simulation of a truck tire rolling resistance under transient conditions. The temperature in the truck tire is measured using thermocouples drilled and inserted into the tire shoulder and infrared sensors that can measure the temperature on the tire treads. Additionally, the tire's temperature was measured on the inside during the on-road tests. The transient behavior of the tires was recorded, and it was found that the rolling resistance and shoulder temperature were higher for higher speeds. For simulations of a tire, a lumped thermal capacitance model is used to predict the rolling resistance. The lumped thermal model is used to obtain a master curve that is then used to

simulate the tire shoulder and inner liner temperatures during warmup. The model compensates for different factors such as loading, ambient temperature, and speed. The model is seen to agree very well with measurements, and it is concluded that the rolling resistance decreases significantly at lower ambient temperatures and highlights the importance of the transient effect of rolling resistance in range estimation calculations.

2.1.3 Master's Thesis by Chirag Rajopadhye and Bharat Govardhan Raju [7]

The thesis titled "Influence of inflation pressure, speed, load and warm-up phase on rolling resistance of passenger car tyres" investigates the effect of changes in tire inflation pressure, vehicle speed and vehicle load on the rolling resistance. The study is done to analyze the effect of different on both the steady state rolling resistance coefficient and the energy loss due to rolling resistance brought about by the warmup phase of the tire. The thesis explores the effect on the rolling resistance and energy loss due to changes in the aforementioned parameters individually, as well as the interactive effect of changing 2 of the parameters at a time. The additional contribution of change in rolling resistance due to parameter changes in the warmup phase was also explored. The fundamental findings were that the rolling resistance coefficient shows a negative correlation with a change in inflation pressure and load and a positive correlation with a change in speed. It was concluded that the consideration of the warm-up phase for estimating the energy efficiency of tires is warranted, especially in the context of short distance travel.

2.1.4 White Paper by IZZE Racing [8]

The white paper titled "Influence of Temperature on Tire Grip" provides a compelling argument for the use of infrared temperature sensors to monitor tire temperature. It describes dominant modes that generate heat within a tire namely strain energy loss (i.e., heat generation due to hysteresis) and surface heat due to tire-road tangential interaction. It briefly illustrates the modes of heat exchange from the tire to the environment. Much of the white paper is spent on establishing the effect of varying temperature (considering different tire treads) on the different mechanisms of tire grip (namely indentation and molecular adhesion), primarily from the viewpoint of motorsports. It finally highlights the different ways the temperature data obtained can be used to tune and build a faster race car.

2.1.5 Journal Article by Vieira et al [9]

The journal article titled "Rolling Resistance Evaluation of Winter Tires on In-Service Road Surfaces" explores how rolling resistance is impacted by the different types of tires. The experiments were carried out with 50 different tires of 5 different types – all-season tires, summer tires, winter tires without studs, winter tires with studs, and specialized winter tires embedded with hard particles. The experiments were done independently on a steel drum rig and on road testing. One of the major takeaways was that the drum results led to lower RRC values compared to road conditions but did not lead to any significant correlations. Labelled values of rolling resistance of the tires correlated quite well with the drum measurement values, however were significantly different from road measurement values (road values were higher). Considering the effect on rolling resistance by the type of tires, there was no conclusive proof that studded tires have higher rolling resistance than non-studded winter tires. The specialized winter tires showed relatively lower rolling resistance than the regular winter tires. The summer tire showed the least rolling resistance consistently. Finally, all-season tires have relatively high rolling resistance since they are a compromise between winter and summer performance.

2.1.6 Journal Article by Dieter J. Schuring [3]

The journal article titled "Transient Versus Steady-State Tire Rolling Loss Testing" develops and tests a formula for computing the "rolling loss" i.e., the energy loss per unit distance, of the tires operating under two transient scenarios – a warmup test with constant speed and zero torque (free-rolling) and an urban driving scenario (namely EPA) with rapidly varying speeds thus incorporating the influence of driving and braking torques on rolling loss. A very strong correlation was observed between the averaged warmup rolling loss and steady state rolling loss. The rolling losses during the urban driving test were found to be between 26% and 47% higher than the steady state losses, the reason being additional losses added by the varying torque application. The article, being old at this point, has technological limitations regarding sensors, data acquisition, and torque application control, amongst other things. However, it serves as an initial benchmark to transient testing, with future research adding value and credibility to its findings.

2.1.7 Journal Article by Ejsmont et al [10]

This journal article, "Influence of load and inflation pressure on the tyre rolling resistance" experimentally determines the effect of normal load and inflation pressure on the rolling resistance. The tires were tested on a drum as well as a road with different surface finishes also to obtain the effect of surface roughness. The load and inflation pressure were varied, and it was found that the load affects the rolling resistance force but does not significantly affect the rolling resistance coefficient. The inflation pressure was found to significantly affect the rolling resistance, with both the rolling resistance force and coefficient decreasing when tested at higher inflation pressure. The researchers also concluded that tires with a higher rolling resistance coefficient have a higher dependence on inflation pressure. With respect to surface roughness, smoother surfaces were found to have similar effect on rolling resistance amongst themselves compared to a rougher surface.

2.1.8 Journal Article by Dieter J. Schuring et al [11]

This journal article titled "Transient Speed and Temperature Effects on Rolling Loss of Passenger Car Tires" explores the effect of speed and temperature on rolling resistance as the authors underline the need to understand the transient behavior of the tire. The authors also model the behavior of the tire using an exponential equation and temperature and speed as inputs. The temperature dependence of rolling resistance is analyzed for 2 different temperature measurements: ambient temperature and tire temperature. The results identified in the paper match the theoretical explanations and follow similar trends. The speed dependence is also tested experimentally, and it is shown that the tire achieves an equilibrium temperature irrespective of the starting temperature but depends on the speed. Finally, a model is developed, and its parameters are calculated. This model developed in this paper forms the basis of one of the models in this thesis work.

2.1.9 Master's Thesis by Redrouthu and Das [12]

The thesis titled "Tyre Modelling for Rolling Resistance" establishes a mathematical model for rolling resistance, focusing on a free-rolling tire and ignoring the effect of longitudinal slip considerations. The thesis work also lists the different ways of modeling the tire and the rolling resistance. The model developed in the thesis incorporates multiple factors contributing to rolling resistance, including vertical tire stiffness affecting tire deflection and counter deflection, tire viscous and Coulomb damping effects, and rolling aerodynamic drag, and combines some existing models with new ones. The study investigates the isolated and combined impacts of tire inflation pressure, tire size, velocity, and normal load on rolling resistance. Validation of the model is accomplished through comparison with experimental data derived from tests conducted by Michelin and LeanNova, ensuring a solid foundation for the proposed mathematical framework.

2.1.10 Master's thesis by Tevell and Zetterberg [13]

The thesis titled "Creating a Virtual Tyre Temperature Sensor" focuses on developing a virtual tire temperature sensor to determine the temperature under dynamic driving conditions using a recurrent neural network. The virtual sensor uses onboard signals from the vehicle to predict the temperature. A virtual sensor can be used in real-time to determine the tire rolling resistance and hence improve the range estimation. The limitation of using a virtual sensor based on neural networks is that the sensor is only accurate in the driving scenarios it is trained on. Correlation analysis and feature selection were done to remove onboard signals that do not have much influence on the tire temperature, and selected signals were used to train the neural network. The trained model was found to be 90% accurate in predicting the temperature that was confirmed using a temperature sensor mounted in the tire.

2.2 Theory

The theory section elaborates on important concepts surrounding rolling resistance and the causes and factors that affect it. In addition, it includes information on the measurement techniques used and information on past efforts in modeling rolling resistance.

2.2.1 Rolling Resistance Force and Rolling Resistance Coefficient

Rolling Resistance Force (RRf) is a force at the tire's contact patch that acts opposite to the direction to rotation. The Rolling Resistance Coefficient (RRc) is defined as the rolling resistance force per unit load. The RRc is a metric used to quantify this resistance. The unit N/kN is used because a free rolling tire is considered, and the load in the order of kN results in rolling resistance in the order of N. The RRc values range from 6 to 10 N/kN for passenger car tires on asphalt. Rolling resistance force comprises the losses from the tire due to deformation and losses from other rotational sources, including aerodynamic losses and tire-rim friction. In standardization methods, the value of the rolling resistance coefficient is calculated once the measured rolling resistance force stabilizes. The resistance arising from the tire can be understood by two different mechanisms.

2.2.1.1 Rolling resistance due to viscoelastic hysteresis

As the tire rolls, the part of the tire at the leading edge of the contact patch undergoes deformation due to loading. The parts of the tire at the trailing edge of the contact patch get unloaded. Due to the viscoelastic nature of rubber compounds, the pressure distribution on the contact patch is not symmetric but generally tends to be higher in the direction of rolling. In the following figure, the spring and damper represent the rubber material's viscoelastic behavior. The spring represents the elastic properties, and the damper represents the viscous losses.

The centroid of the pressure distribution integrated over the length of the contact patch is offset by some distance (L) from the center of the contact patch. This offset of the centroid causes a braking/resistive torque, which can be represented in terms of a vertical force (F_{res}), as seen in Figure 2.1. This force is responsible for the loss of energy between loading and unloading, generally termed hysteresis, but in the case of tires, termed as rolling resistance (energy consumed per unit distance with units (J/m)). This phenomenon is majorly responsible for converting the mechanical energy at the wheel to heat that warms up the tire and is lost to the environment.

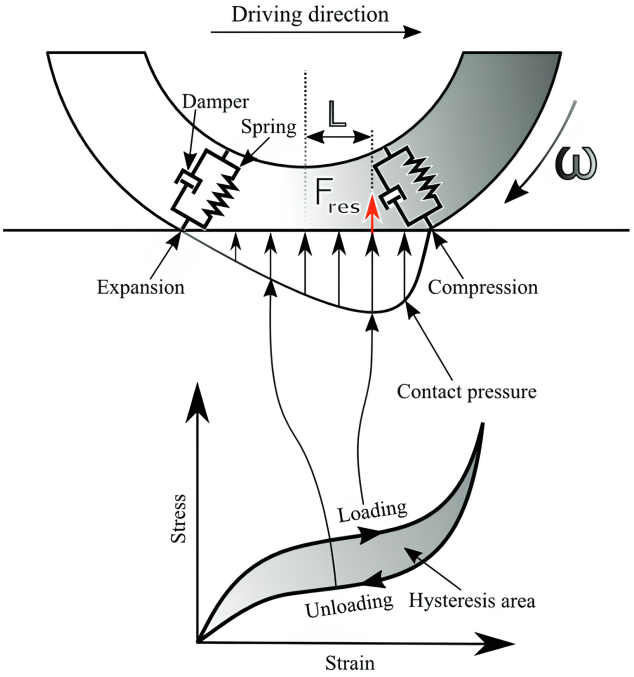

Figure 2.1: Mechanism of Rolling Resistance due to Viscoelasticity (Figure from [14])

Thus, reducing the tire's viscoelastic hysteresis will result in a lower rolling resistance. However, another important effect of the hysteresis property is the grip caused by the asymmetrical deformation due to the microtexture of the road in the road [15]. This type of grip is important, especially when the road is wet. Thus, there must be a compromise between reducing rolling resistance and retaining grip in wet conditions.

2.2.1.2 Rolling Resistance Due to Aerodynamic Drag

Hysteresis from tire deformation primarily contributes to rolling resistance losses. However, aerodynamic drag is a secondary contributor to the losses, accounting for up to 15% at high speeds [16]. It results from the pure rotational motion of tires (without any longitudinal movement), e.g., in a rolling drum test rig.

Aerodynamic drag comprises form drag, arising from the object's shape moving through the air, and skin friction, arising from fluid (air) and object surface friction, and ventilation moment. If the tires are flat (without any tread grooves), the drag caused will be mostly due to skin friction. However, in normal car tires, the grooves induce a small amount of form drag as well.

2.2.2 Factors Affecting Rolling Resistance

The following is the theory surrounding the key factors that are tested in this thesis work:

2.2.2.1 Effect of Tire Outer Diameter on Rolling Resistance

When the tire's outer diameter is increased (with everything else being similar), some factors increase the rolling resistance, while other factors decrease it. These factors are listed as follows:

Factors which decrease rolling resistance:

- A larger diameter tire typically has a larger contact patch, which distributes the vehicle's weight over a larger area. This results in lower contact pressure, reducing hysteresis losses.
- A larger diameter tire often has lower sidewall flexing for the same load, which can decrease energy losses due to flexing and improve overall tire efficiency. The reduced sidewall flexing also contributes to a more efficient rolling motion.
- A larger diameter tire tends to have lower tread deformation, further minimizing energy losses.

Factors which increase rolling resistance:

- Aerodynamic drag increases rolling resistance force as the surface area in contact with air increases.
- Tires with larger diameters weigh more, which increases the normal load and, consequently, the rolling resistance force.

Previous research by Pillai and Russel-Fielding [17] found that there is an overall decrease in rolling resistance as diameter increases and established the relationship between rolling resistance and outer tire diameter, which can be represented by the formula:

$$RRf \propto D^{-\frac{1}{3}} \tag{2.1}$$

This indicates that the rolling resistance decreases as the outer diameter increases.

2.2.2.2 Effect of Aspect Ratio on Rolling Resistance

The aspect ratio of the tire is the sidewall height expressed as a percentage of the tire's section width. Thus, a higher aspect ratio for a constant section width indicates a larger tire.

It has been observed by Pillai and Russel-Fielding [17] that an increase of the aspect ratio increases energy dissipation, thus a higher rolling resistance. The reasoning is that a higher aspect ratio would have longer sidewalls, which results in more sidewall flexing, increasing the magnitude of the compression-relaxation cycles and leading to higher hysteresis.

2.2.2.3 Effect of Inflation Pressure on Rolling Resistance

A tire with higher inflation pressure is stiffer and will deform less than a tire with lower pressure and, hence, have a lower hysteresis effect. A lower hysteresis effect leads to a lower loss of energy and, hence, lower rolling resistance. Ejsmont et al. [10] tested the effect of increasing inflation pressure for 5 different tires and concluded that increased pressure reduced the rolling resistance coefficient.

Grover, P. S. [18] experimentally determined that an exponentially decreasing dependence for pressure fits most tires. The pressure dependence is hence given as $RRf \propto P^{-\alpha}$, where α is the pressure dependence exponent. The exponent of dependence was found to be between -0.3 and -0.5 by both Hall and Moreland [19] and by Ydrefors et al. [5] with the latter observing that an exponent of -0.4 presented the best fit for the tires tested. Previous research works have also noted that the pressure dependence of the rolling resistance coefficient changes depending on whether the tire is tested on the road or a drum.

2.2.2.4 Effect of Temperature on Rolling Resistance

Three different temperatures affect the rolling resistance:

- **Tire temperature:** Increase in the tire temperature leads to a lowered hysteresis effect as higher temperature increases the elasticity of the rubber used in tires and increases the inflation pressure, both resulting in a lowered rolling resistance [20].
- **Ambient temperature:** The ambient air temperature does not affect the rolling resistance directly, rather, it affects the internal temperature of the tire and consequently, the rolling resistance [21].
- **Road temperature:** Like the ambient temperature, the road temperature affects the rolling resistance indirectly by increasing the tire temperature and reducing the rolling resistance [21].

Comparing the effect of ambient and road temperatures on the rolling resistance of the tire, it is found that the tire temperature is more sensitive to the road temperature than to the ambient temperature. Yokota et al. [21] have used FEM and physical correlation for different tires tested in the range of 10-30℃ for ambient temperature and 10-50℃ for road temperature. They found that for every 10℃ rise in the ambient temperature, the tire temperature rises by ∼1-2℃ and for every 10℃ rise of the road temperature, the tire temperature rises by ∼6-7℃.

2.2.2.5 Effect of Speed on Rolling Resistance

Speed affects the rolling resistance in various ways, due to its different effects on the various mechanisms that cause rolling resistance.

- **Effect on hysteresis:** Schuring [22] found that the hysteresis of the tire is dependent on the frequency of tire deformation, which increases with an increase in speed.
- **Effect due to aerodynamic losses:** Research by Michelin [16] indicates that, at constant load and inflation pressure, running the tires at a higher speed increases the aerodynamic losses.
- **Effect due to generation of standing waves:** Higher speeds also cause standing waves to arise. Previous research [19], [20] have found that driving at high speeds — 120 km/h or more—standing waves in the tires will quickly and significantly increase rolling resistance. When the next deflection starts while the thread and side walls are still being affected by the previous one, a standing wave is formed.
- **Effect on achievement of temperature steady state:** Rajopadhye and Govardhan Raju [7] found that at higher speed, the steady state temperature is achieved faster, which reduces the average energy loss during the warmup phase, which results in a lesser contribution of warmup rolling resistance, and overall lower rolling resistance during the test run.

2.2.3 Rolling Resistance Measurement Techniques

Measurement of the rolling resistance can be divided into lab measurements and on-road measurements. Lab measurements allow for carefully controlled conditions, whereas on-road measurements provide realistic conditions for measurements.
Sandberg et al. [23] classifies rolling resistance measurement techniques as follows:

- **Lab test of tires:** Lab measurements can, in turn, be classified as drum-based measurements and rolling road-based (belt-based) measurements.
  - **Drum test:** A drum test has the tire to be tested pressed against a large rolling drum with a prescribed load. The drum is then rotated, and the resistive torque due to the tire is measured. The tested setup is shown in the figure below. In this thesis work, lab measurement using a drum-based method is focused upon.

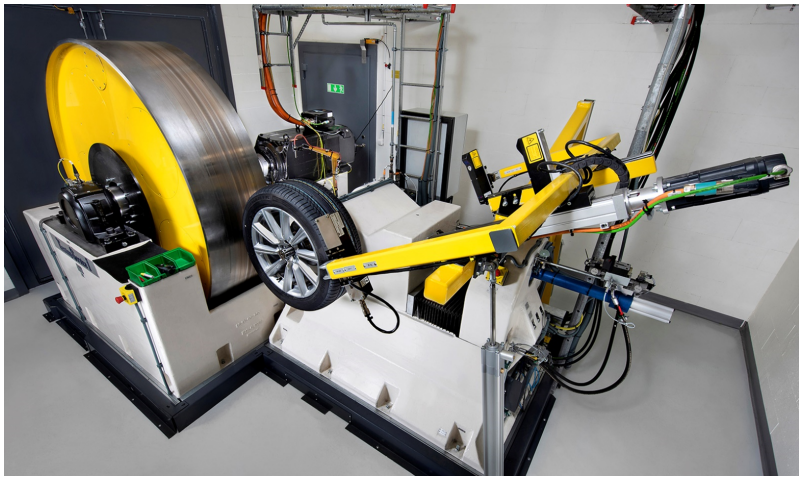

Figure 2.2: ISO Rolling Resistance testing rig
(Image from Volvo Car Corporation Internal Media)

  - **Belt test:** The belt test has a similar setup to the drum test but uses a rolling belt instead of a drum.

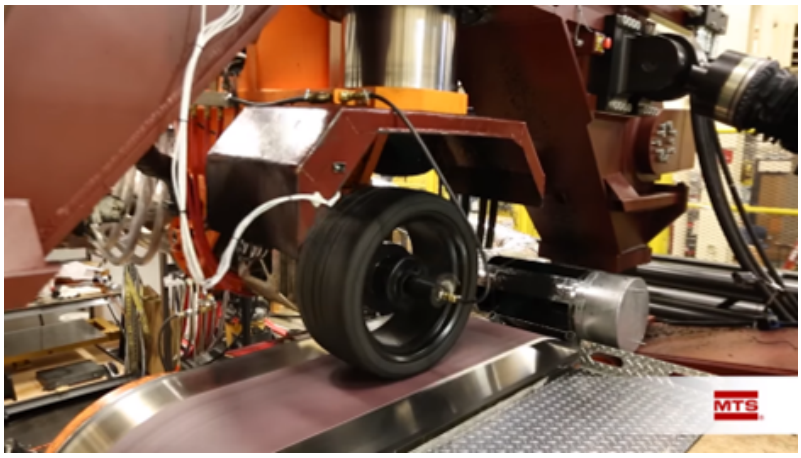

Figure 2.3: Flat belt rig (Image from [24])

- **On road testing:**
  - **Trailer method:** The Trailer method of rolling resistance measurements is the most versatile method and, at the same time, the most difficult one. It is based on towing a test "rig" (as visualized in the figure below) behind a vehicle and measuring the towing force, and thus calculating the rolling resistance. The influence of aerodynamic drag can be reduced by using an enclosure to isolate the rig from airflow. The ability to conduct measurements on different surfaces is a major advantage of using the trailer method to measure rolling resistance.

Figure 2.4: Trailer rig (R^2 MK.II, Image from [25])

  - **Coast-down method:** It is one of the more popular on-road testing methods. In this, the vehicle is accelerated to a set speed, after which the gearbox is switched to neutral, and the vehicle decelerates due to resistive forces. This method utilizes established mathematical models to remove inertial and aerodynamic resistances (provided accurate windspeed data is captured and the coast-down is performed under windstill conditions) and finally evaluates the rolling resistance.
  - **Fuel consumption method:** It is an indirect method that mathematically evaluates the amount of fuel consumed by different resistances and losses and calculates the rolling resistance. This method is highly dependent on the driving style of the operator as well as the drive cycle, and in order to get any significant results, tires must be tested over long distances consistently in the same manner—ideally on a test track.

2.2.4 Modeling of Rolling Resistance

2.2.4.1 Empirical models

Tires, being very susceptible to minute changes in operating conditions, are jokingly referred to as 'black magic.' This is because it is incredibly difficult to include different environmental parameters to perfectly describe how a tire behaves, partially because each tire differs from another of the same brand and make and partially because the road and operating conditions differ slightly.

Empirical (also known as statistical) models are based on fitting the model to the data collected from experiments and are grounded in observations, which are supported by theory. A mathematical relationship between input and output is created after performing a statistical analysis of the data. Repeating the same tests provides statistical significance to this mathematical relationship, after which an observed input can be used to predict output with high certainty. This is why it has become a common practice in the research and development sector.

2.2.4.2 Physical models (spring, friction, damper)

A physical (also known as constitutive) model formulates the varying effects of different physical quantities on the systems using equations based on the relations between the quantities. It is a common practice in industry to define rolling resistance as a ratio of rolling resistance force and normal force. However, a more detailed model can be established by utilizing the definition of the offset "e_x" of the normal pressure distribution along the contact patch length. This leads to the formulation described in Section 2.2.1.1

To create a physical model, certain foundational assumptions are necessary to reduce the complexity of a model and set limitations for its applications. The modeling process involves integrating various fundamental concepts and existing models to develop a new (and/or improved) model.

Following the model development, simulation becomes crucial, and correlation with experimental data (if available) is essential to validate accuracy, repeatability, and reproducibility with different input parameters.

An example of a physical model for rolling resistance is described in the master's thesis by Redrouthu and Das [12]. This model combines concepts and models such as tires as radial springs and dampers, balloon modeling of stiffness, constant belt model, damping model, and rotational aerodynamic drag. Ficht et al. [26] developed and demonstrated a steady state as well as a transient rolling resistance physical model and verified the model's accuracy with experimental data.

3
Methods

3.1 Testing Methodology, Tires and Sensor

The flowchart in Figure 3.1 overviews the procedure followed in this thesis. Considering the emphasis on experimentation in the thesis, a large part of the first testing phase was dedicated to performing tests to establish the baseline values at 2 different (but equally important) conditions: at ISO Test Load and Vehicle Load. Following the baseline tests were tests that vary one of the parameters from normal load, inflation pressure, and speed while keeping others constant. This was followed by testing and analysis of the tire warmup and the transient behavior of the parasitic losses.

The second part of the thesis focused on modeling tire behavior. Using data from the tests, the parameters and coefficients needed for modeling were found. Two models were developed, one to simulate the thermal behavior of the tire and one to simulate the rolling resistance. After verifying the models separately, a combined tire model was created that predicts the behavior of the tire given only the test conditions.

The third part focused again on testing, this time using a dynamometer and a complete vehicle by running drive cycles. A drive cycle test is more indicative of real-world performance as compared to a single tire on the ISO test rig. The results from the drive cycle test were analysed to obtain knowledge of the rolling resistance and losses of the tires during realistic driving.

The rolling resistance testing rig at PV16 at Volvo Cars Torslanda facility, as shown in Figure 3.2, was the first testing facility used in this thesis. Different tires, described later in Section 3.1.1, were tested in PV16 at different loads, inflation pressures, and speeds. Some specific tests to determine the behaviour of rolling resistance while warmup were also performed, which are discussed in Sections 3.2.6 and 3.2.7.

The data acquired from these tests was then used to develop a Rolling Resistance Model to calculate instantaneous rolling resistance provided tire temperature and pressure data, which is described in Section 3.3.1. A thermal model, described in Section 3.3.2, was also developed to calculate the warmup behaviour of the tire, given the initial conditions, drive cycle and empirically calculated parameters pertaining to heat transfer coefficients for different tires. These models were tested separately to

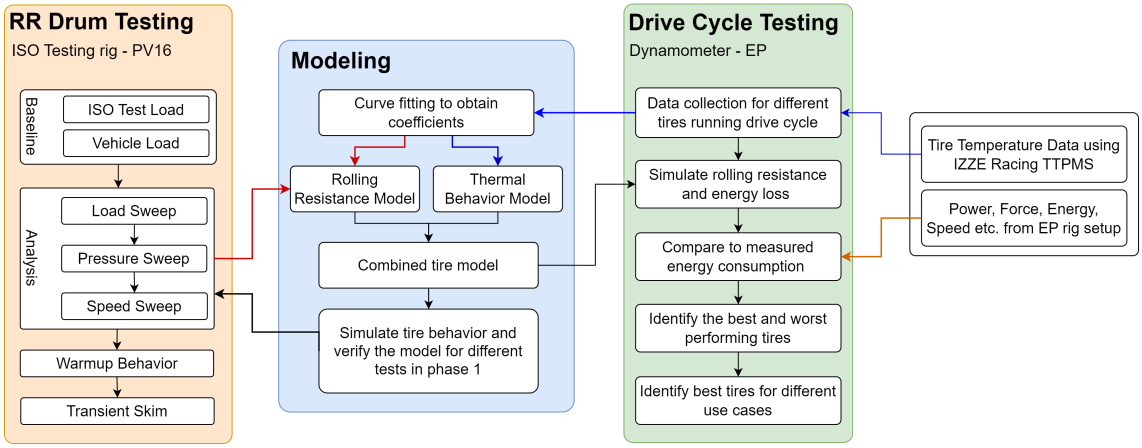

Figure 3.1: Methodology followed in the thesis work

check their validity and then combined to form a model that calculates the warmup of the tire as well as the rolling resistance, given the initial conditions, tire heat transfer parameters and drive cycle, as described in Section 3.3.3.

Drive cycle tests were conducted on the dynamometer rig at EP, shown in Figure 3.2, to verify and compare the results of the rolling resistance coefficient obtained from the ISO testing rig at PV16 to the dynamometer at EP. The rolling resistance and losses of the tires under realistic driving were obtained from the drive cycle tests.

Figure 3.2: (L) Drum Test rig at PV16; (R) Dynamometer rig at EP (Images from Volvo Car Corporation Internal Media)

3.1.1 Test Tires Specifications

Three tires were tested, which are geometrically identical except for the outer diameter (affected by different aspect ratios). The difference in the aspect ratio gives the tires different outer diameters. All 3 tires tested are A-class summer tires of the same manufacturer. The rims used for all 3 tires are 7.5” in width with 19” diameter.

The outer diameter of the tire is calculated using the formula,

Table 3.1: Test Tire Specifications

Tire ID	**Tire Specs**	**Inner Diameter** (mm)	**Width** (mm)	**Aspect Ratio** (%)	**Outer Diameter** (mm)
A40	235/40 R19	482.60	235	40	670.6
A50	235/50 R19	482.60	235	50	717.6
A60	235/60 R19	482.60	235	60	764.6

$$\text{Outer Diameter} = \text{Inner Diameter} + 2 \cdot \text{Aspect ratio} \cdot \text{Width}.$$

Figure 3.3: Test tires (L to R: A40, A50, A60)

3.1.2 Temperature and Pressure Measurement System

The following figure shows the temperature and pressure measurement sensor used in this thesis work to measure the inner liner temperature of the tire and the instantaneous inflation pressure. The sensor is the TTPMS from IZZE Racing.

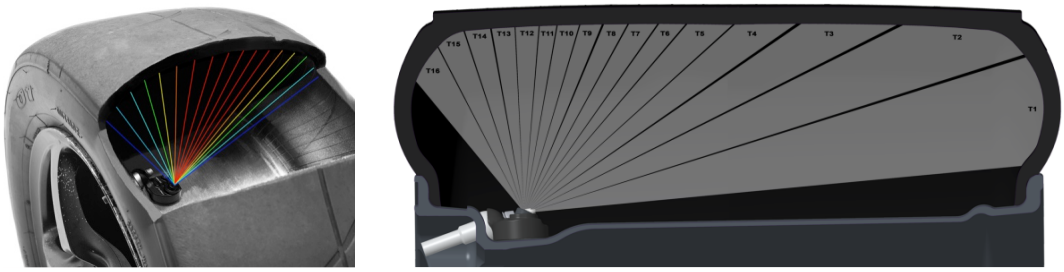

Figure 3.4: IZZE Racing TTPMS
(Images from [27])

The following table presents the manufacturer specifications of the sensor.

Table 3.2: TTPMS specifications (from [27])

Infrared temperature range	-20 – 300°C
Infrared temperature measurement error	±0.5°C
Internal temperature range	-40 – 150°C
Internal temperature measurement error	±0.25°C (at full scale)
Temperature measurement resolution	0.1°C
Pressure range	0 – 5 bar
Pressure measurement error	± 5 mbar (at full scale)
Pressure resolution	1 mbars

3.2 Rolling Resistance Testing on Drum Rig

This section elaborates on the tests conducted in Drum Rig.

3.2.1 Definitions

1. **ISO Test Load:** ISO test load is the normal load specified by the ISO 25280 standard [2] (which is 80% of the rated load) for each tire. The ISO test loads are 5570 N, 6865 N, and 7649 N for tires A40, A50, and A60, respectively.
2. **Vehicle Load:** In this thesis, the vehicle load represents the normal load acting on a tire when used in a car. This load is considered to be a quarter of the overall vehicle curb weight, which equals 5400 N.
3. **Drum Torque:** The torque measured at the drum (in Nm) in the PV16 rig is referred to as drum torque through this thesis.
4. **Drum Torque Measurement Uncertainty:** The torque sensor used to obtain the drum torque has a measurement uncertainty of ±0.9 Nm as stated in the calibration report by VCC.
5. **Parasitic Loss:** As per [2], the parasitic loss is defined as the loss of energy (or energy consumed) per unit distance excluding internal tire losses, attributable to aerodynamic loss of the different rotating elements of the test equipment, bearing friction and other sources of systematic loss which may be inherent in the measurement.
6. **Skim Test Reading:** As per [2], the skim test reading is the type of parasitic loss measurement in which the tire is kept rolling without slippage while reducing the tire load to a level at which energy loss within the tire itself is virtually zero. In the PV16 rig, the skim test load is 200 N.
7. **Warmup Cycle:** In this thesis, the warmup cycle consists of 30 minutes under set load, followed by a skim test for 3 minutes. The warmup cycle brings the test tire up to the working temperature (steady state) before taking measurements.
8. **Measurement Cycle:** In this thesis, the measurement cycle consists of 10 minutes under test load, followed by a skim test for 3 minutes. The measurement cycle is done to obtain the RR measurement of the tire. This is usually repeated multiple times to ensure repeatability.

The warmup cycle, measurement cycle and skim test are visualized by the following figure:

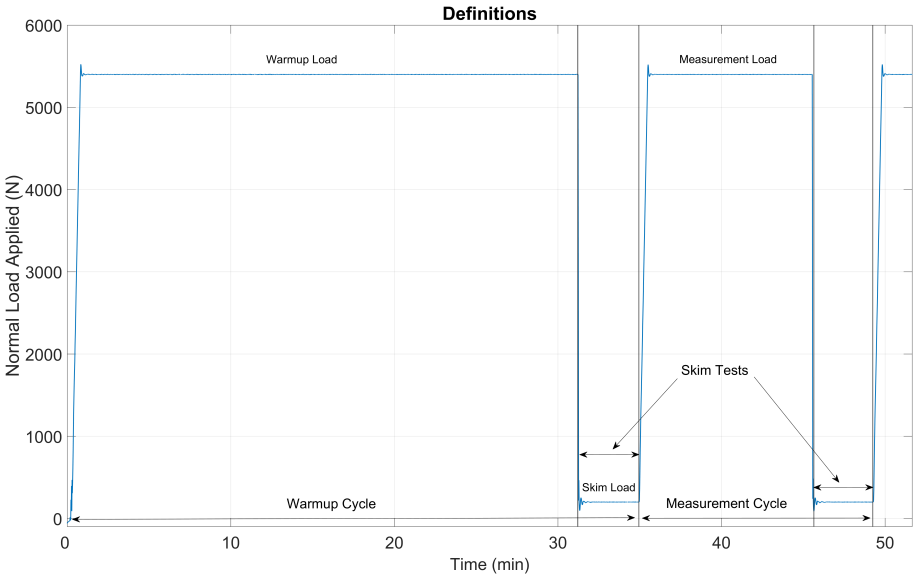

Figure 3.5: Test definition (Skim Test, Warmup cycle and Measurement Cycle)

3.2.2 Test Equipment and Specification

Rolling Drum
The rolling drum, which is visualized in Figure 3.2, is a smooth steel drum with a diameter of two meters. The rig is set up in a temperature-controlled environment such that the temperature remains constant.

Testing Environment
The ambient temperature, which must be measured at a distance not less than 0.15 m and not more than 1 m from the tire sidewall, is to be maintained at 25°C [2] and the drum is also maintained at the same temperature.

3.2.3 ISO Standard Rolling Resistance Test

The following information is referred from the documentation for the ISO 28580:2009 standard [2]:

3.2.3.1 Test Procedure

The test procedure is as follows:

1. The tires to be tested must be placed in the thermal environment of the test location for at least 3 hours to attain thermal equilibrium.
2. After thermal conditioning, the tire's inflation pressure is adjusted to 210 kPa for standard tires and 250 kPa for reinforced tires before the test. The pressure has to be verified 10 minutes after the adjustment is made.

3. The load on the tire is 80% of its rated load pressed against the rotating drum. brought up to a speed of 80 km/h and held at that speed for 30 minutes. This ensures that the torques due to rolling resistance reach a steady state equilibrium.
4. The torque required to maintain the tire speed at 80 km/h is then recorded and used along with the parasitic losses to calculate the rolling resistance.

The loading cycles can be visualized in the following figure:

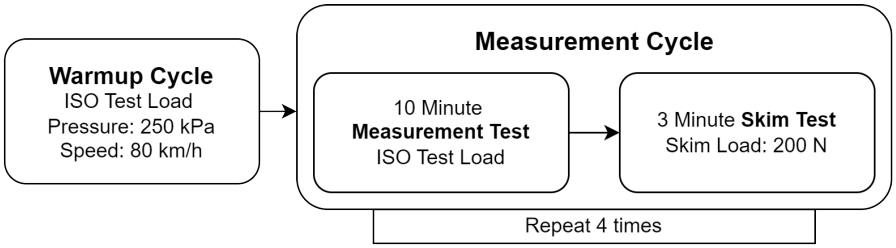

Figure 3.6: ISO Rolling Resistance Test Procedure

3.2.3.2 Calculation of Rolling Resistance

A representation of the data measured by the drum torque sensor is shown in the figure below:

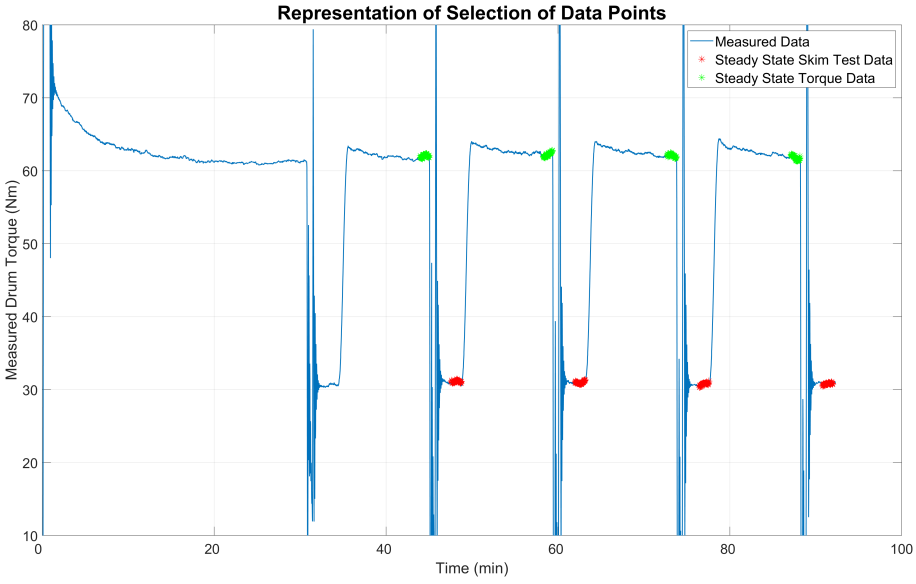

Figure 3.7: Representation of Selection of Data Points for Rolling Resistance Calculation

The green and red markers represent the data points where the total drum torque and parasitic losses reach a steady state, respectively.
The rolling resistance force calculation is as per the ISO standard using the formula,

$$F_r\,(in\,N) = \frac{T_t\,(in\,Nm)}{R\,(in\,m)} - F_{pl}\,(in\,N),$$

where,

T_t is measured torque,
R is the radius of the drum, and
F_{pl} is the parasitic loss measured during the skim test. It is measured as a torque and converted to a force.

Comparing the equation to measured data pictured in Figure 3.7, the green markers in the figure correspond to T_t and the red markers denote the measured torque relating to F_{pl}.

The rolling resistance coefficient can be calculated from the measured rolling resistance force as

$$RRc\,(in\,N/kN) = \frac{F_r\,(in\,N)}{F_z\,(in\,kN)},$$

where F_z is the normal load.
The calculation also remains valid for the calculation of rolling resistance force and coefficient in non-standard tests.

3.2.3.3 Compensations for Test Conditions

Correction for Varying Drum Diameter: To calculate the ISO rolling resistance coefficient, the diameter of the drum in a test rig must be 2 m. If the drum diameter is other than 2 m, the following correction factor must by applied:

$$F_{r02} \approx K_r \cdot F_{r01} \quad where \quad K_r = \sqrt{\frac{(\frac{R_1}{R_2}) \cdot (R_2 + r_T)}{R_1 + r_T}}. \tag{3.1}$$

Here,

R_1 is the radius of test drum 1 in (m),
R_2 is the radius of test drum 2 in (m),
r_T is one-half of the nominal design tyre diameter in (m),
F_{r01} is the rolling resistance value measured on test drum 1 in (N), and
F_{r02} is the rolling resistance value measured on test drum 2 in (N).

This compensation is later used to correlate results between the rolling resistance calculated in the PV16 (drum) and EP (dynamometer) rigs, where the drum sizes differ.

3.2.3.4 Comparison between ISO Load & Vehicle Load

The operating conditions are quite different between the ISO standard test and what the vehicle (generally) experiences. The vehicle load conditions in comparison to ISO standard conditions are as follows:

- Pressure: 280 kPa as compared to 250 kPa.
- Load: 5400 N as compared to 80% of load index.

3.2.4 Load & Pressure Sweep

3.2.4.1 Load Sweep

The load sweep is performed to analyze the effect of load on rolling resistance. The test is performed at 3 loads: ISO test load, vehicle load (5400 N), and a load lying between those two loads, all at an inflation pressure of 280 kPa. The tests are performed at an increased pressure of 280 kPa (from 250 kPa for the ISO RR test) as the tires used on the road are generally inflated to 280 – 300 kPa as is recommended by Volvo Cars for daily driving. The generalized test procedure is visualized below:

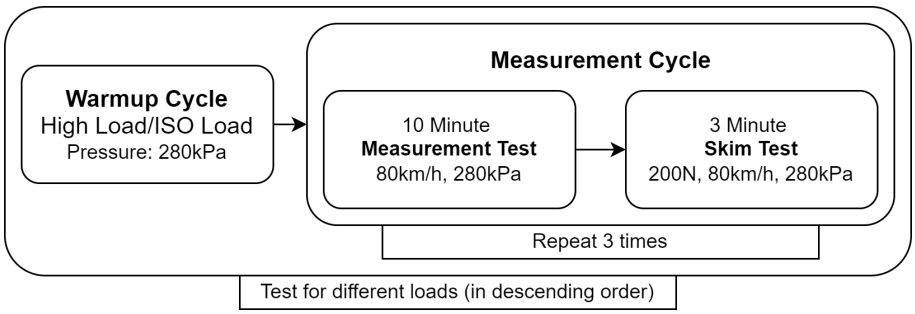

Figure 3.8: General Procedure for Load Sweep Test

The loads for A50 and A60 tires are as follows:

Tire ID	ISO Load (N)	Intermediate Load (N)	Vehicle Load (N)
A40	7649	6500	5400
A50	6865	6100	5400

Table 3.3: Load Sweep Test Specifications for Tires A50 and A60

The loads in the sweep for tire A40 have been selected differently from those of other tires as the ISO load is quite similar in magnitude to the vehicle load. This does not provide significantly different results when analyzing the load dependence of rolling resistance. To address this issue, additional tests labelled "high load" and "low load" conditions have been chosen, with the test specification for A40 being as follows:

Tire ID	High Load (N)	ISO Load (N)	Vehicle Load (N)	Low Load (N)
A40	6100	5570	5400	4800

Table 3.4: Load Sweep Test Specifications for Tire A40

3.2.4.2 Pressure Sweep

The pressure sweep is performed to analyze the effect of pressure on rolling resistance. The load sweep test is also performed at 3 different inflation pressures for all 3 tires at inflation pressures of 250 kPa, 280 kPa and 300 kPa. By performing the load sweep at 3 different pressures, the effect of inflation pressure on the rolling resistance under different loads can be analyzed.

3.2.5 Speed Sweep

The speed sweep was done to understand the impact of speed on the rolling resistance and the warmup evolution of all the tires. The test procedure is as follows:

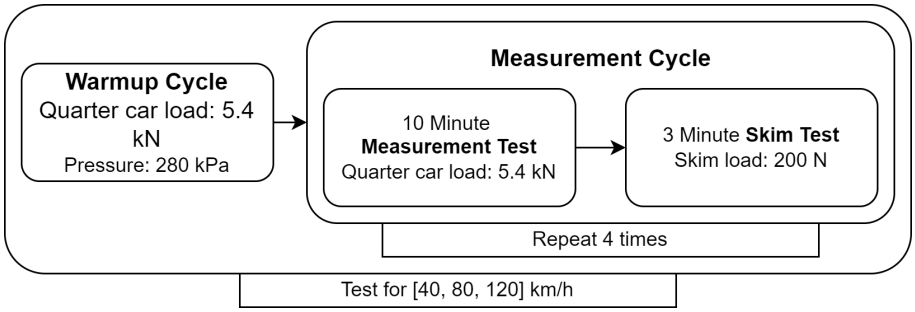

Figure 3.9: Speed Sweep Test Procedure

The warmup cycle at 280 kPa and 5.4 kN load is completed, which is followed by a measurement cycle, all at a constant speed. The measurement cycle is repeated 4 times to ensure consistent and reliable results. The test procedure is repeated at various speeds (40 km/h, 80 km/h, and 120 km/h), and the linearity of the behavior can also be checked.

3.2.6 Warmup Behaviour

The test was done to isolate and understand the effect of the warmup on the tire on rolling resistance. In this test, only the warmup cycle, described in Section 3.2.3, is used.

Data on the rolling resistance and temperature from this test is used to parameterize the Rolling Resistance Model as described in Section 3.3.1.1.

3.2.7 Transient Skim Test Measurement

While the ISO standard test is good at comparing different tires fairly, it only considers the steady state rolling resistance and does not account for energy loss due to transient changes in rolling resistance during the warmup phase. Generally, the skim test reading is taken after the tire has warmed up completely and does not consider transient changes. Since a constant skim test reading is used to calculate the rolling resistance, the resulting value of the rolling resistance force may not be accurate if the skim test reading is dependent on the warmup phase. To understand if and how the skim test reading changes with the warmup of the tire, the transient skim measurement test was conducted.

In this test, the skim test reading is taken at various points in the tire warmup phase to establish the dependence of the skim reading on the temperature of the tire, which can be visualized as follows:

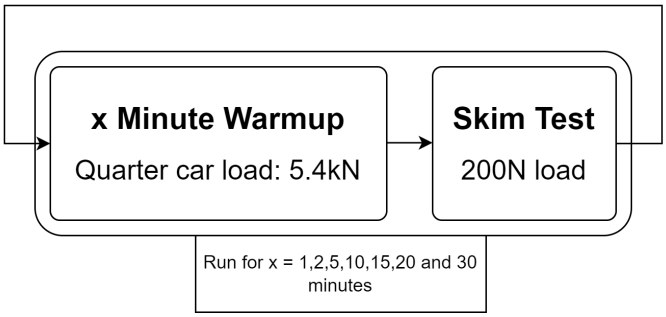

Figure 3.10: Procedure for Transient Skim Test Measurement

The application of normal load on the tire is visualized in the following figure:

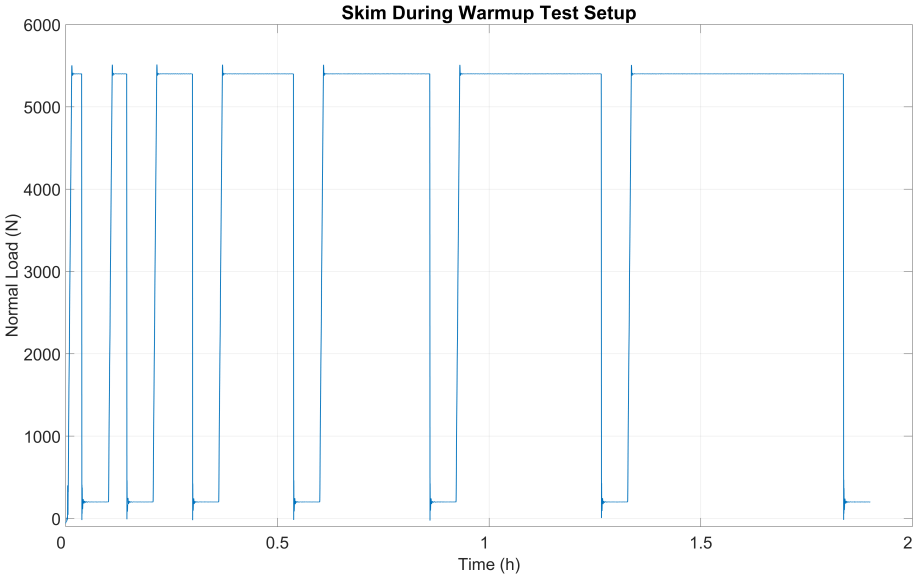

Figure 3.11: Normal Load Application Skim During Warmup

A sample of data collected from this test is shown in the figure below. The red markers represent the last minute of each skim test, where the skim test reading of torques has reached a steady state. The mean of each set of the red markers gives the mean value of skim reading for that test, which is visualized along with measurement noise, in Section 4.1.7 in Figure 4.10.

The green markers represent the last minute of the measured drum torque for the tire under test load, the mean of which is taken. Using the two sets of mean values (measurement test reading and skim test reading), the mean rolling resistance force corresponding to each warmup duration is calculated using the formula shown in section 3.2.3.2, and visualized later in Section 4.1.7 in Figure 4.11.

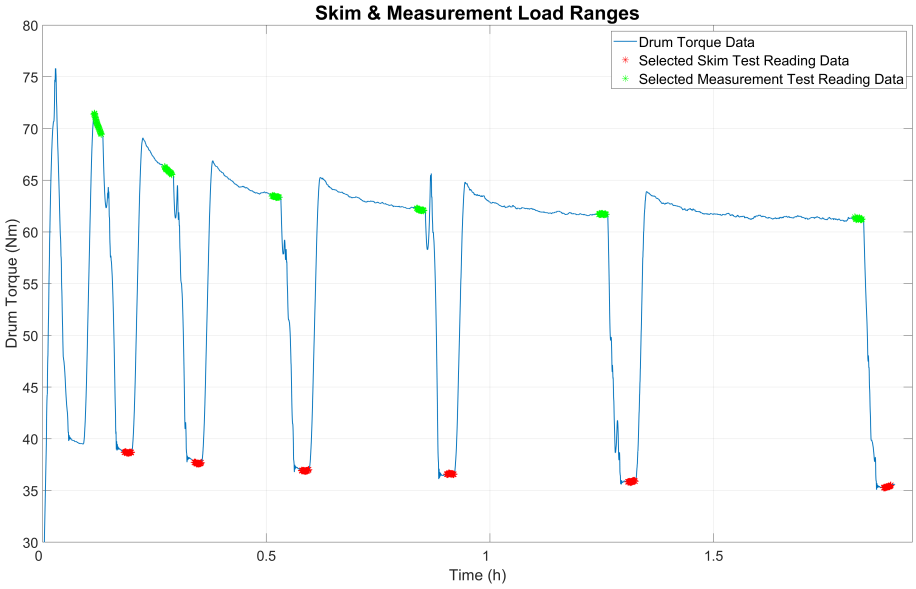

Figure 3.12: Drum Torque Data from Transient Skim Measurement Test

3.3 Modelling

This section elaborates on the models developed in this thesis work.

3.3.1 Rolling Resistance Model

The Rolling Resistance model developed in this thesis work is an empirical model based on the warmup behaviour of the tire. The model uses the temperature of the tire and speed as an input to calculate the rolling resistance.

3.3.1.1 Theory

Janssen and Hall [28] and later Schuring et al. [11] showed the dependence of rolling resistance on the speed and temperature can be expressed by an exponential relation of the form,

$$RRf = (A'_0 + A'_1 v_x) e^{(B'_0 + B'_1 v_x)T}, \tag{3.2}$$

where v and T are speed and temperature respectively, and A'_0, A'_1, B'_0 and B'_1 are empirically determined parameters that must be fitted to every tire (referred to as fitting parameters). Once the fitting parameters are determined, the equation can then be used to predict the rolling resistance force for input temperatures and speeds.

Such a model can be used to predict the expected rolling resistance force under transient conditions of speed and temperature. By using the model during a drive cycle test, the instantaneous rolling resistance can be predicted, and hence, the energy

consumption can be predicted with a higher degree of accuracy.

To represent the exponential reduction of rolling resistance with increasing temperature, equation 3.2 is rewritten with a negative exponent as,

$$RRf = (A'_0 + A'_1 v_x)e^{-(B_0+B_1 v_x)T}. \tag{3.3}$$

3.3.1.2 Parameter Identification

The model of the form used by Schuring does not take the inflation pressure into account and hence cannot accurately predict the behavior of the tire under conditions of inflation pressure different from what is used to determine the fitting parameters. Following the observations by Ydrefors et al. [5] and the results from our tests conducted to determine how pressure affects rolling resistance, which is discussed later in Section 4.1.4, the pressure dependence is assumed as follows in the model,

$$\begin{gathered} RRf \propto P^{-0.4} \\ \Rightarrow RRf = \left(\frac{P}{P_{ref}}\right)^{-0.4} (A'_0 + A'_1 v_x)e^{-(B_0+B_1 v_x)T}. \end{gathered} \tag{3.4}$$

Where P_{ref} is the reference pressure for the fitting parameters. Therefore, the pressure compensation term can be applied to the equation. The individual effects of each tire's ISO rolling resistance and the applied normal load are isolated when modelling. It is assumed that the rolling resistance force has a linear dependence on the normal load and ISO RRc and the equation is rewritten as,

$$RRf = \left(\frac{P}{P_{ref}}\right)^{-0.4} \cdot \frac{F_z}{1000} \cdot RRc_{ISO} \cdot (A'_0 + A'_1 v_x)e^{-(B_0+B_1 v_x)T}, \tag{3.5}$$

where $A_0 = \frac{A'_0}{RRc_{ISO} \cdot F_z/1000}$ and $A_1 = \frac{A'_1}{RRc_{ISO} \cdot F_z/1000}$.

The equations fitted can be used to obtain the fitted coefficients A_0,A_1,B_0 and B_1 by using data from 2 different speeds.

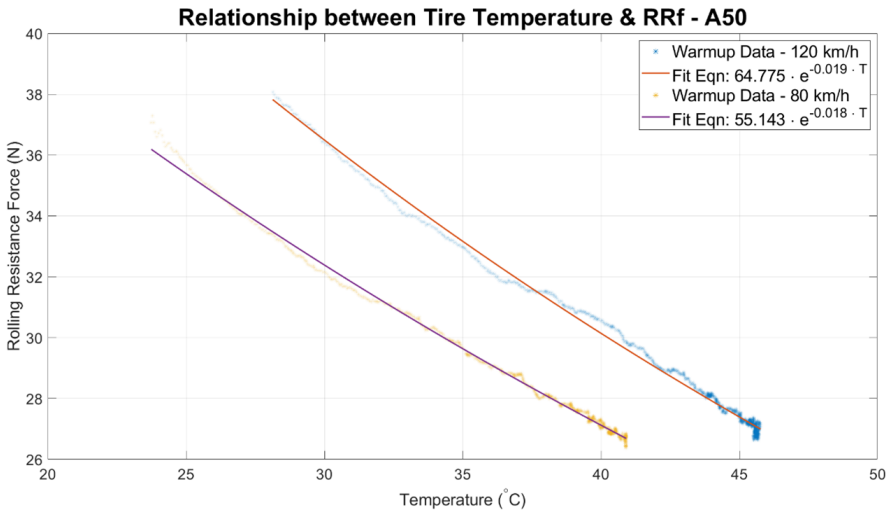

Figure 3.13: Curve Fitting for Coefficients in the Rolling Resistance Model

The graph shows the measurement data (points) and exponent fit (lines). Using the fitted constant and exponent terms (A and B) and the speed, the fitted coefficients (A_0,A_1,B_0 and B_1) can be calculated from warmups at two different speeds of 120 km/h and 80 km/h (33.33 m/s and 24.24 m/s respectively) at the PV16 ISO testing rig. Comparing the fitted line and equation 3.3,

$$Ae^{-BT} = (A'_0 + A'_1 v_x)e^{-(B_0+B_1 v_x)T} \tag{3.6}$$

Example: Comparing the equation with the fitted lines in Figure 3.13

64.7752=$A_0 + A_1 \cdot$ (33.33 m/s), -0.0191 =$B_0 + B_1$ (33.33 m/s)
55.1434=$A_0 + A_1 \cdot$ (24.24 m/s), -0.0177 =$B_0 + B_1$ (24.24 m/s)

The obtained coefficients can then be used to predict the rolling resistance force and coefficient given the temperature and speed. This must be repeated for every tire to obtain the coefficients for that tire.

The parametrization conditions are 5400 N, 280 kPa and temperatures used correspond to 80 km/h and 120 km/h.

3.3.1.3 Load Compensation

As the tire is subjected to a higher normal load, the tires experience a higher rolling resistance force, which increases the internal heat generation, resulting in a higher steady-state temperature. This affects the relation between rolling resistance force and temperature, as visualized in Figure 3.14, and subsequently the fitting coefficients (A_0,A_1,B_0 and B_1).

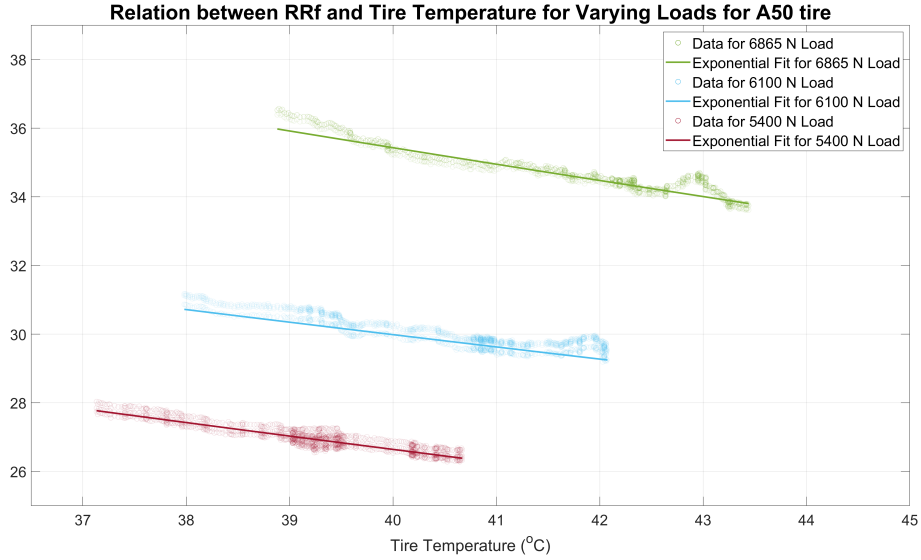

Figure 3.14: Relation between RRf & Tire Temperature for Varying Loads

It is unclear which and to what magnitude the fitting coefficients (A_0,A_1,B_0 and B_1) are impacted by the varying load as tests need to be run at different speeds for each load to solve for the fitting coefficients. One way to account for normal load variations would be a compensation factor, which could be of the following form (similar to that discussed in [16]):

$$\text{Load} \quad \text{Compensation} \quad \text{Factor} = \left(\frac{F_z}{F_{z,ref}}\right)^{\beta} \tag{3.7}$$

where, $F_{z,ref}$ is the normal load at which the fitting coefficients are calculated, and β is an empirically fitted exponent.

Another method would be to calculate the fitting coefficients at different normal loads. This would require a sweep of varying loads at different speeds. This would create a lookup table (or map) of fitting coefficients, and thus the effect of normal loads on RRf prediction can be included in the Rolling Resistance Model.

However, this implementation has not been completed in this thesis due to constraints related to time and data availability.

3.3.2 Thermal Model

A thermal model is developed in this thesis work to calculate the temperature of the tire as well as the temperature of the inflation gas, given only the speed, the rolling resistance, and the environmental conditions such as the road and ambient temperature.

3.3.2.1 Theory

The thermal model of the tire uses a lumped thermal capacity approach to calculate the temperature of the tire rubber and the inflation gas given the operating conditions (speed, load, and inflation pressure) and tire parameters (rolling resistance coefficient, heat transfer coefficients, etc). The simplification of lumped thermal capacity means that the tire as a whole, has the same temperature. Figure 3.15 describes the generation and transfer of heat as used in the model.

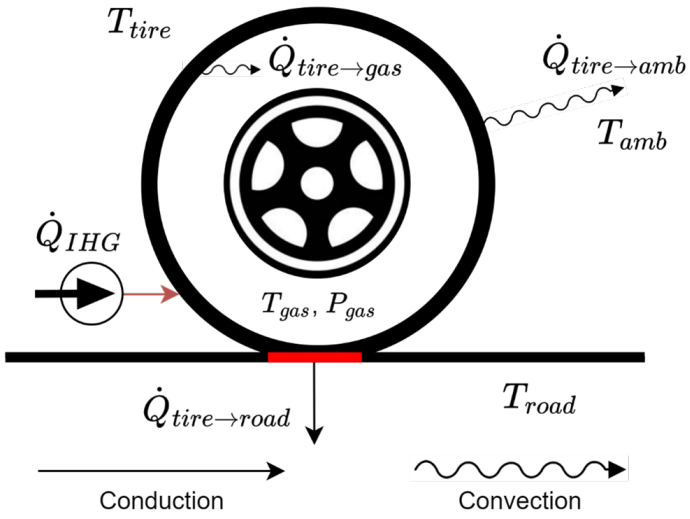

Figure 3.15: Representation of Heat Transfers
(IHG represents the internal heat generation due to rolling resistance)

Figure 3.16 represents the same, however in form of a thermal circuit diagram, with the heat transfer parameters (highlighted in red) being unknown quantities.

It is also assumed that the heat transfer from the tire to the rim is negligible compared to other forms of heat transfer. This is due to the minimal contact surface area between the tire and the rim, making it relatively insignificant in the overall thermal dynamics of the tire. The heat transfer from the inflation gas to the rim is also considered to be low due to the low heat transfer coefficient. Therefore, it is not taken into consideration in this model.

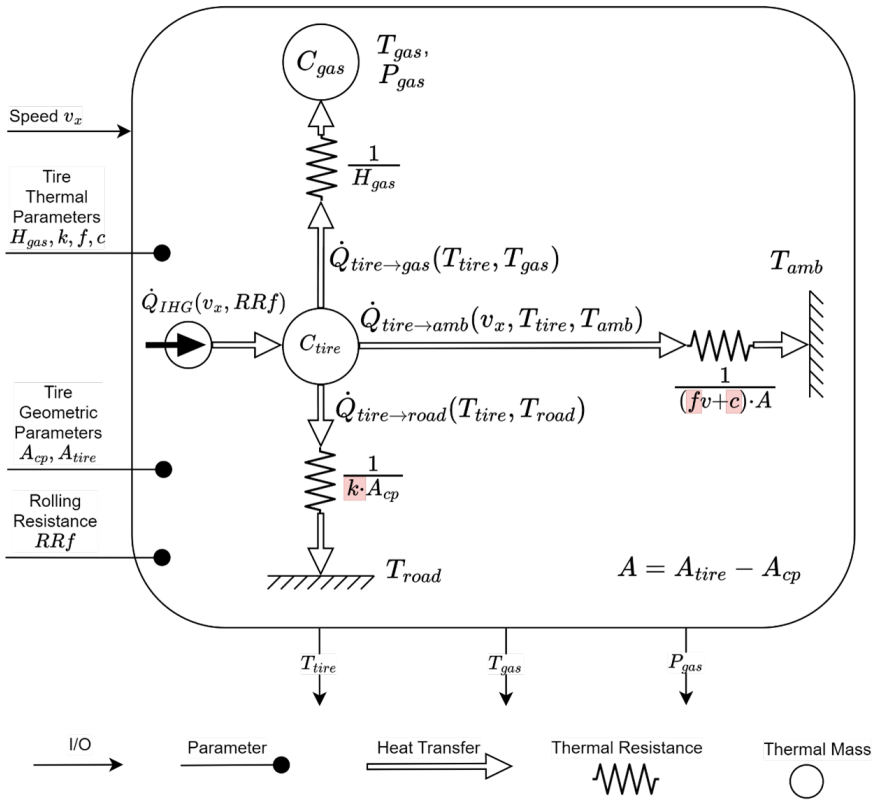

Figure 3.16: Thermal Circuit Diagram with heat transfer parameters (highlighted in red) being unknown quantities

The thermal model in this thesis work considers the tire rubber material into a single unit that has one source of heat input, rolling resistance (heat generation due to hysteresis), and 3 heat outputs: to the road, to the ambient, and to the inflation gas. The road and ambient are both assumed to be kept constant and equal in a controlled environment and act as a heat sink. The heat transfer equations for the thermal model are as follows.

Heat generation due to RR,

$$\dot{Q}_{IHG} = v_x \cdot RR_f, \tag{3.8}$$

heat loss to ambient,

$$\dot{Q}_{\text{tire}\to\text{amb}} = (f \cdot v_x + c) \cdot (A_{\text{tire}} - A_{cp}) \cdot (T_{\text{Tire}} - T_{\text{amb}}), \tag{3.9}$$

heat loss to road,

$$\dot{Q}_{\text{tire}\to\text{road}} = k_{\text{tire}\to\text{road}} \cdot A_{cp} \cdot (T_{\text{Tire}} - T_{\text{road}}), \tag{3.10}$$

heat loss to inflation gas,

$$\dot{Q}_{\text{tire}\to\text{gas}} = H_{\text{tire}\to\text{gas}} \cdot (T_{\text{Tire}} - T_{\text{gas}}), \tag{3.11}$$

heat balance equation for tire temperature,

$$\frac{d}{dt}T_{\text{Tire}} = \frac{\dot{Q}_{IHG} - (\dot{Q}_{\text{tire}\to\text{amb}} + \dot{Q}_{\text{tire}\to\text{gas}} + \dot{Q}_{\text{tire}\to\text{road}})}{C_{p,\text{tire}} \cdot m_{\text{tire}}}, \tag{3.12}$$

heat balance equation for gas temperature,

$$\frac{d}{dt}T_{\text{gas}} = \frac{\dot{Q}_{\text{tire}\to\text{gas}}}{C_{p,\text{gas}} \cdot m_{\text{gas}}}, \tag{3.13}$$

and the pressure evolution equation derived from the ideal gas law,

$$P_{\text{gas}}(t) = \left(\frac{P_0}{T_0}\right) \cdot T_{\text{gas}}(t). \tag{3.14}$$

3.3.2.2 Parameter Identification

The parameters that need to be identified are the conductive heat transfer coefficient ($k_{tire\to road}$), speed factor for convective coefficient (f), and constant factor for convective coefficient (c). Simplifications to the model:

1. The inflation gas temperature is calculated using an assumed value of the heat transfer coefficient $H_{tire\to gas}$ from Kelly et al. [29]. This is because the measured inflation gas temperature is unreliable and hence cannot be used to calculate $H_{tire\to gas}$.

   If the inflation gas temperature was measured accurately, then the differential equation for inflation gas temperature can be used to calculate $H_{tire\to gas}$ as:

   $$\frac{d}{dt}T_{gas} = \frac{\dot{Q}_{tire\to gas}}{C_{p,gas} \cdot m_{gas}}, \dot{Q}_{tire\to gas} = H_{tire\to gas} \cdot (T_{Tire} - T_{gas}). \tag{3.15}$$

   Substituting for $\dot{Q}_{tire\to gas}$ and rearranging,

   $$H_{tire\to gas} = \frac{\frac{d}{dt}T_{gas} \cdot C_{p,gas} \cdot m_{gas}}{(T_{Tire} - T_{gas})}. \tag{3.16}$$

2. In the thesis work, the ambient and road temperatures are assumed to be the same and constant since the temperatures inside the ISO Tire testing rig and dynamometer are controlled and maintained at 23℃. Hence, $T_{road} = T_{amb}$.

   The conductive heat transfer and the speed independent convective heat transfer are of the same form. Due to the assumption that road and ambient temperature are the same, they depend on the same independent variable ($T_{road} = T_{amb}$). Hence, the two terms can be combined to the following form:

   $$\dot{Q}_{\text{speed independent}} = z \cdot (T_{\text{tire}} - T_{\text{amb}}), \text{ where } z = (c \cdot (A_{\text{tire}} - A_{cp}) + k \cdot A_{cp}), \tag{3.17}$$

   $$\dot{Q}_{\text{speed dependent}} = f \cdot v_x \cdot A_{cp} \cdot (T_{\text{tire}} - T_{\text{amb}}), \tag{3.18}$$

   $$\frac{d}{dt}T_{\text{tire}} = \frac{\dot{Q}_{IHG} - (\dot{Q}_{\text{speed independent}} + \dot{Q}_{\text{speed dependent}} + \dot{Q}_{\text{tire}\to\text{gas}})}{C_{p,\text{tire}} \cdot m_{\text{tire}}}. \tag{3.19}$$

The equation is solved using mldivide [30] in MATLAB to obtain the values for the coefficients f and z.

3.3.3 Combined Model

The combined model is developed using the Rolling Resistance Model and the Thermal Model developed previously. The combined model uses only the speed as an input and calculates the rolling resistance and temperature in every iteration.

3.3.3.1 Theory

A combined model is created to predict the temperatures and rolling resistance of the tire given only the test conditions (speed, normal force, initial temperature, and initial pressure values). The combined model uses the previously developed Rolling Resistance and Thermal models, and the rolling resistance force used to calculate the internal heat generation at every timestep uses the temperature and inflation pressure calculated in the previous timestep. The following figure shows the schematic of the combined model.

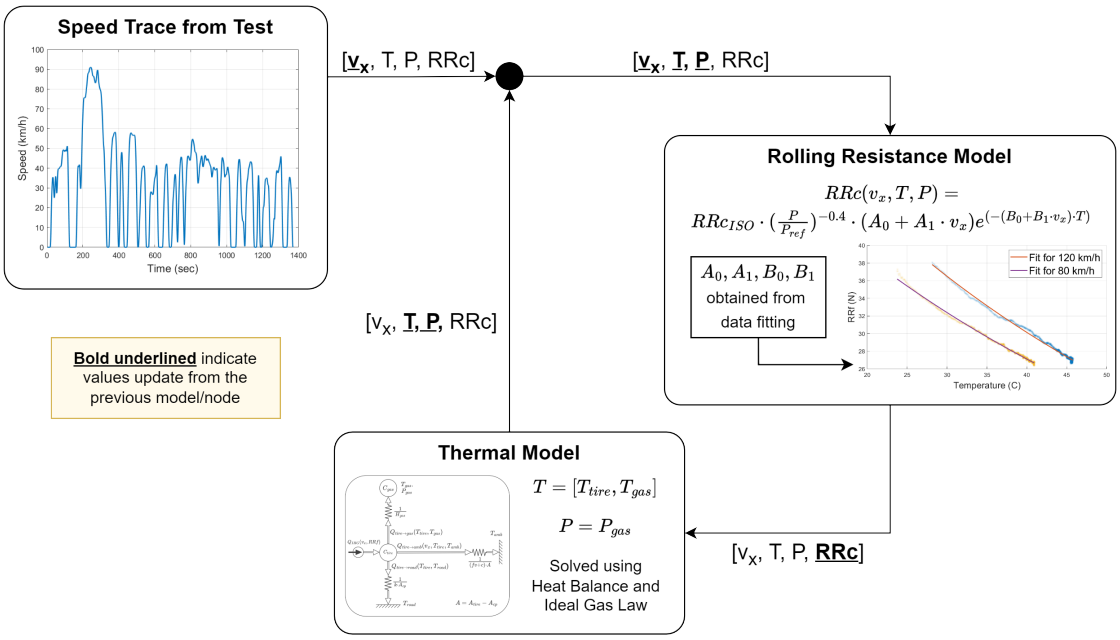

Figure 3.17: Combined Model Schematic

The fitting parameters for the rolling resistance model (namely A_0, A_1, B_0, B_1) are calculated for the PV16 rig. To account for the change in roller diameter between the PV16 rig and the dynamometer EP rig, a correction factor needs to be included, which is explained by equation 3.1.

3.4 Drive Cycle Tests on Dynamometer

This section elaborates on the drive cycle tests conducted in this thesis work.

3.4.1 Definitions

Road Load: The road load is the resistive forces experienced by the vehicle while driving at a constant speed on a smooth, flat surface. The road load consists of rolling resistance, driveline and powertrain losses, and aerodynamic losses.

Coastdown: Coastdown is performed by taking the vehicle up to a predefined speed and letting it roll freely down to a stop under no propulsion or braking forces.

3.4.2 Dynamometer Rig Setup

As shown in Figure 3.2, the dynamometer testing rig at EP consists of 4 rollers of 1.2 m diameter, one under each wheel. The vehicle is also mounted to the rig using the front tow point and rear tow hitch to prevent any movement. A secure mounting is needed to prevent any weight transfer due to roll or pitch motion and to hold the wheels vertically over the rollers.

Figure 3.18: (L) Dynamometer Rig without Vehicle and (R) Single Drum (Images from Volvo Car Corporation Internal Media)

Figure 3.19: (L) Front Tow Point Mounting and (R) Rear Hitch Point Mounting (Images from Volvo Car Corporation Internal Media)

3.4.3 Dyno Setting/Coastdown Test

A dynamometer setting is performed before a drive cycle test to obtain the correct resistive forces for the vehicle to be used when running a drive cycle. Since the vehicle is mounted on the dynamometer with the resistive forces being applied by the drums, the force applied by the dynamometer should match the forces as it would experience on road.

The total resistive force (called dyno load) on a vehicle is given by the equation

$$F = A + Bv + Cv^2, \tag{3.20}$$

where

A: Rolling resistance
B: Speed dependent rolling resistance and drivetrain losses
C: Aerodynamic drag (predominantly)

As the dyno load is affected by the rolling resistance, it has to be recalculated for different tires so that the vehicle experiences the same resistive force as it would on road. The dyno setting is performed as two highway cycles to bring the vwarm the vehicle up, followed by coastdowns from 130 km/h. The coastdown behaviour of the complete vehicle is compared to the behaviour on road, and the resistive forces to be applied by the dynamometer are calculated. The following figure shows the speed trace followed during the dyno setting.

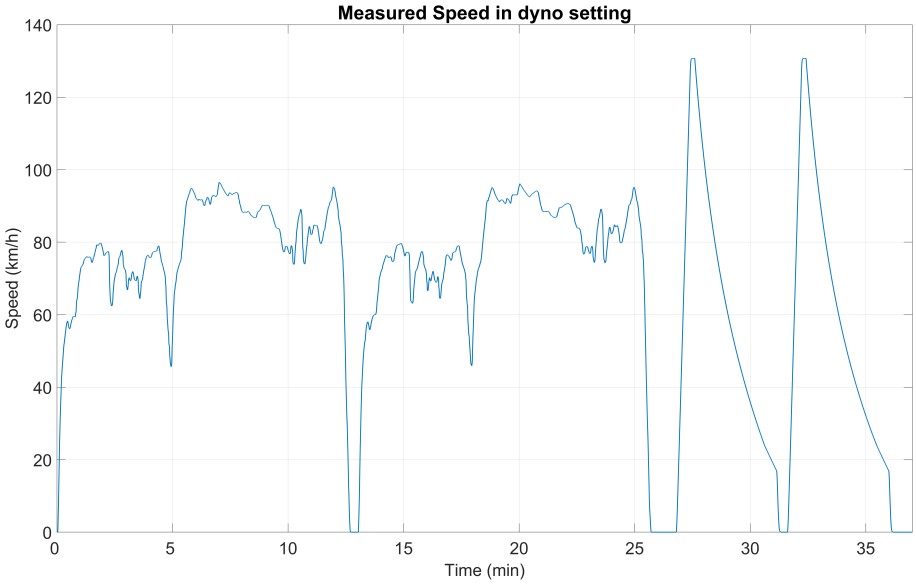

Figure 3.20: Speed trace followed in Dyno Setting

In the highway sections of the dyno setting, the resistive forces on the vehicle applied by the dynamometer will be the same irrespective of the tires. As a result, the difference in the energy consumed will be dependent only on the difference in the rolling resistance between the different tires tested. An analysis of the same is presented in Section 4.3.

3.4.4 Drive Cycle Description

A drive cycle is used to simulate the vehicle's driving behavior in a controlled environment. The drive cycle used is based on the Multi Cycle Range and Energy Consumption Test (SAE J1634 standard [31]). The drive cycle used consists of 4 city (urban driving) sections, 2 highway sections, and 2 constant speed sections. The following figure shows the speed trace in the city and highway sections.

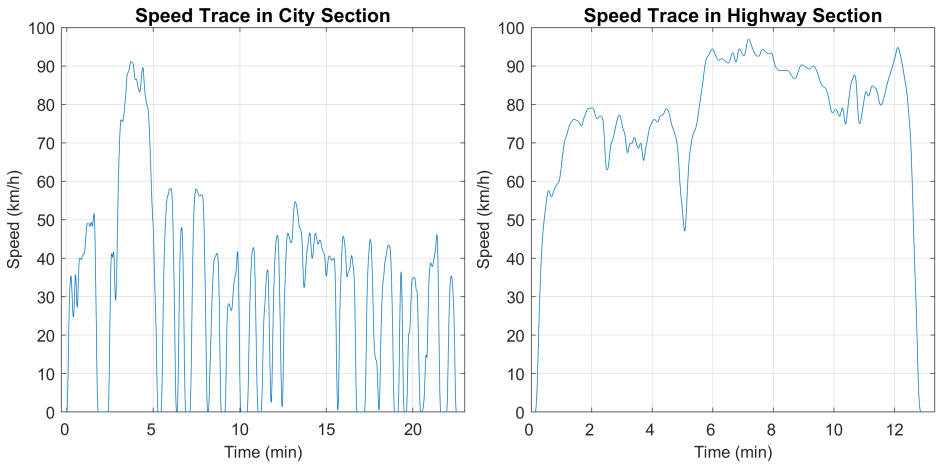

Figure 3.21: (L) City and (R) Highway Section Speed Trace

The following figure shows the speed trace followed in the drive cycle.

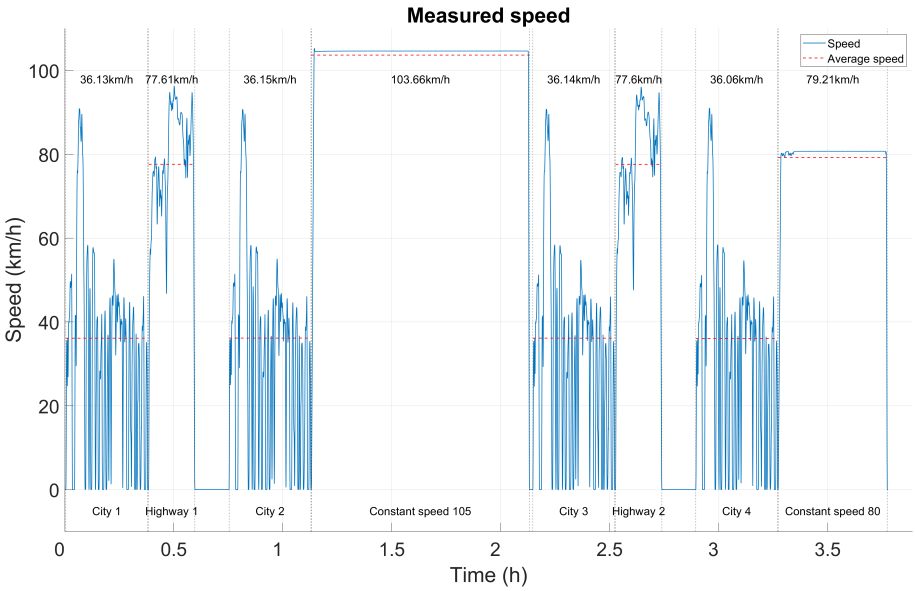

Figure 3.22: Speed trace followed in the drive cycle

The city cycle has frequent starts and stops with low and intermediate speed driving. This is representative of most commutes in daily driving. Frequent starts and stops prevent the tires from reaching optimal working or steady-state temperatures. An addition to the SAE standard is the addition of two intervals of 10 minutes duration after the highway cycles. The intervals are termed 'hot soak' and is important as the

tire has a non-uniform temperature distribution. The part of the tire close to and at the contact patch will have a different temperature than the rest of the tire due to a combined effect of conduction to the road surface and hysteresis heat generation. The hot soak allows the temperatures in the tires to equalize.

The second constant speed section is at 80 km/h compared to 105 km/h as in the standard. This is to compare the predicted rolling resistance in the section to the rolling resistance value obtained in the ISO testing rig.

3.4.5 Rolling Resistance Power and Energy Loss

This section explains the power and energy loss calculation due to rolling resistance.

3.4.5.1 Rolling Resistance Power Loss

One of the main objectives of this thesis work is to estimate the difference in losses due to rolling resistance between a dynamic model and a constant rolling resistance value in terms of power and energy loss.

The power lost due to rolling resistance, termed as Rolling Resistance Power Loss in this thesis work, is calculated using both the Rolling Resistance Model ($RRc(v_x, T)$) and ISO standard test value for all tires using,

$$\text{Rolling Power Loss (model)} = RRc(v_x, T) \cdot F_z \cdot v_x$$
$$\text{and, Rolling Power Loss (ISO RRc)} = RRc_{ISO} \cdot F_z \cdot v_x.$$

The rolling resistance power loss will have a speed dependence irrespective of whether a model or a constant value is used for calculation. However, the rolling resistance power loss calculated for the modelled rolling resistance will have complex dependence as the rolling resistance model has a dependence on speed as described in section 3.3.1.1

It must be kept in mind that the rolling resistance power loss is related only to the tire and not the vehicle being tested.

3.4.5.2 Rolling Resistance Energy Loss

The energy consumption due to rolling resistance, termed as rolling resistance energy loss in this thesis work, is calculated from the rolling power loss using the fundamental relation between power and energy:

$$E = \int P \cdot dt$$

4

Results & Analysis

The results of the different tests and models and analyses of the same are presented in this section.

4.1 Rolling Resistance Testing on Drum Rig

This section presents the results of the tests run on the Drum Rig.

4.1.1 ISO Standard Test

The ISO Test is done according to the test procedure in Section 3.2.3. The RRc uncertainty is calculated from the measurement uncertainty in the rolling resistance force measurement and included in the graph. The uncertainty in the torque measurement is ±0.9 Nm, and the radius of the drum being 1 m results in a ±0.9 N error in measured force. The results are as follows:

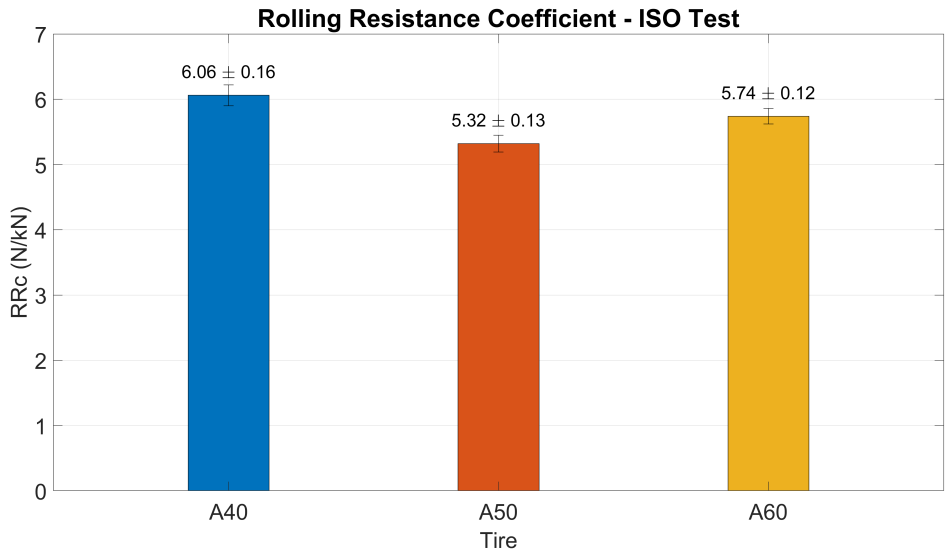

Figure 4.1: ISO Standard Rolling Resistance Coefficient Comparison

The ISO RRc of the different tires increases in the order A50<A60<A40.

4.1.2 Vehicle Load Test

The comparison between ISO Load and the actual vehicle load, i.e., 5400 (N), is of interest, and it can be observed that even though the rolling resistance force changes significantly due to varying normal load, the rolling resistance coefficient changes very little between the two loads. The change is small enough to be considered within the measurement uncertainty of the sensor. The inflation pressure is also changed to 280 kPa to match the inflation pressure recommended by the vehicle manufacturer.

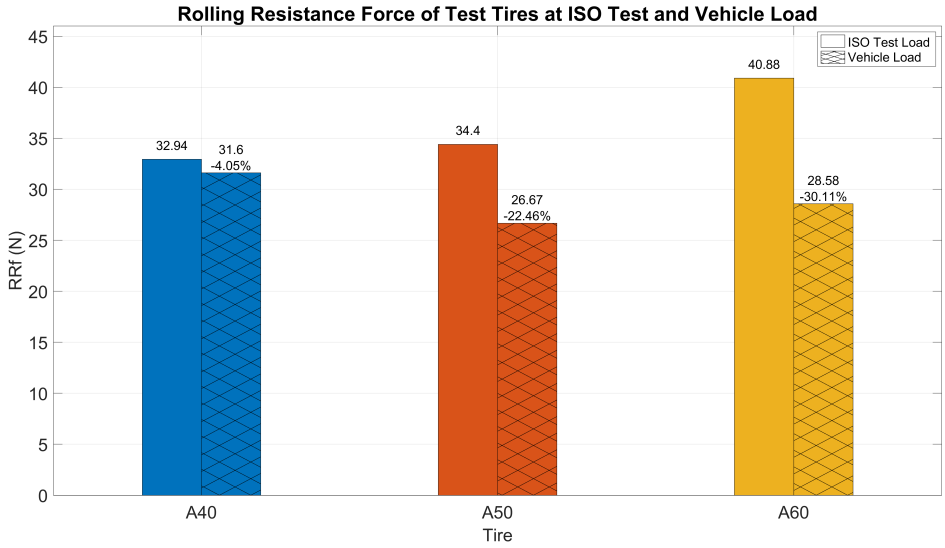

Figure 4.2: Comparison of Rolling Resistance Force under ISO and Vehicle Load

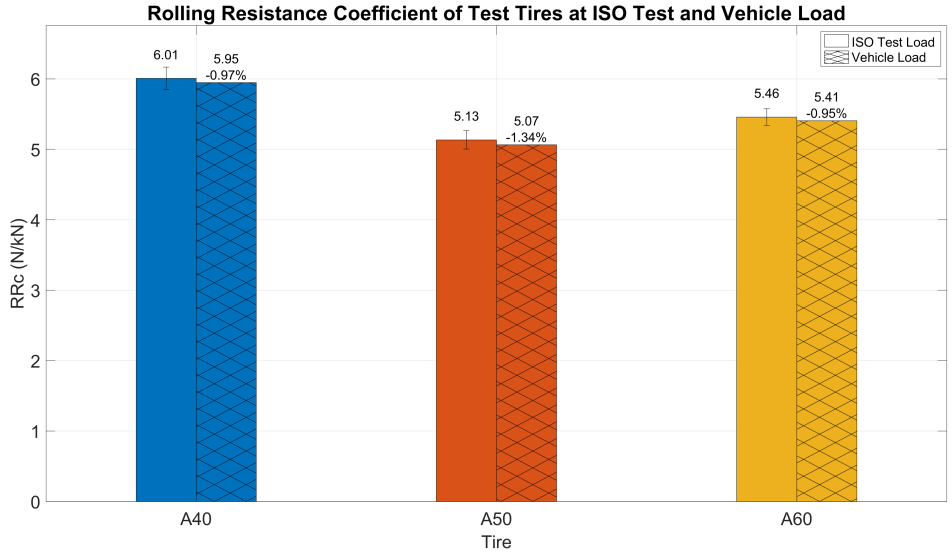

Figure 4.3: Comparison of Rolling Resistance Coefficient under ISO and Vehicle Load

4.1.3 Load Sweep

The result of the load sweep performed to study the effect of load on the rolling resistance coefficient is as follows:

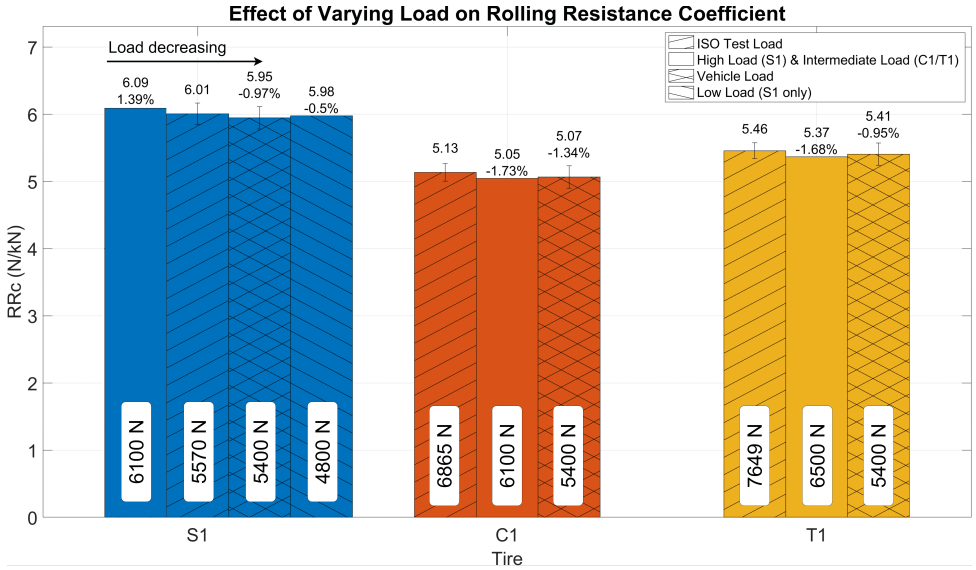

Figure 4.4: Comparison of Rolling Resistance Coefficient for Complete Load Sweep

It can, therefore, be said that the RRc is constant (within measurement uncertainty) with a change in the normal load while the RRf increases with increasing load. A reasoning for the behavior can be that the increasing load causes an increase in the rolling resistance force but also increases the deformation in the tire. An increase in deformation would lead to an increase in the internal heat generation, increasing the tire's temperature. This is discussed further in Section 4.1.8.

4.1.4 Pressure Sweep

A pressure sweep was run to understand the effect and significance of pressure change on rolling resistance. The pressure was changed in steps to 250 kPa, 280 kPa, and 300 kPa for 80 km/h speed and ISO test load and vehicle load for each tire.

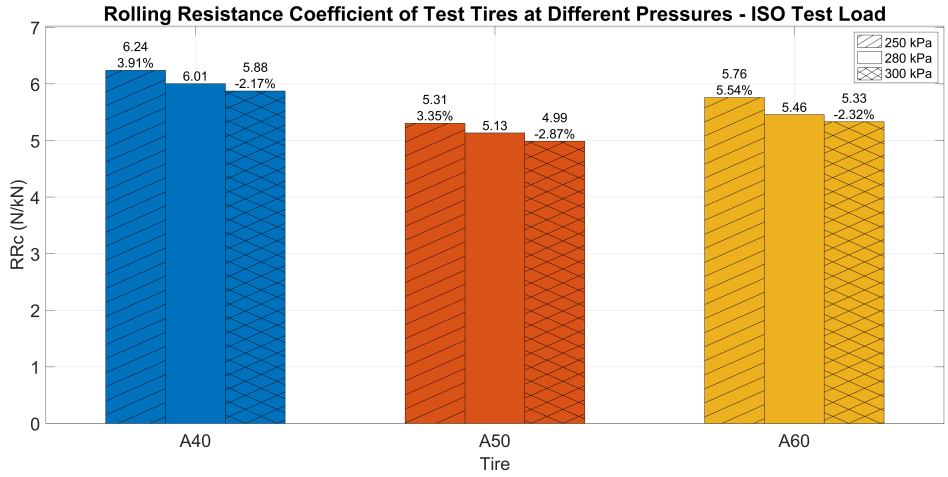

Figure 4.5: Comparison of RRc of Different Tires at Different Pressure at ISO Test Load

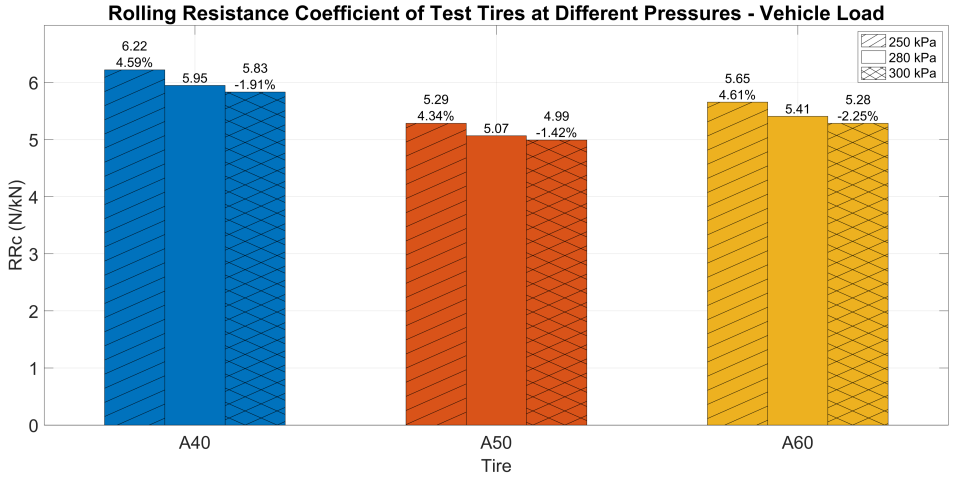

Figure 4.6: Comparison of RRc of Different Tires at Different Pressure at Vehicle Load

The test results match the theory described in Section 2.2.2.3 – the rolling resistance decreases as pressure increases, and the decrease is significant enough not to be accounted for as sensor uncertainty. From Section 2.2.2.3, the equation $RRf \, \alpha \, P^{-\alpha}$ can be used to compare the pressure dependence. For tire A40, at pressures 250 kPa and 280 kPa, the following relation is obtained:

$$\frac{RRf \ at \ 250\,kPa}{RRf \ at \ 280\,kPa} = 1.0453 \quad \left(\frac{280}{250}\right)^{-0.4} = 1.0463 \tag{4.1}$$

An exponent of –0.4 fits the pressure dependence well for all the tires with the experimental data obtained. These results support using -0.4 as the exponent for the pressure dependence in the rolling resistance model.

The decrease in rolling resistance can be explained as the increase in pressure causing an increase in the tire stiffness. A stiffer tire deforms less and has lower hysteresis, leading to lower generated resistance force and lower coefficient.

4.1.5 Speed Sweep

The speed was changed from 40km/h to 80 km/h to 120km/h to understand the effect of speed on the rolling resistance. The normal force applied was the vehicle load and inflation pressure of 280kPa. The following bar graph shows the change in RRc for different speeds.

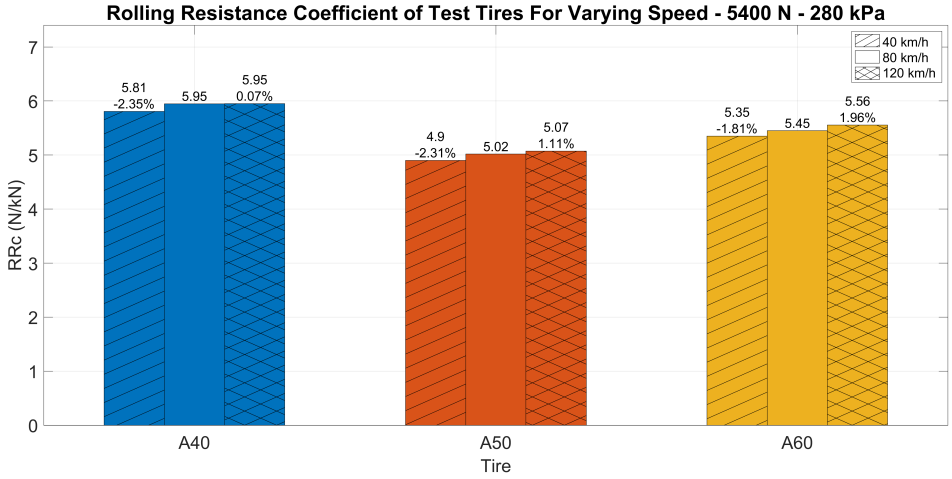

Figure 4.7: Comparison of RRc of Different Tires at Different Speeds

The test results match the theory described in section 2.2.2.5 – the rolling resistance increases with speed, and the change is large enough to not be accounted as sensor uncertainty.

The increase in RRf is due to the increased frequency of deformation with increasing speed, which leads to an increased force. Since the load is kept constant, the coefficient also increases.

4.1.6 Warmup Behavior

The warmup of the tires from a cold start was done to analyze and obtain the temperature evolution during the warmup along with the rolling resistance and establish the relation between the rolling resistance and temperature of the tire.

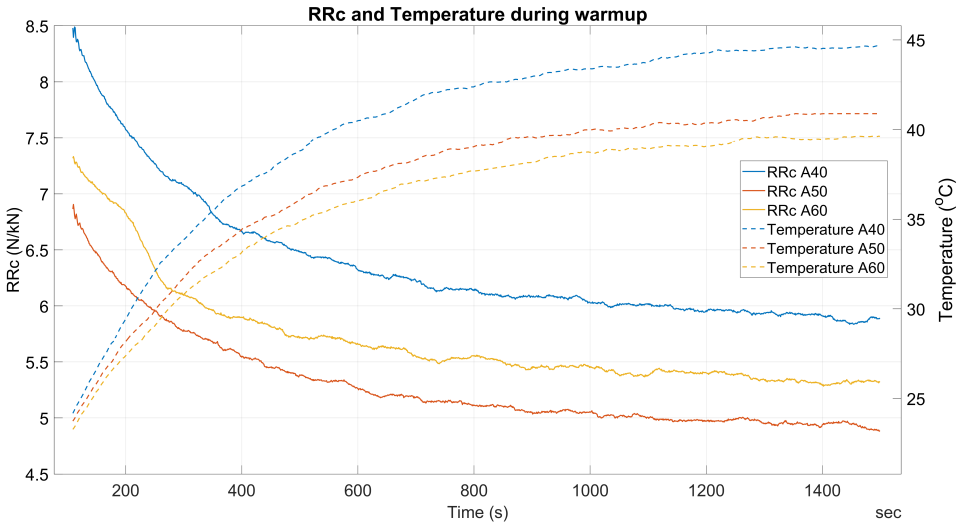

Figure 4.8: Warmup behavior of different tires

The figure above shows the warmup region behavior of different tires. From the figure, it can be inferred that all tires measured have similar starting temperatures (∼23°C) but reach different steady-state temperatures. The RRf reaches a steady state value as the temperature reaches a steady state.

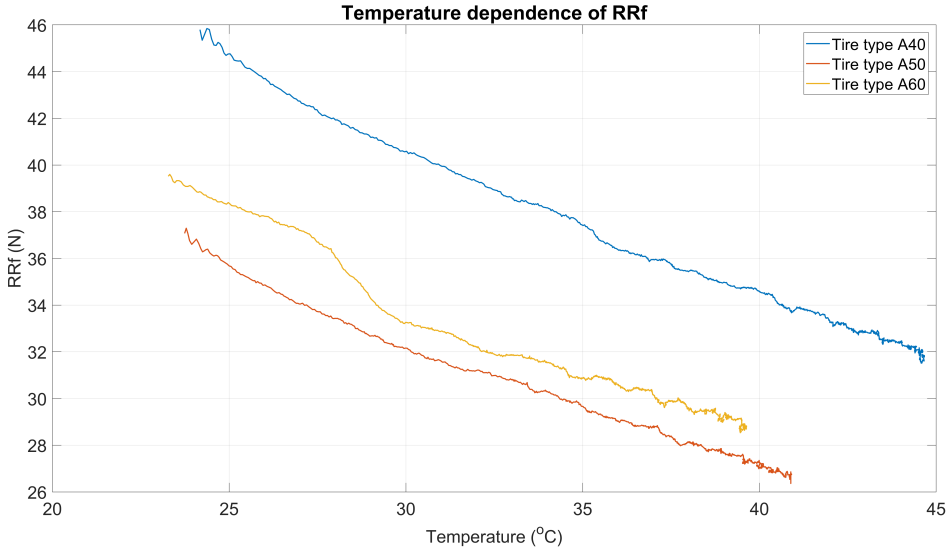

Figure 4.9: Temperature Dependence of RRf as tested

The figure above shows the temperature dependence of RRf. The temperature dependence of RRc is obtained by correlating the temperature and measured RRf

at each given time. In a 5°C interval between 30 and 35°C, the decrease in RRf is as follows:

- A40: 14.17% (-3.15 N)
- A50: 7.82% (-2.50 N)
- A60: 7.12% (-2.37 N)

The relation between RRf and has an exponential decrease as described previously, but for a small temperature range, a linear behaviour can be approximated.

The values are subject to measurement errors in both the torque and the temperature sensors. This assessment demonstrates that the tire of type A40 is more sensitive to changes in rolling resistance per unit change in temperature compared to A50 and A60, which have similar temperature dependence.

4.1.7 Transient Skim Measurement

The test is performed as described in section 3.2.7. Figures 4.10 and 4.11 show the evolution of the parasitic losses with increasing warmup duration and the resulting evolution of rolling resistance with increasing warmup duration respectively.

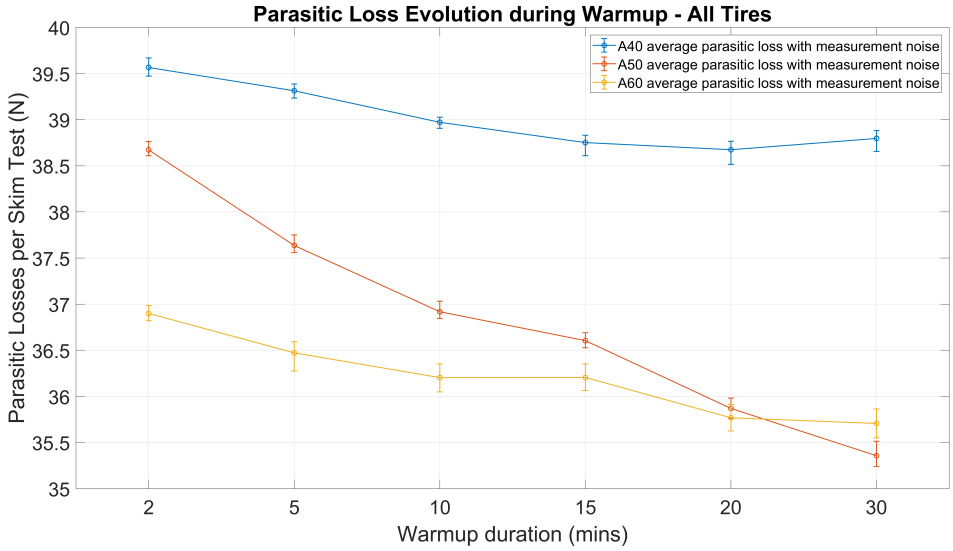

Figure 4.10: Evolution of Parasitic Loss due to Tire Warmup - All Tires

To understand the impact of higher parasitic losses during the warmup phase, the evolution of the rolling resistance force is analysed. The rolling resistance force is calculated by subtracting the means of the last sixty seconds of the measurement load and skim load, and error bars show the sensor uncertainty.

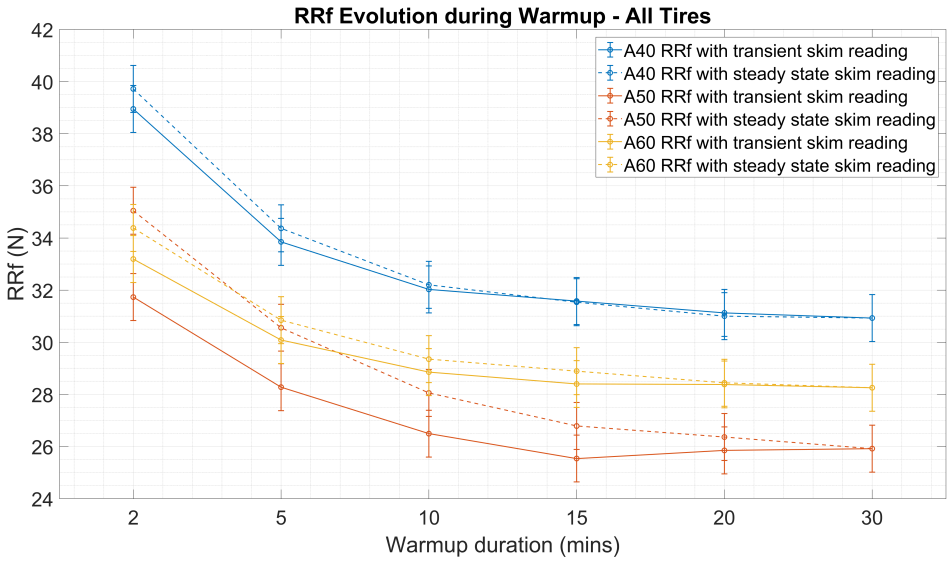

Figure 4.11: Temperature Dependence of RRf as tested

The data suggests a notable shift in RRf and parasitic losses as the temperature increases, one that surpasses measurement uncertainty. The understanding from the test is that the parasitic losses of the tire depend on its thermal state. As seen in the figure above, when analysing a tire that has not reached thermal equilibrium, it is important to use (or measure, when possible) the parasitic losses corresponding to the temperature of the tire. Since the normal load for all these tests is the same (5400 N), the rolling resistance coefficient should also exhibit the same trends.

4.1.8 Comparison of RRc in relation to Tire Temperature for Varying Loads

The rolling resistance of a tire is negatively correlated to the temperature of the tire and is dependent on the normal load on the tire. To try to understand this relationship, the rolling resistance coefficient corresponding to each load and the average temperature of the tire's inner lining (at steady state) is plotted for every tire. The markers on the plot indicate the values of rolling resistance and average tire temperature, with error bars showing the measurement uncertainty of RRc measurements and temperature measurements.

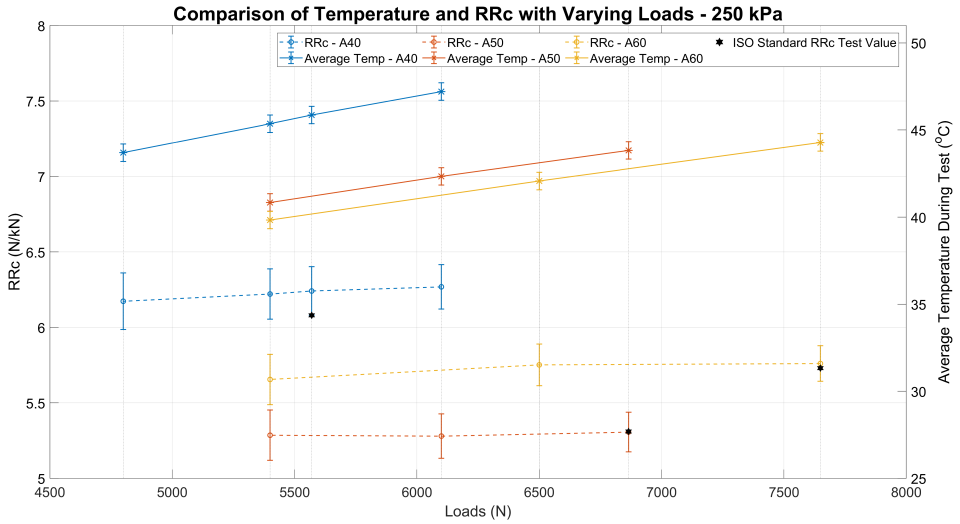

Figure 4.12: Comparison of Temperature and RRc with Varying Loads

It can be inferred from the plot that there is no significant change in the rolling resistance coefficient with an increase in load, and the average temperature increases for increasing loads. This increase in temperature leads to a reduction in the rolling resistance force, as shown in Section 4.1.6. Though the average temperatures shown in 4.12 are after steady state is achieved, the relationship between increasing temperature and reducing RRc still holds. The conclusion is that the load does not significantly affect the rolling resistance coefficient and remains the same across different tires and different initial inflation pressures. Similar plots for other capped inflation pressures are in Appendix A.1.

4.2 Modeling

4.2.1 Rolling Resistance Model

The model is parameterized for the warmup cycle data and validated using different tests. The following figure shows the modelled and measured RRf along with the measurement error. As it can be inferred, the model can calculate the RRf within the error margins.

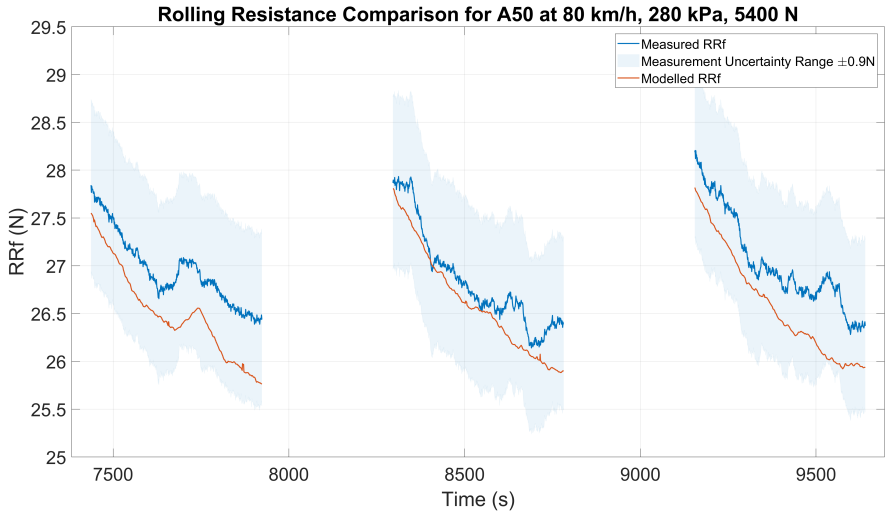

Figure 4.13: Comparison of Measured and Modelled Rolling Resistance Force

The following figures show the error and percentage error between the modelled and measured rolling resistance.

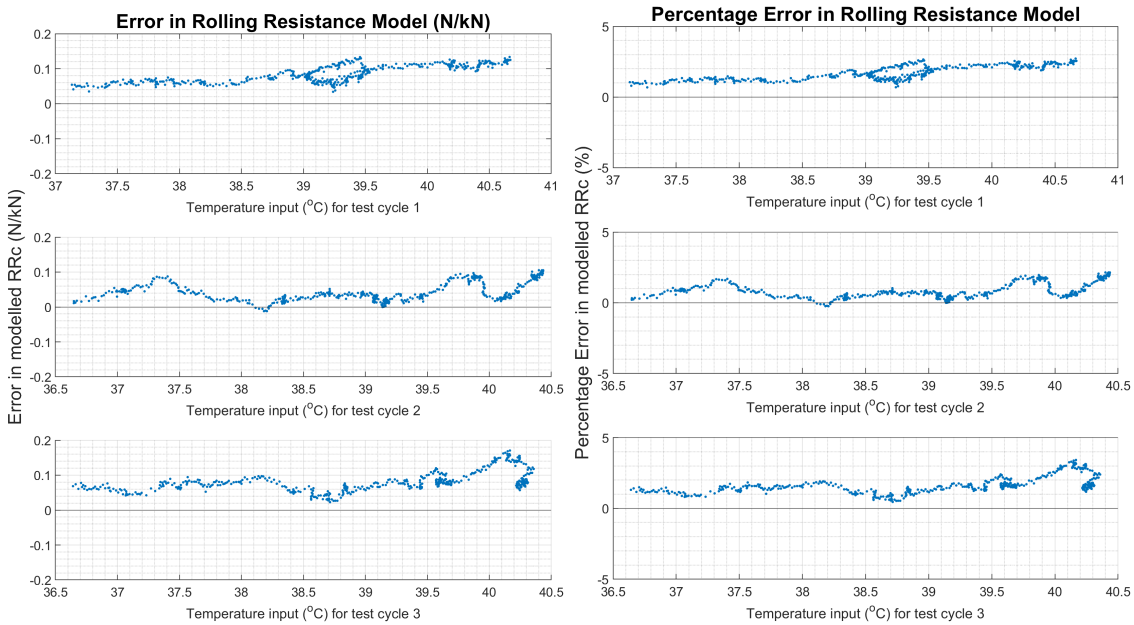

Figure 4.14: (L) Error in Modelled RRf (N/kN); (R) Percentage Error in modelled RRf

From the above figures corresponding to the speed sweep for tire A50, it can be inferred that the model can calculate the rolling resistance force and coefficient to a high accuracy. The modelled RRc is within ±0.2 kN/N of the measured RRc, which is considered a valid range of variation.

As discussed in Section 3.3.1.2, the Rolling Resistance Model is can accurately model the rolling resistance at and close to the parametrization values of vehicle load (5400 N) and inflation pressure (280 kPa). Additionally, the model also includes a term to account for the variations in pressure during the tests.

When the model is input a vehicle load of 5400 N and an inflation pressure capped at 300 kPa for tire A50 and at 250 kPa for tire A40, and subsequently compared with test data, the graphs in Appendices A.2.1 & A.2.2 were obtained.

The model has not been compensated for varying loads as mentioned in Section 3.3.1.3, and as a result, the model cannot calculate the rolling resistance accurately. The modelled and measured rolling resistance force is shown for tire A50 when a load of 6865 N is used instead of a vehicle load in Appendix A.2.4

The limitations of the rolling resistance model are listed as follows:

1. The parameters identified are at vehicle load (5400N) and no normalization is done. Hence, the model is valid only for loads close to the parametrization load and will not be accurate for loads considerably different.
2. The rolling resistance model cannot predict data at low speeds, as it was not parameterized for such conditions, limiting its capability. The parameterization could not be completed due to issues with the temperature data obtained during these low-speed tests. Additionally, the ISO testing rig cannot accurately measure rolling resistance force at low speeds. Consequently, a cutoff of 20 km/h has been set as the useful lower limit for the model output.
3. The data used to parametrize the model is from the ISO testing rig. Since the testing rig is run on a drum, the RRf generated in the ISO testing rig will be higher than what will be generated on a flat road. As a result, the RRf calculated by the model will be equivalent to a value obtained in the testing rig as compared to a flat surface.

4.2.2 Thermal Model

The following figure shows the modelled and measured temperature for tire A50 in the drive cycle test. The model is fitted to the data obtained from the drive cycle tests at the dynamometer rig in EP. The data obtained from the ISO drum rig in PV16 cannot be used as the parameter identification described in Section 3.3.2.2 uses the speed to identify the speed dependent and speed independent heat transfer terms.

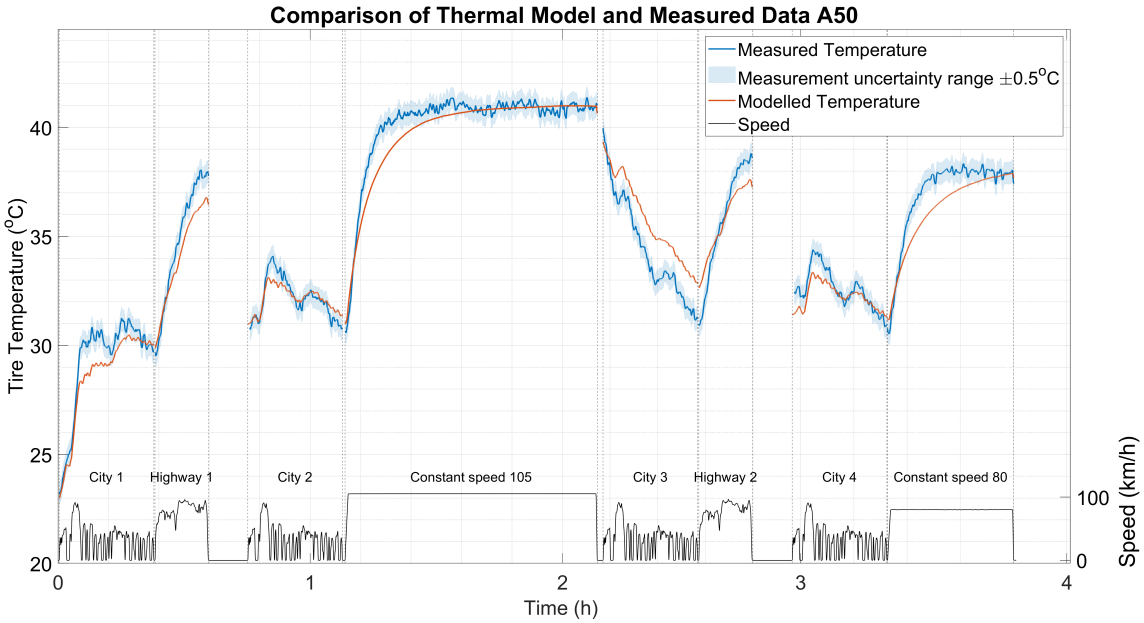

Figure 4.15: Comparison of Thermal Model & Measured Data for A50 tire

As seen in the figure above, the thermal model can model the tire temperature accurately in most cases. In regions of warmup or cooldown (large temperature difference), the predicted temperature varies outside the measurement error range. The limitations of the thermal model are listed as follows:

1. The heat transfer coefficient from tire to inflation gas has been taken from [27]. This is because the temperature of the inflation gas, as measured by the sensor, is not reliable.
2. The speed independent heat transfer coefficient from tire to road (conduction) and tire to ambient (convection) are lumped together in a single term since they are dependent on the same independent variable ($T_{tire} - T_{amb}$) rising from the assumption that $T_{tire} = T_{amb}$.
3. The individual contributions of conduction and convection cannot be determined since they are lumped into the same parameter 'z'.

4.2.3 Combined Model

The following figures show the modelled temperature and the deviation from the measured temperature data.

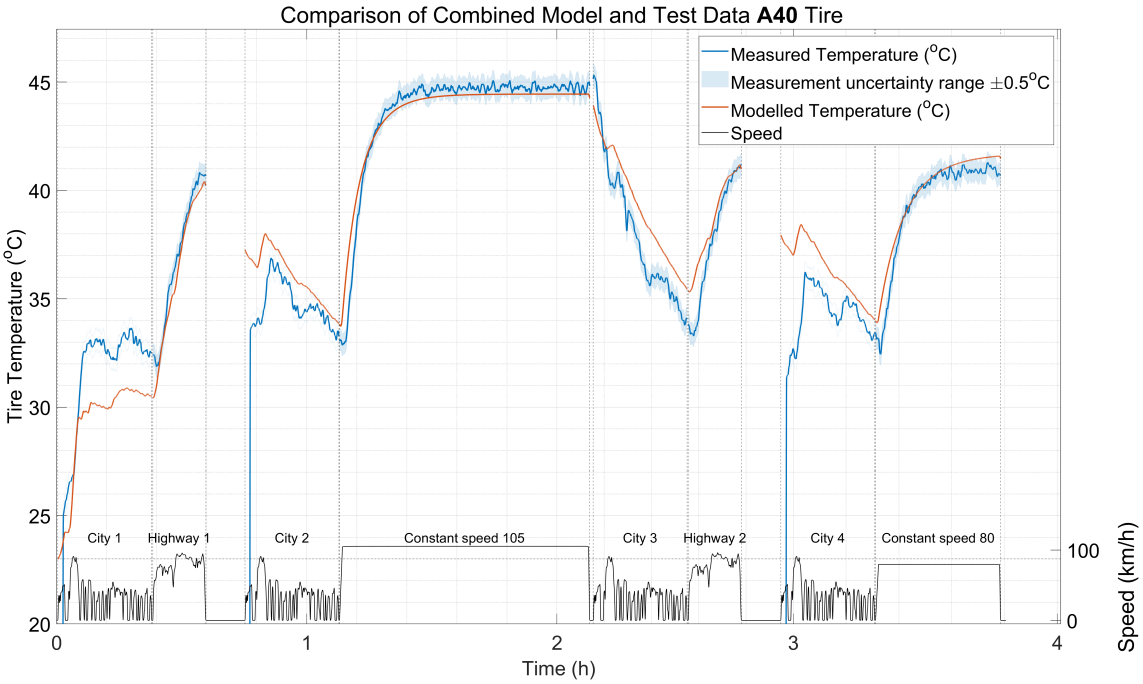

Figure 4.16: Comparison of Combined Modelled & Measured Data for A40 tire

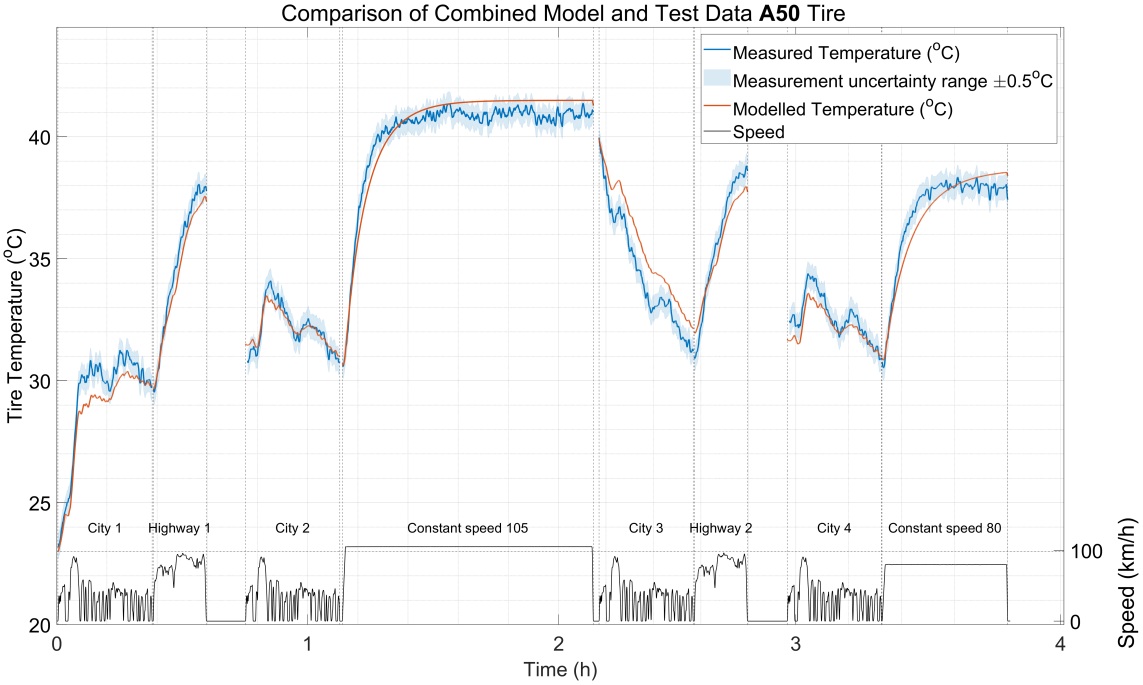

Figure 4.17: Comparison of Combined Modelled & Measured Data for A50 tire

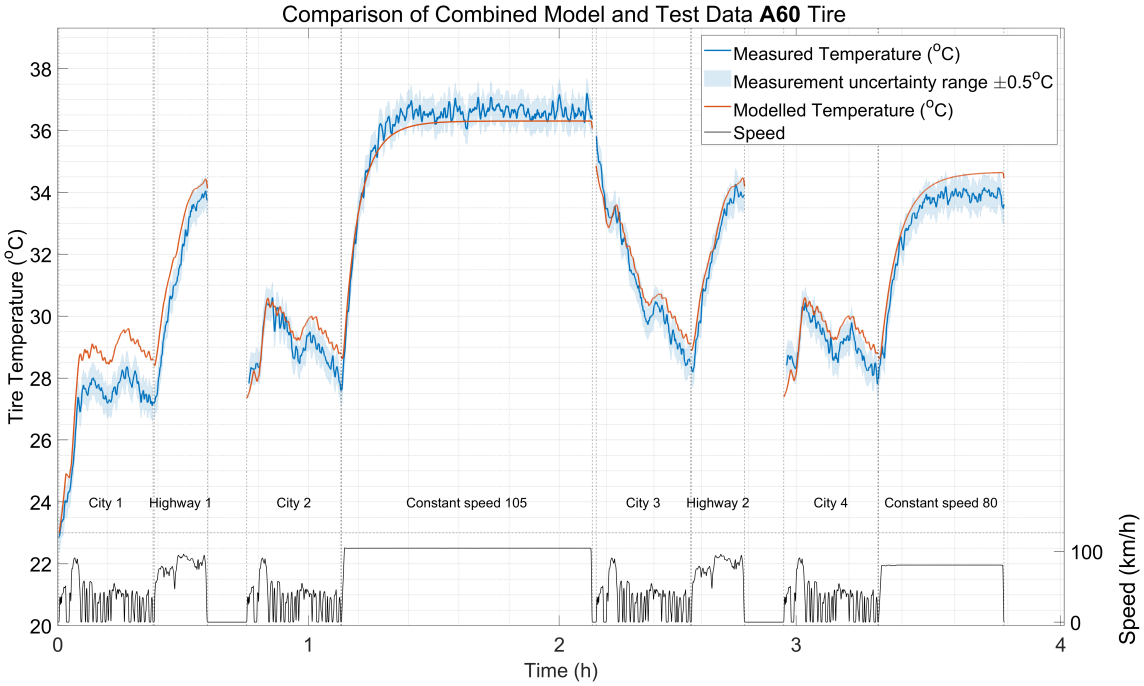

Figure 4.18: Comparison of Combined Modelled & Measured Data for A60 tire

The performance of the model is quantified in the following table.

Table 4.1: Section-wise RMS Error Temperature for Combined Model for all Tires (top) All City sections and (bottom) Highway & Constant Speed (CS) Sections

Tire	Section-wise Temperature RMSE for Combined Model (°C)			
	City 1	City 2	City 3	City 4
A40	2.14	0.41	1.19	0.41
A50	0.12	0.1	0.76	0.62
A60	1.3	1.08	0.45	0.82

Tire	Section-wise Temperature RMSE for Combined Model (°C)			
	Highway 1	Highway 2	CS 105 km/h	CS 80 km/h
A40	0.75	0.44	0.84	0.5
A50	0.66	1.09	0.01	0.75
A60	0.23	0.01	0.52	0.66

It can be observed that the modelled temperature is within the measurement uncertainty range (±0.5°C), especially in the highway and constant speed segments. The city sections have higher errors, which could be attributed to the effect of acceleration and braking torques on rolling resistance, which in turn affects temperature evolution, as well as the limitation set by the simplifications made to the thermal model, discussed in Section 3.3.2.2.
The limitations of the combined model stem from its constituent models.

The rolling resistance parameters (A_0, A_1, B_0 and B_1) are identified at the ISO testing rig and heat transfer coefficients identified are at the dynamometer rig. A correction factor for the drum sizes is used to convert the rolling resistance obtained. The heat transfer coefficients are identified at the dynamometer rig (EP) and cannot be used for other test environments. The dynamometer rig has a controlled ambient and roller temperature different from the real world.

4.3 Drive Cycle Tests – Dynamometer Setting

The following section presents and analyses the results of the dyno setting, which is explained in 3.4.3.

4.3.1 Temperature

The following temperature measurements were obtained for the three different tires during the dyno setting.

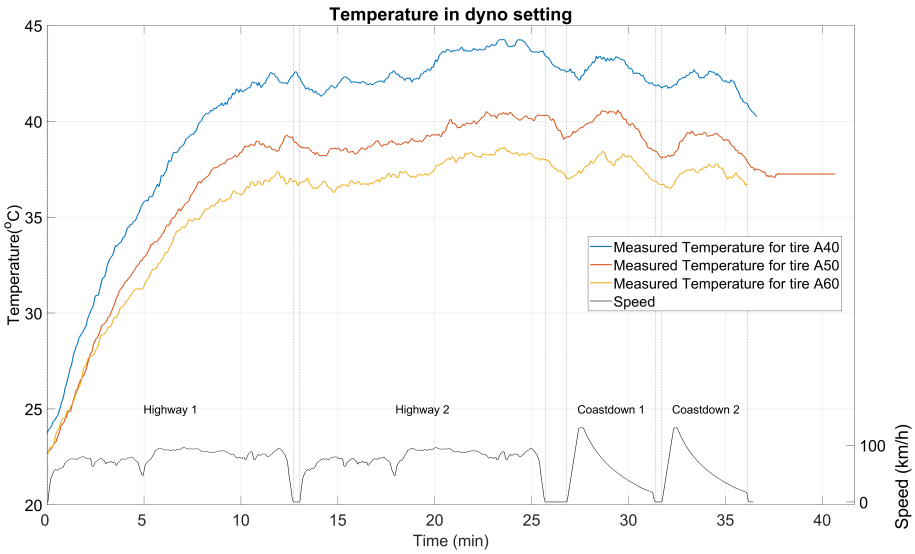

Figure 4.19: Measured Temperature in Dyno Setting

A few observations can be made from the temperature evolution:

1. The temperatures of the different tires are in the order $A40 > A50 > A60$.
2. The temperature increases in the first highway section but remains does not vary much ($\pm 2°C$) in the second highway section.
3. Type A40 has the highest variation in measured temperature, followed by A50 and then A60.

4.3.2 Modelled Rolling Resistance

The Rolling Resistance Model developed previously is used to model the rolling resistance of the tires with the measured temperature and speed data. The following rolling resistance was obtained for all three tires.

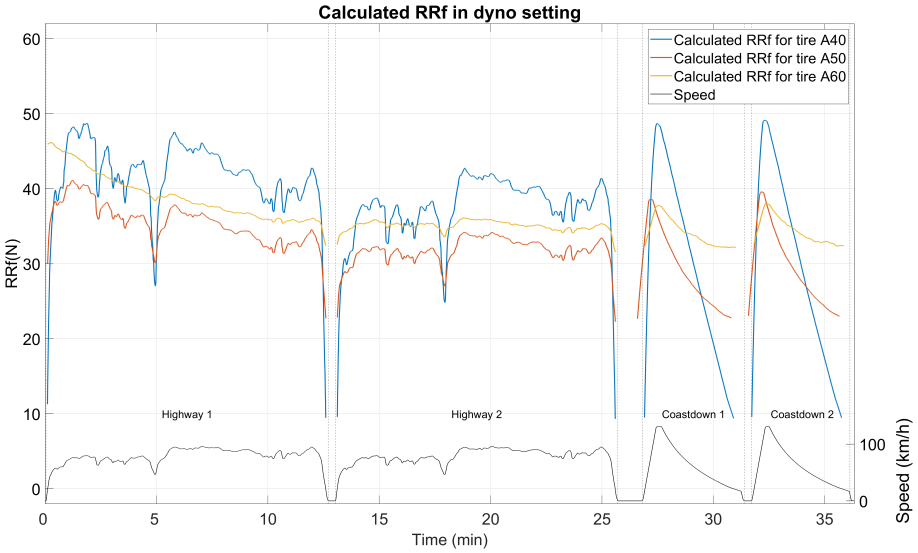

Figure 4.20: Modelled Rolling Resistance for Dyno Setting

The relative dependence on speed can be seen from the modelled rolling resistance. type A40 has the highest dependence on speed followed by A50 and then A60.

4.3.3 Rolling Resistance Energy Loss

As explained in Section 3.4.3, the resistive forces applied by the dynamometer is the same for all three tires in the highway section. Therefore, the accuracy of the Rolling Resistance Model can be verified by calculating the difference in energy consumption of the full vehicle and the difference in energy loss due to rolling resistance. Additionally, the increased energy loss due to transience in rolling resistance can be quantified by comparing the difference in energy consumption to the difference in energy loss calculated with the ISO RRc.

Using the formulae in Section 3.4.5, the difference in energy is calculated and tabulated:

Tires compared	**Δ Energy (Wh)**	**Δ RR Energy (model) (Wh)**	**Δ RR Energy (ISO) (Wh)**
A40-A50	112.9	109.4	71.8
A60-A50	64.0	59.7	39.9

Table 4.2: Energy Loss due to Rolling Resistance in Dyno Setting

From the calculated values, it can be seen that the modelled loss due to rolling resistance is within 5% of the measured value. This validates the output from the Rolling Resistance Model. Also, it can be be seen that the measured loss due to rolling resistance is higher than the value calculated from the ISO RRc, indicating that the energy lost due to rolling resistance is dependent on the transient state of the tire.

4.4 Drive Cycle Tests – Temperature & Rolling Resistance

The following section presents and analyses the results of the drive cycle tests.

4.4.1 Temperature

The following temperature measurements were obtained for one of the front tires of the three different types of tires. A tire on the front axle was chosen as the vehicle is a rear-wheel drive, and the analysis was done for tires that are not powered/driven.

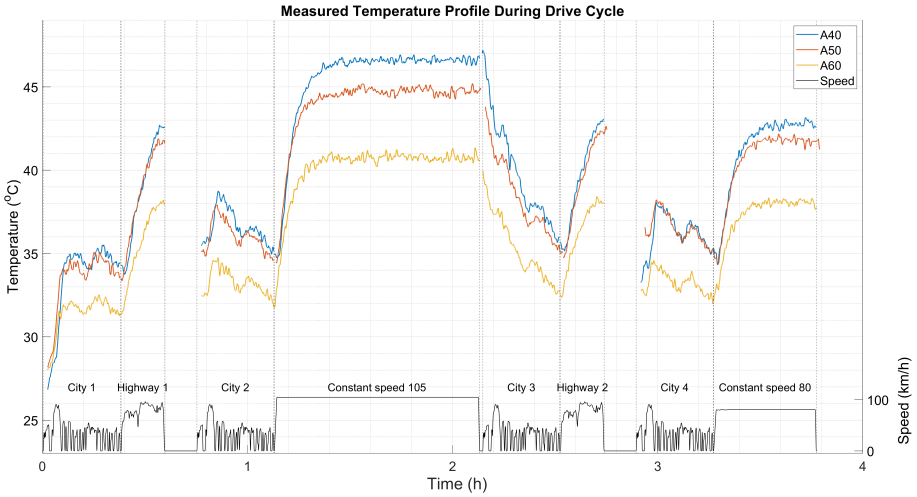

Figure 4.21: Averaged Measured Temperature for Front Left Tire

A few observations can be made from the temperature evolution:

1. The temperatures of the different tires are in the order $A40 > A50 > A60$.
2. The temperature attains steady state in the constant speed sections for all three tires.
3. The heat generation increases the temperature in the continuous driving section in the city section and in the highway and constant speed sections.
4. The city section with frequent stopping is not sufficient for the tire to generate enough heat and the temperature built up from the previous sections reduces.
5. The temperature between different city sections is in the order City 3 > City 2 ≈ City 4 > City 1. This applies to all three types of tires.

6. Type A40 has the highest variation in measured temperature, followed by A50 and then A60. This can be attributed to the combined effect of lower volume of rubber (lower aspect ratio leads to a smaller tire), higher speed of rotation (due to a smaller outer diameter), and higher magnitude of sidewall deflection in type A40.

4.4.2 Modelled RRc

The following figures show the modelled RRc for the front left tire through the drive cycle tests for the different tires in order of increasing aspect ratio. Numbers above each section show the average RRc in section and the difference to ISO RRc value in parentheses.
It must be noted that the modelled RRc is being compared to the following:

- ISO RRc value (calculated at ISO Test Load and 250 kPa inflation pressure).
- Road RRc (calculated at vehicle load of 5400 N and 280 kPa inflation pressure).

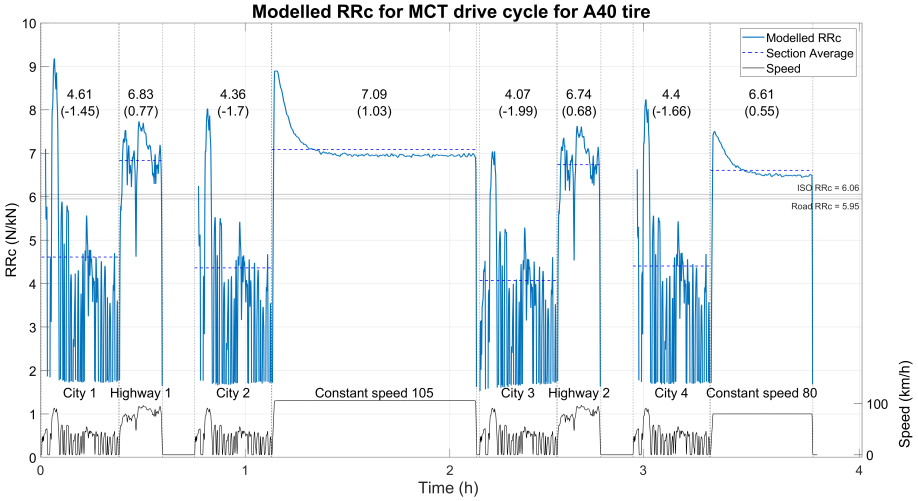

Figure 4.22: Modelled RRc for A40 tire type

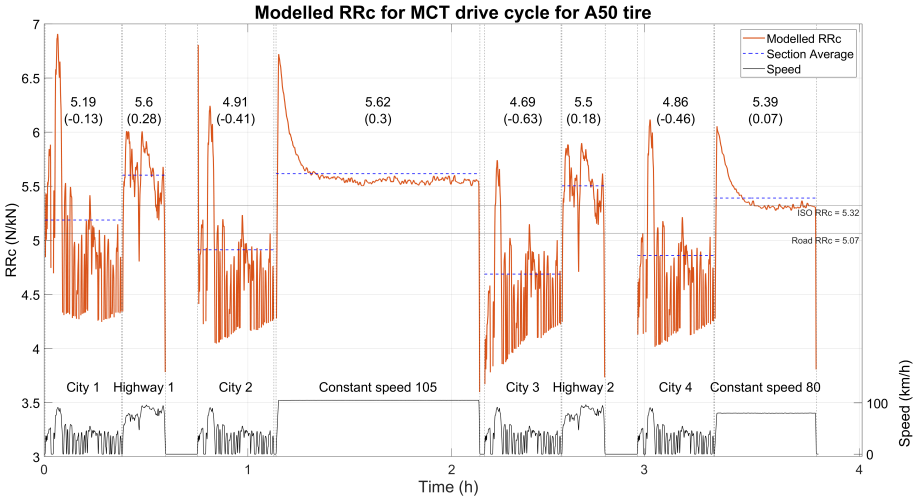

Figure 4.23: Modelled RRc for A50 tire type

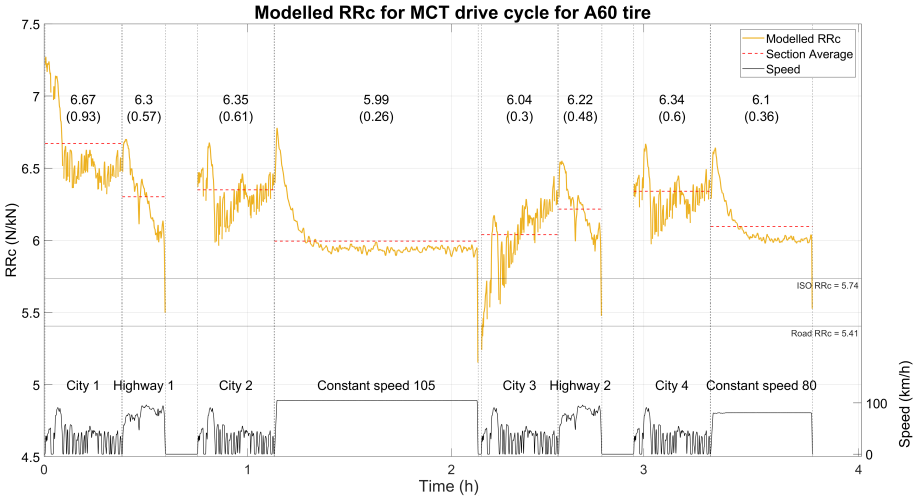

Figure 4.24: Modelled RRc for A60 tire type

Since the RRc is predicted using the Rolling Resistance Model developed in Section 3.3.1, it shows a dependence on both speed and temperature. The RRc is calculated only for speeds above 20 km/h as the model may not be accurate for very low speeds.

4.4.3 Comparison of City Sections

Different city sections in the drive cycle can be compared to understand how the rolling resistance and temperature of tires change with varying initial thermal states. City sections 2 and 3 are chosen for comparison as city section 2 presents a tire that is slightly warmed up after highway section 1 followed by a 5-minute soak, whereas city section 3 presents a tire with a steady state after the 105km/h constant speed section.
The following figures compare the calculated RRc for city section 2 and city section 3 for the different types of tires, in increasing order of aspect ratio.

Tire type A40

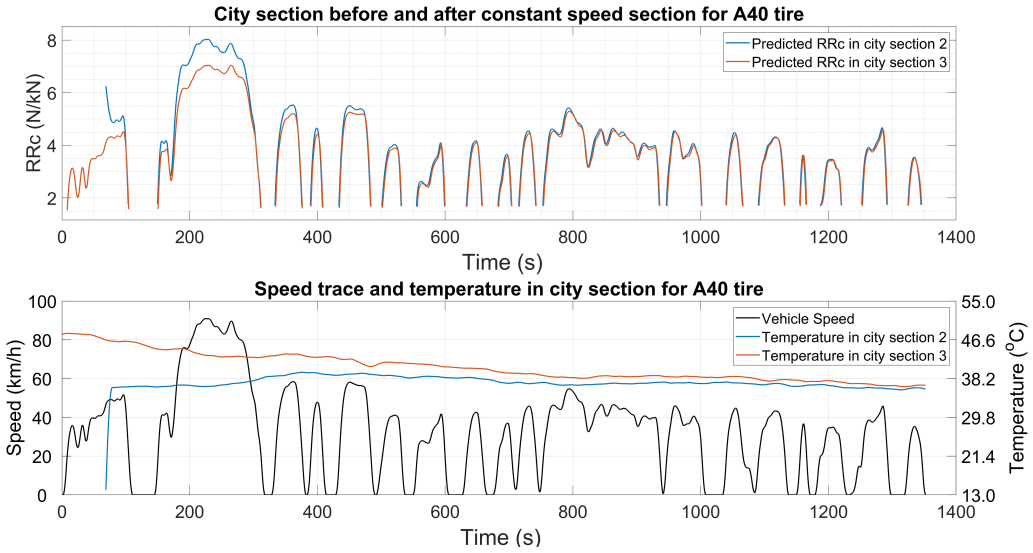

Figure 4.25: Comparison of different city sections, RRc (T) and temperature (B), type A40

Observations for A40:

1. The dependence of RRc on speed and tire temperature is high. In the initial part of the city sections, change in speed and temperature both cause large changes in RRc (approx. 4 N/kN due to 50km/h change and 1 N/kN due to 6°C change).
2. In city section 2, the temperature varies within the cycle, but the final temperature reaches a similar value to the initial temperature. In city section 3, the final temperature is much lower than initial temperature (∼10°C).

Tire type A50

Figure 4.26: Comparison of different city sections, RRc (T) and temperature (B), type A50

Observations for A50:

1. The dependence of RRc on speed and tire temperature is not as high as A40 tire. Variation in RRc due to speed and temperature exists, but the magnitude of change is much lower.
2. In city section 2, the temperature varies within the cycle, but the final temperature reaches a similar value to the initial temperature. In city section 3, the final temperature is much lower than the initial temperature ($\sim$7°C).

Tire type A60

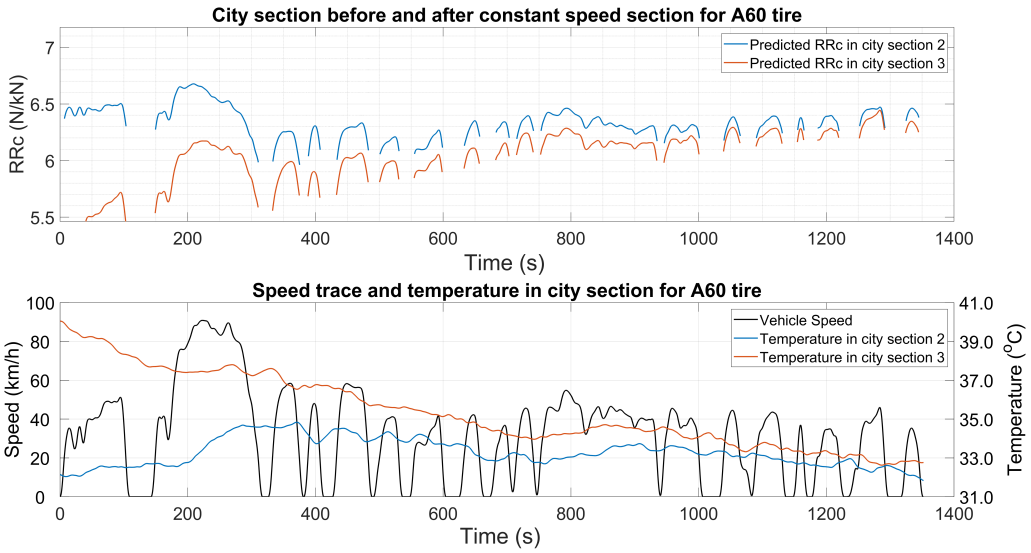

Figure 4.27: Comparison of different city sections, RRc (T) and temperature (B), type A60

Observations for A60:

1. The dependence of RRc on speed and tire temperature is even lower than type A50.
2. In city section 2, the temperature varies within the cycle, but the final temperature reaches a similar value to the initial temperature. In city section 3, the final temperature is lower than the initial temperature (∼5°C).

The figures show that the instantaneous value of RRc is more indicative of the speed, whereas the trend of RRc is more indicative of the temperature. Looking at the behavior of the RRc during the entire section, as the difference in temperatures of the 2 sections reduces towards the end of the section, the difference in RRc also reduces.

4.5 Rolling Resistance Power and Energy Loss

4.5.1 Rolling Resistance Power Loss

The following figures show the difference in modeled and standardized values for A50 tire. The rolling resistance power loss will exhibit speed-dependent behavior, as power depends on speed, irrespective of whether the ISO constant RRc or modeled RRc is used for calculation. However, the rolling resistance power loss calculated from the modeled RRc will have a non-linear dependence on speed, as the power calculated depends on speed directly and on the speed indirectly through the rolling resistance model, as described in Section 3.3.1.

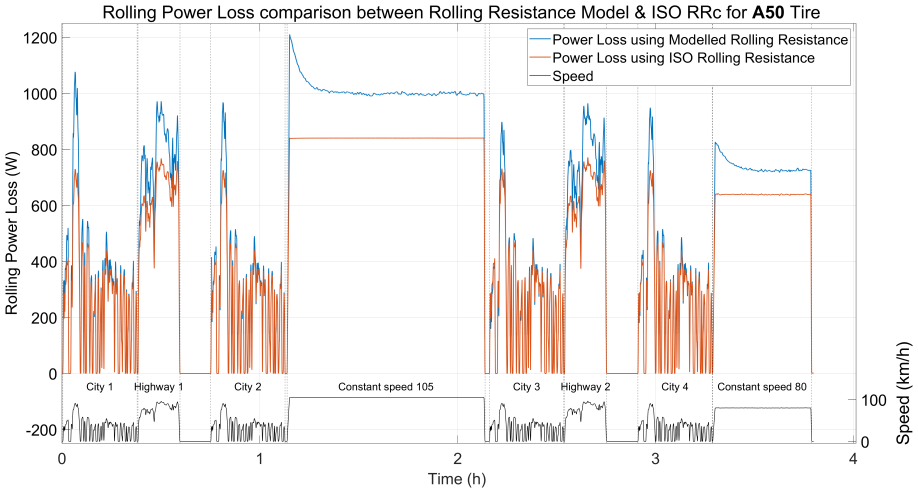

Figure 4.28: Rolling Resistance Power Loss comparison between Rolling Resistance Model and ISO Rolling Resistance

The following figures compare the modelled and measured rolling resistance power loss in different sections for the tire A50.

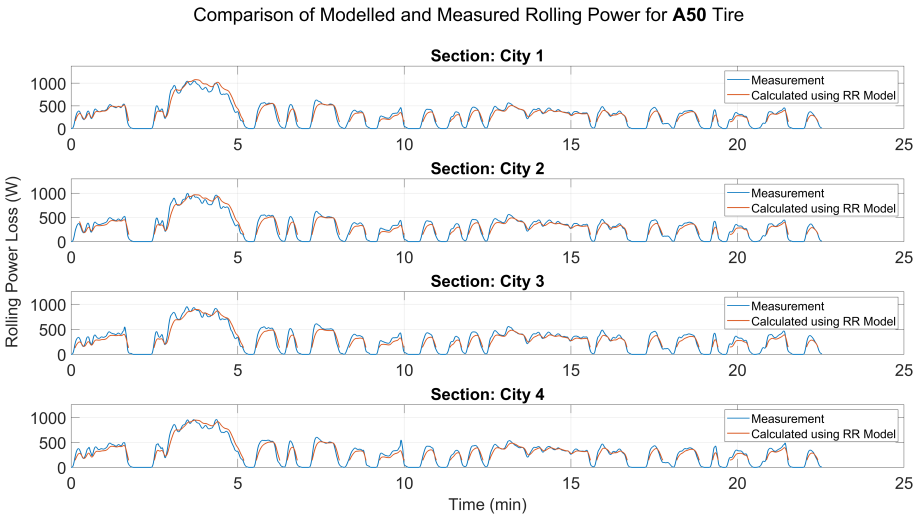

Figure 4.29: Comparison of Modelled and Measured Rolling Power for A50 Tire – Different City Sections

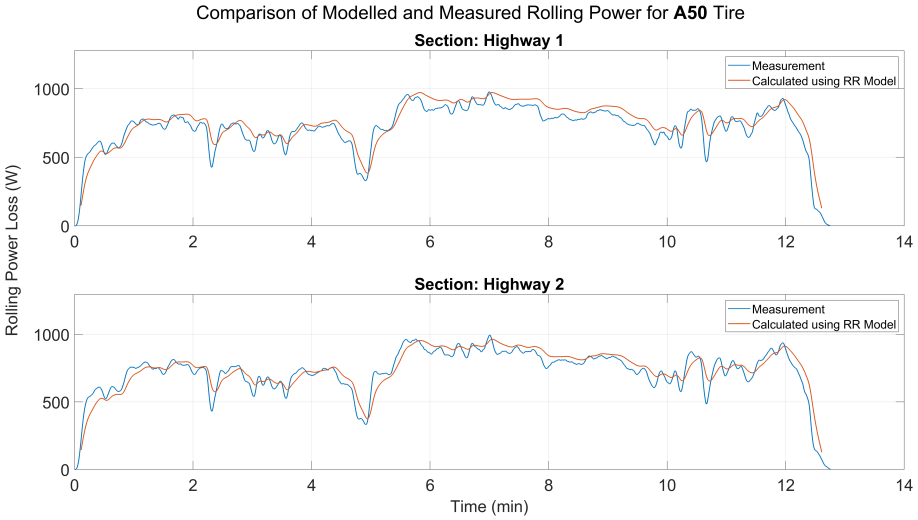

Figure 4.30: Comparison of Modelled and Measured Rolling Power for A50 Tire – Different Highway Sections

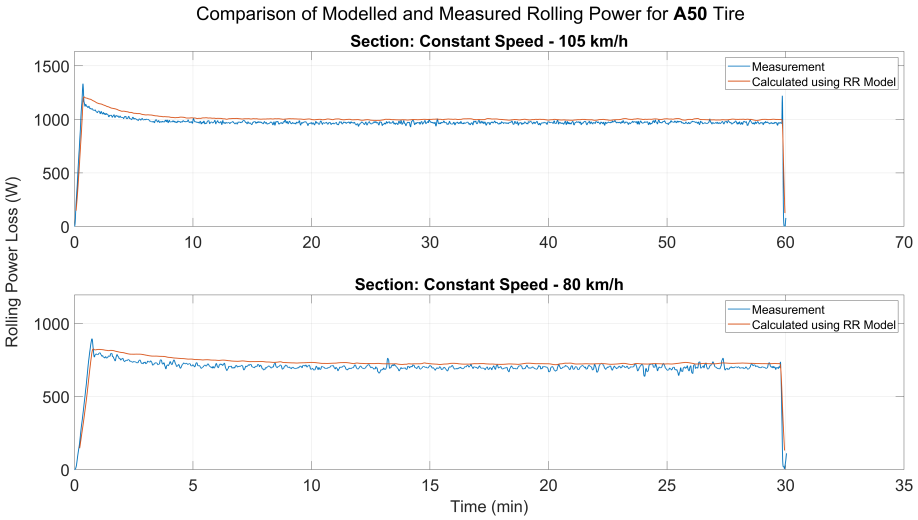

Figure 4.31: Comparison of Modelled and Measured Rolling Power for A50 Tire – Constant Speed Sections

The following table shows the section-wise mean percentage error between the modelled and measured rolling power losses for all tires.

Table 4.3: Mean Percentage Error between Modelled & Measured Rolling Loss Power for All Tires

Tire	Mean Percentage Error (%)		
	City Sections	Highway Sections	Constant Speed Sections
A40	35.5	20.3	21.1
A50	16.9	9.3	9.5
A60	20.3	15.3	12.8

4.5.2 Rolling Resistance Energy Loss

The energy loss due to the isolated effect of rolling resistance using the Rolling Resistance Model and the constant ISO rolling resistance is calculated and plotted in the figure below.

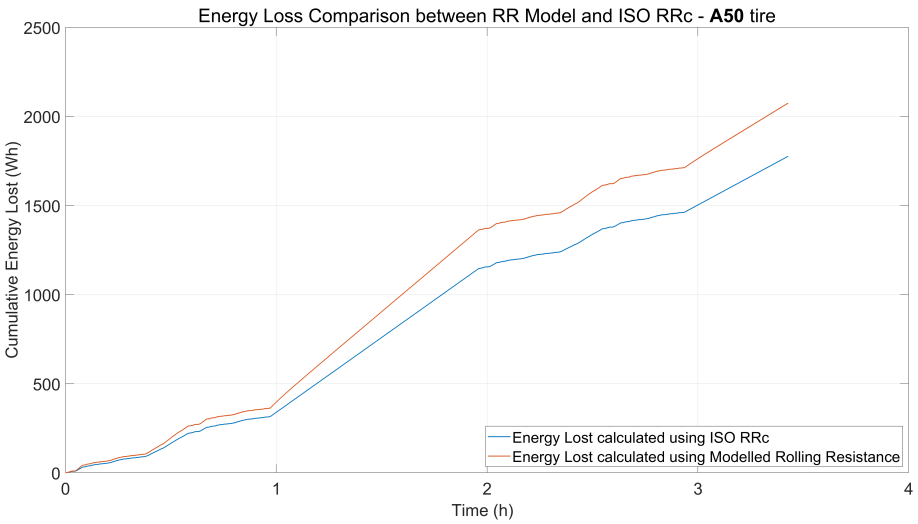

Figure 4.32: Energy Loss Comparison between RR model and Constant ISO RRc– A50 tire

Referring to Figures 4.33-4.35 below, the City 1 section exhibits the highest predicted rolling resistance energy loss because the tires start at ambient temperature (∼23°C), as shown in Figure 4.21. As the tire warms up, the rolling resistance decreases, subsequently reducing the rolling resistance energy loss. This trend can be observed in all the other city sections, with the lowest rolling resistance energy loss occurring in City 3 section. This section comes after the Constant Speed at 105 km/h section, at the end of which the tire has reached thermal equilibrium. This trend of lowest rolling resistance energy loss calculated by the Rolling Resistance Model in the City 3 section and highest in the City 1 section can be observed across all tires.

Another observation, particularly for A40 tire, is that the rolling resistance energy loss from the Rolling Resistance Model is similar to the ISO constant loss in City 1 section. The Rolling Resistance Model predicts lower losses than the ISO constant calculation in the subsequent city sections. This is because the A40 tire shows a high speed dependence and the lower speeds in the city section lead to a lower calculated rolling resistance.

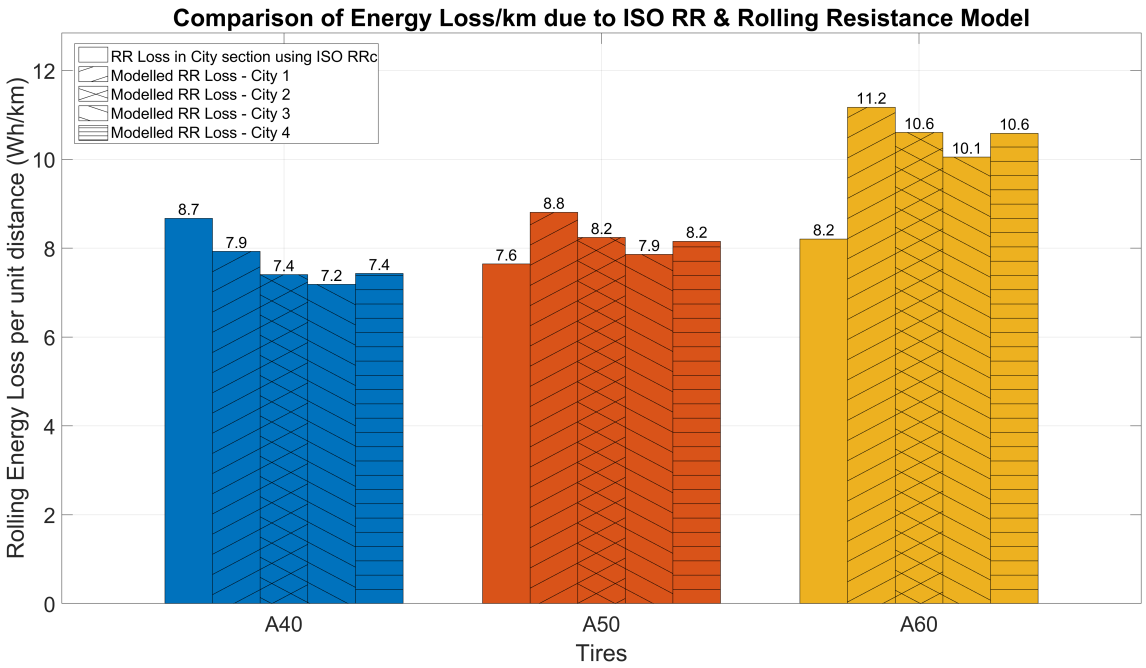

Figure 4.33: ISO Constant and Rolling Resistance Modelled Energy Loss Comparison for City Sections

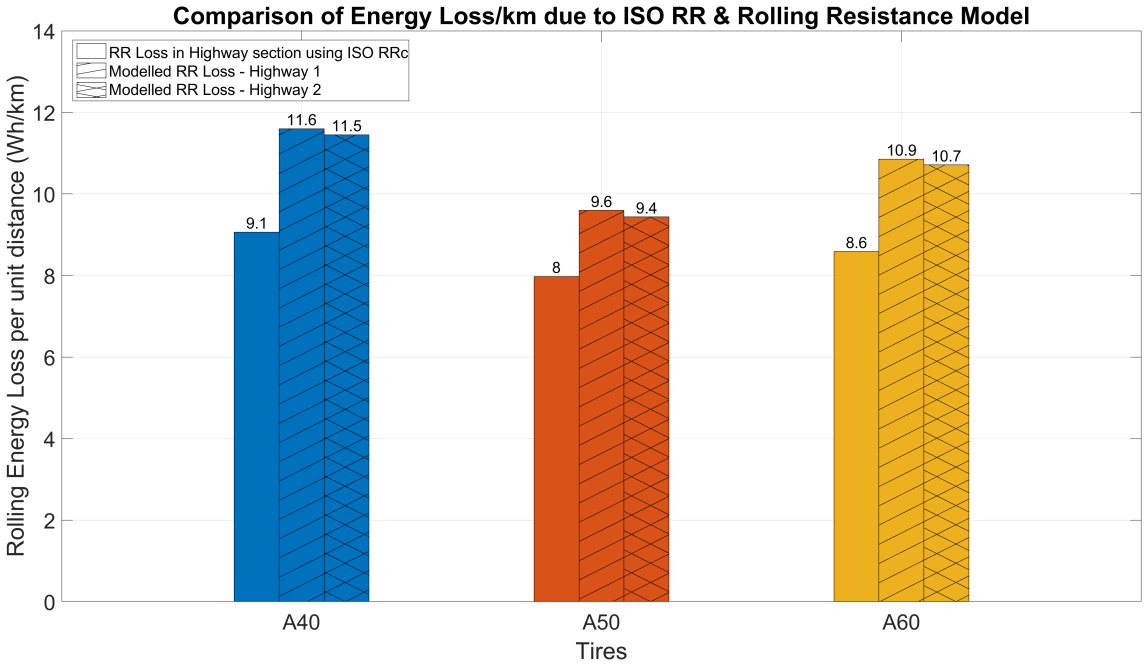

Figure 4.34: ISO Constant and Rolling Resistance Modelled Energy Loss Comparison for Highway Sections

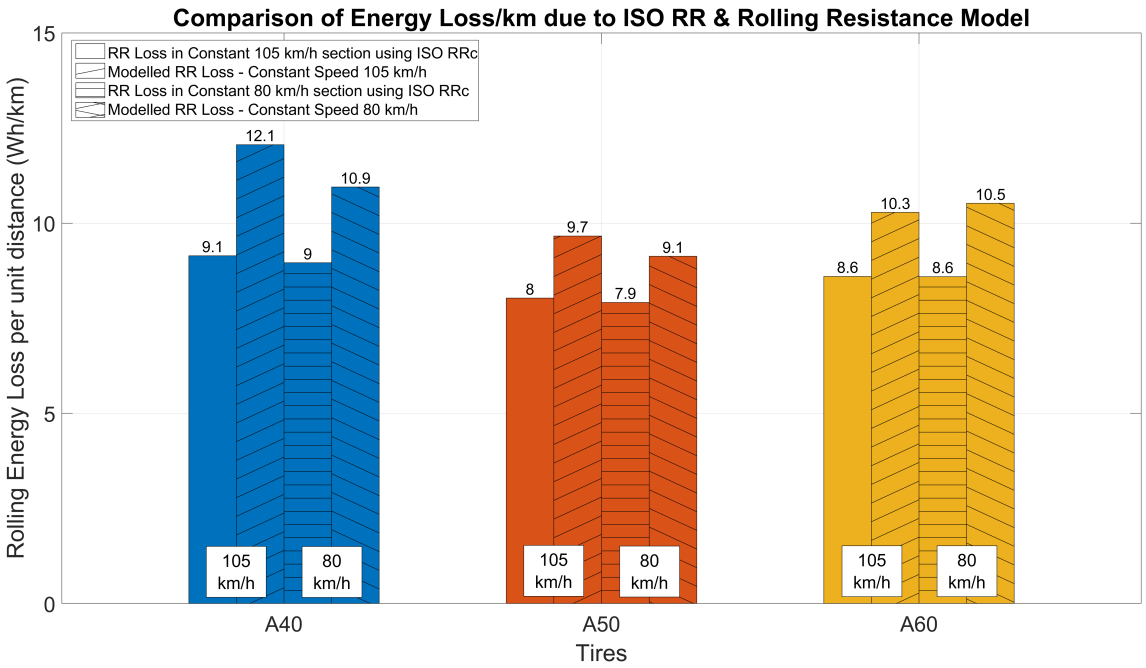

Figure 4.35: ISO Constant and Rolling Resistance Modelled Energy Loss Comparison for Constant Speed Sections

A less dramatic yet significant comparison arises in the highway and constant speed sections, where the Rolling Resistance Model consistently predicts higher rolling resistance energy loss than the ISO rolling resistance-based energy consumption. This difference is caused by the varying speeds, which subsequently affect the tire temperatures and is a fundamental limitation of the ISO standard rolling resistance test.

Figures 4.33-4.35 above show the energy loss of different tires in different sections. In a way, the 3 separate bar graphs highlight the findings of the thesis work. The section-wise percentage difference in rolling resistance energy loss from ISO Constant to Rolling Resistance Model is summarized in Tables 4.4 & 4.5 below.

The percentage difference being negative denotes that the rolling energy loss calculated from the ISO constant is more than that being calculated by the rolling resistance model.

Table 4.4: Comparison between ISO Constant & Modelled Rolling Resistance Energy Loss in City Sections

Tire	Section-wise % Difference between Rolling Energy Losses			
	City 1	City 2	City 3	City 4
A40	-8.6%	-14.6%	-17.0%	-14.1%
A50	15.2%	7.7%	2.9%	7.2%
A60	36.1%	29.3%	22.6%	29.1%

Table 4.5: Comparison between ISO Constant & Modelled RR Energy Loss in Highway and Constant Speed (CS) Sections

Tire	Section-wise % Difference between Rolling Energy Losses			
	Highway 1	**Highway 2**	**CS 105**	**CS 80**
A40	28.0%	26.3%	31.9%	22.2%
A50	20.3%	18.3%	20.3%	15.3%
A60	26.4%	24.7%	19.5%	22.4%

5
Discussion

5.1 Transient Behavior of Rolling Resistance

As the tire warms up, an increase in temperature leads to a decrease in RRf and RRc. This effect was present for all tire (in different amounts). Since the rolling resistance is higher when a tire is being warmed, the vehicle experiences a higher resistance before the tire reaches working temperature. When compared to the ISO RRc, the actual resistance and loss will be higher. This is captured by Figure 4.8. The temperature change during warmup and its effect on the rolling resistance varies between tires. Tire A40 heats up much faster and reaches a higher temperature compared to the other two tires. This is followed by type A50 and then A60. A faster rate of heating leads to a higher change in RRc. When compared to the ISO RRc value no tire matches the value initially. However, as the tires warm up, they reach the ISO RRc and even show a lower value as the temperature increases further.

5.2 Transient Behavior of Parasitic Losses

The parasitic losses in the tire rolling resistance measurement rig reduce as the tire warms up to the steady state temperature, as demonstrated in Figure 4.11. The parasitic losses are relatively higher when the tire is being warmed up than at a steady state, which means that the actual value of rolling resistance during tire warmup will be slightly lower than what is obtained if using the parasitic losses obtained at a steady state.

Interestingly, the impact of warmup of parasitic losses varies across different tires, which could be caused by diverse underlying factors. In an ideal case, the parasitic losses would be found with just enough load on the tire to turn it with no slip to keep the tire deformation to a minimum. However, limitations in our measurement and testing equipment mean that such a low load cannot be applied on the tires. A solution would be to make a series of skim test measurements and extrapolate to zero load.

One important factor in this analysis could be the tire's aspect ratio, which affects the temperature evolution on the tire's inner lining, which, in turn, affects how quickly a steady state is achieved.

In this thesis work, we have identified the phenomenon but did not have enough

data from required test conditions to analyze and reach a conclusion as to what influences parasitic loss during warmup. Hence, we have not included the effect of the parasitic losses in any of the models developed. We are of the impression that more research must be done on the same to establish a relation between the tires and the transient effect of parasitic losses and to understand if the transient behavior is a tire related phenomenon or is dependent on the measurement/testing equipment.

5.3 Rolling Resistance Power and Energy Loss

The estimation of the energy and power loss due to rolling resistance forms a major part of this thesis work. As shown in Figure 4.28 and summarized in Table 4.4 & Table 4.5, the rolling resistance loss for tire A50 from the calculated rolling resistance is higher almost through the entire cycle.

While this increased energy loss is accounted for official range certifications (the vehicle runs on a test rig as described in Section 3.4.2 and the tires experience the warmup and cooldown), the estimation of range done real-time in a vehicle can be improved by accounting for the increased losses. The models developed in thesis work can be used as the basis to develop a more robust model to include the different environmental and operational conditions and predict the rolling resistance and temperature of the tire.

Looking at the section wise differences in energy loss, one key observation is that the A50 tire exhibits the least overall deviation from the energy loss using ISO constant RRc. A possible reason for the same could be that tire A50 is the only tire amongst the 3 tires tested that is used for the recommended vehicle type. Tire A40 is recommended for a smaller vehicle and is hence rated for a lower load than the vehicle load in this thesis (5400N), while tire A60 is for a larger vehicle and rated for a much higher load.

Even though we have established that the steady state rolling resistance is not dependent on the load (in the range of loads tested), the warmup of the tire is still dependent on the load. As most of the driving in the drive cycle takes place with changes in speed, a steady state temperature is not reached, and hence the steady state rolling resistance value is not achieved.

Knowledge of the power and energy loss in the tire can be useful in selecting the best tire for a particular application. Given a vehicle type, a factor influencing the selection of tires could be the energy loss.

Table 5.1: Comparison Section-wise Rolling Resistance Energy Loss between all tires

Tire	City Section Average (Wh/km)	Highway Sections Average (Wh/km)	Average Overall Loss (Wh/km)	Rolling Loss as per ISO RRc (Wh/km)	Difference from RR Model Loss to ISO Loss (%)
A40	7.5	11.6	9.5	8.9	6%
A50	8.3	9.5	8.9	7.8	12%
A60	10.6	10.8	10.7	8.4	22%

The table shows the average overall loss and the difference in the ISO loss. Taking the tires in the thesis work as an example, tire A40 performs well in the city sections and deviates the least from the ISO loss but the overall energy loss is higher than A50. For the tires tested and the vehicle used in the testing, it can be concluded that tire A50 has the least energy loss over a drive cycle.

6
Conclusion

This thesis work investigated the warmup behavior of geometrically different tires along with the effect of different operating parameters such as normal load, inflation pressure and speed. All the tires tested were found to have an initially high value of rolling resistance that reduced as the tire warmed up before reaching a steady state value during constant speed testing. The change in rolling resistance coefficient during warmup was then modelled and important parameters were identified.

From the first phase of testing (at constant speed), and the subsequent modelling phase, it can be concluded that the tires have 30-40% higher rolling resistance force at the start compared to when fully warmed up and hence have the corresponding increased energy loss. This validates the initial assumption that the accuracy of the energy consumption (and by extension, range) calculated using steady state ISO rolling resistance value can be improved by using a dynamic model of rolling resistance.

The Rolling Resistance Model developed can simulate the rolling resistance, incorporating the influence of variations in speed, inflation pressure and tire temperature. The model developed in this thesis is within the measurement uncertainty of the torque sensor on the drum rig (± 0.9 N). The Thermal Model developed was found to have some limitations due to the testing environment but can simulate the instantaneous temperature of the tire given the rolling resistance force and speed to an error of only ± 2°C.

The rolling resistance and the thermal model were then combined to form a physical model of the tire capable of predicting the instantaneous rolling resistance and temperature with only the speed as the input. Despite the limitations in the constituent models, the combined model can predict the temperature to an error of ± 2°C and the rolling resistance to an error of ± 5 N for a single tire.

The drive cycle tests at the dynamometer can be used to understand the behavior of the tires in a dynamic scenario that resembles real-life driving. Figures 4.33-4.35 shows the energy loss of each tire in each section, compared to the energy loss due to ISO Rolling Resistance.

Referring to Table 5.1, it can be observed that there is a discrepancy between the rolling energy loss calculated by the rolling resistance model and using the ISO rolling resistance coefficient, which can vary from 6 to 22% and can be attributed to

what the tires are optimized for. A40 tire performed better in the city sections (than its expected ISO RRc rolling loss) and had the least overall deviation; however, it is the A50 tire that has the least overall loss.

The findings in this thesis show that the tire's temperature (and hence its warmup) affects the rolling resistance. Using the ISO Rolling Resistance value obtained after the tire has reached a steady state, the additional contribution of the warmup region to rolling resistance loss is ignored, and as a result, the overall range can be overestimated. In terms of the tires, each tire performs differently in each section and the best tire for the vehicle must be chosen to minimize the overall energy loss due to rolling resistance. These types of insights can be obtained from the model, which can be used to understand better how various tires are affected by warmup and can help make better design choices.

7

Recommendations for Future Work

Different types of tires (all season, winter) can be tested to verify if the observations made in thesis work hold true for other types of tires as well. Tires with different geometry (different rim diameter, section widths) can also be tested to understand the influence of other geometric factors. Following are some possible more work that can be done in the specific sections of this thesis work:

7.1 Rolling Resistance Testing on Drum Rig

More tests can be run at both higher and lower speeds as well as loads to understand the influence of extreme cases. It is noted in previous research that high speeds (>130km/h) lead to a large increase in rolling resistance. Similarly, low speeds may not allow the tire to build up any temperature and remain as a 'cold tire' thermally. Low loads are unlikely in actual usage but can be possible due to use of tires of incorrect specification. Higher loads are more likely as users can overload the vehicle.

7.2 Modeling

7.2.1 Rolling Resistance Model

The functionality of the rolling resistance model can be improved by including either a load dependent scaling factor for the rolling resistance or by parametrizing the model at different loads and using different fitted parameters for different loads. The effect of load greater than the parameterization load in predicting the rolling resistance is highlighted in Appendix A.2.4. The same has been noted by those working on similar models. If enough data is obtained from testing torque loaded tires, the effect can be quantified and included in the model using the steps highlighted in Section 3.3.1.

7.2.2 Thermal Model

In this thesis work, the evolution and effect of inflation gas temperature has been ignored since the measurement of the inflation gas temperature is not reliable. Using the measured inflation gas temperature, the heat transfer coefficient from the tire to

the gas can be calculated and the model can be made more accurate. The observation that $T_{amb} = T_{road}$ was made in the dynamometer rig, was included in the model. However, this is not representative of real world conditions, and the temperature measurements of ambient and road can be used to improve the model.

7.3 Drive Cycle Tests

More drive cycle tests can be conducted to further validate the combined model as well as to analyse the performance of different tires in different types of test sections.

Bibliography

[1] U.S. Department of Energy and U.S. Environmental Protection Agency, *Where the Energy Goes: Electric Cars*. [Online]. Available: https://www.fueleconomy.gov/feg/atv-ev.shtml.

[2] *ISO 28580:2009(en) Passenger car, truck and bus tyres — Methods of measuring rolling resistance — Single point test and correlation of measurement results*. [Online]. Available: https://www.iso.org/standard/44770.html.

[3] D. J. Schuring, "Transient Versus Steady-State Tire Rolling Loss Testing," en, Feb. 1979, p. 790116. DOI: 10.4271/790116. [Online]. Available: https://www.sae.org/content/790116/ (visited on 01/22/2024).

[4] M. Greiner, H.-J. Unrau, and F. Gauterin, "A model for prediction of the transient rolling resistance of tyres based on inner-liner temperatures," en, *Vehicle System Dynamics*, vol. 56, no. 1, pp. 78–94, Jan. 2018, ISSN: 0042-3114, 1744-5159. DOI: 10.1080/00423114.2017.1343955. [Online]. Available: https://www.tandfonline.com/doi/full/10.1080/00423114.2017.1343955 (visited on 01/25/2024).

[5] L. Ydrefors, M. Hjort, S. Kharrazi, J. Jerrelind, and A. Stensson Trigell, "Rolling resistance and its relation to operating conditions: A literature review," en, *Proceedings of the Institution of Mechanical Engineers, Part D: Journal of Automobile Engineering*, vol. 235, no. 12, pp. 2931–2948, Oct. 2021, ISSN: 0954-4070, 2041-2991. DOI: 10.1177/09544070211011089. [Online]. Available: http://journals.sagepub.com/doi/10.1177/09544070211011089 (visited on 01/14/2024).

[6] J. Hyttinen, M. Ussner, R. Österlöf, J. Jerrelind, and L. Drugge, "Truck tyre transient rolling resistance and temperature at varying vehicle velocities - Measurements and simulations," en, *Polymer Testing*, vol. 122, p. 108004, May 2023, ISSN: 01429418. DOI: 10.1016/j.polymertesting.2023.108004. [Online]. Available: https://linkinghub.elsevier.com/retrieve/pii/S0142941823000843 (visited on 01/14/2024).

[7] C. Rajopadhye and B. Govardhan Raju, "Influence of inflation pressure, speed, load and warm-up phase on rolling resistance of passenger car tyres," M.S. thesis, Chalmers University of Technology, Göteborg, Sweden, 2021.

[8] C. Holloway and IZZE Racing, "Influence of Temperature on Tire Grip," White Paper.

[9] T. Vieira, U. Sandberg, and S. Erlingsson, "Rolling Resistance Evaluation of Winter Tires on In-Service Road Surfaces," en, *Tire Science and Technology*, vol. 49, no. 2, pp. 78–103, Apr. 2021, ISSN: 1945-5852, 0090-8657. DOI: 10.2346/tire.20.190225. [Online]. Available: https://meridian.allenpress.

com/tst/article/49/2/78/447981/Rolling-Resistance-Evaluation-of-Winter-Tires-on (visited on 01/22/2024).

[10] J. Ejsmont, S. Taryma, G. Ronowski, and B. Swieczko-Zurek, "Influence of load and inflation pressure on the tyre rolling resistance," en, *International Journal of Automotive Technology*, vol. 17, no. 2, pp. 237–244, Apr. 2016, ISSN: 1229-9138, 1976-3832. DOI: 10.1007/s12239-016-0023-z. [Online]. Available: http://link.springer.com/10.1007/s12239-016-0023-z (visited on 04/03/2024).

[11] D. J. Schuring, J. F. Siegfried, and G. L. Hall, "Transient Speed and Temperature Effects on Rolling Loss of Passenger Car Tires," *SAE Transactions*, vol. 94, pp. 515–523, 1985, ISSN: 0096-736X. [Online]. Available: https://www.jstor.org/stable/44721587 (visited on 03/25/2024).

[12] B. M. Redrouthu and S. Das, "Tyre modelling for rolling resistance," en,

[13] A. Tevell and O. Zetterberg, "Creating a Virtual Tyre Temperature Sensor," en,

[14] J. Hyttinen, M. Ussner, R. Österlöf, J. Jerrelind, and L. Drugge, "Effect of Ambient and Tyre Temperature on Truck Tyre Rolling Resistance," en, *International Journal of Automotive Technology*, vol. 23, no. 6, pp. 1651–1661, Dec. 2022, ISSN: 1229-9138, 1976-3832. DOI: 10.1007/s12239-022-0143-6. [Online]. Available: https://link.springer.com/10.1007/s12239-022-0143-6 (visited on 01/23/2024).

[15] *C.1717 - Grip*. [Online]. Available: https://the-contact-patch.com/book/road/c1717-grip.

[16] Michelin, *The Tyre: Rolling Resistance and Fuel Savings*, 2003.

[17] P. S. Pillai and G. S. Fielding-Russell, "Effect of Aspect Ratio on Tire Rolling Resistance," en, *Rubber Chemistry and Technology*, vol. 64, no. 4, pp. 641–647, Sep. 1991, ISSN: 1943-4804, 0035-9475. DOI: 10.5254/1.3538579. [Online]. Available: https://meridian.allenpress.com/rct/article/64/4/641/91407/Effect-of-Aspect-Ratio-on-Tire-Rolling-Resistance (visited on 05/31/2024).

[18] P. S. Grover, "Modeling of Rolling Resistance Test Data," *SAE Transactions*, vol. 107, pp. 497–506, 1998, ISSN: 0096-736X. [Online]. Available: https://www.jstor.org/stable/44740977 (visited on 05/31/2024).

[19] D. E. Hall and J. C. Moreland, "Fundamentals of Rolling Resistance," en, *Rubber Chemistry and Technology*, vol. 74, no. 3, pp. 525–539, Jul. 2001, ISSN: 1943-4804, 0035-9475. DOI: 10.5254/1.3547650. [Online]. Available: https://meridian.allenpress.com/rct/article/74/3/525/92181/Fundamentals-of-Rolling-Resistance (visited on 01/18/2024).

[20] T. LaClair, "Rolling Resistance," *The Pneumatic Tire*, pp. 475–529,

[21] K. Yokota, E. Higuchi, and M. Kitagawa, "Estimation of Tire Temperature Distribution and Rolling Resistance under Running Conditions Including Environmental Factors," en, Apr. 2012, pp. 2012–01–0796. DOI: 10.4271/2012-01-0796. [Online]. Available: https://www.sae.org/content/2012-01-0796/ (visited on 04/18/2024).

[22] D. J. Schuring, "The Rolling Loss of Pneumatic Tires," en, *Rubber Chemistry and Technology*, vol. 53, no. 3, pp. 600–727, Jul. 1980, ISSN: 1943-4804, 0035-

9475. DOI: 10.5254/1.3535054. [Online]. Available: https://meridian.allenpress.com/rct/article/53/3/600/91289/The-Rolling-Loss-of-Pneumatic-Tires (visited on 05/31/2024).

[23] U. Sandberg, U. Hammarström, M. Haider, *et al.*, "Rolling resistance: Basic information and state-of-the-art on measurement methods," 2011, Publisher: Statens väg-och transportforskningsinstitut.

[24] MTS Systems, *Light Truck & Racing Tire Testing*. [Online]. Available: https://www.mts.com/en/articles/automotive/flat-trac-tire.

[25] Gdansk Tech, *Mobile Set for Rolling Resistance Measurements "R2 mk.2"*. [Online]. Available: https://wimio.pg.edu.pl/en/imikm-en/section-mvmt/activity/research.

[26] A. Ficht and M. Lienkamp, "Rolling resistance modeling for electric vehicle consumption," en, in *6th International Munich Chassis Symposium 2015*, P. Pfeffer, Ed., Series Title: Proceedings, Wiesbaden: Springer Fachmedien Wiesbaden, 2015, pp. 775–798, ISBN: 978-3-658-09710-3 978-3-658-09711-0. DOI: 10.1007/978-3-658-09711-0_49. [Online]. Available: https://link.springer.com/10.1007/978-3-658-09711-0_49 (visited on 01/23/2024).

[27] IZZE Racing, *Tire Temperature and Pressure Monitoring System - Datasheet*. [Online]. Available: https://www.izzeracing.com/products/ewExternalFiles/Izze_TTPMS_V2_Datasheet.pdf.

[28] M. L. Janssen and G. L. Hall, "Effect of Ambient Temperature on Radial Tire Rolling Resistance," en, Feb. 1980, p. 800 090. DOI: 10.4271/800090. [Online]. Available: https://www.sae.org/content/800090/ (visited on 01/22/2024).

[29] D. P. Kelly and R. S. Sharp, "Time-optimal control of the race car: Influence of a thermodynamic tyre model," en, *Vehicle System Dynamics*, vol. 50, no. 4, pp. 641–662, Apr. 2012, ISSN: 0042-3114, 1744-5159. DOI: 10.1080/00423114.2011.622406. [Online]. Available: http://www.tandfonline.com/doi/abs/10.1080/00423114.2011.622406 (visited on 01/25/2024).

[30] Mathworks, *Mldivide MATLAB documentation*. [Online]. Available: https://se.mathworks.com/help/matlab/ref/mldivide.html#bt4jslc-6.

[31] SAE International, *SAE J1634: Battery Electric Vehicle Energy Consumption and Range Test Procedure*.

A

Appendix A: Additional Figures

A.1 Load Sweep at Different Pressures

The load sweep is carried out at different inflation pressures and plotted below:

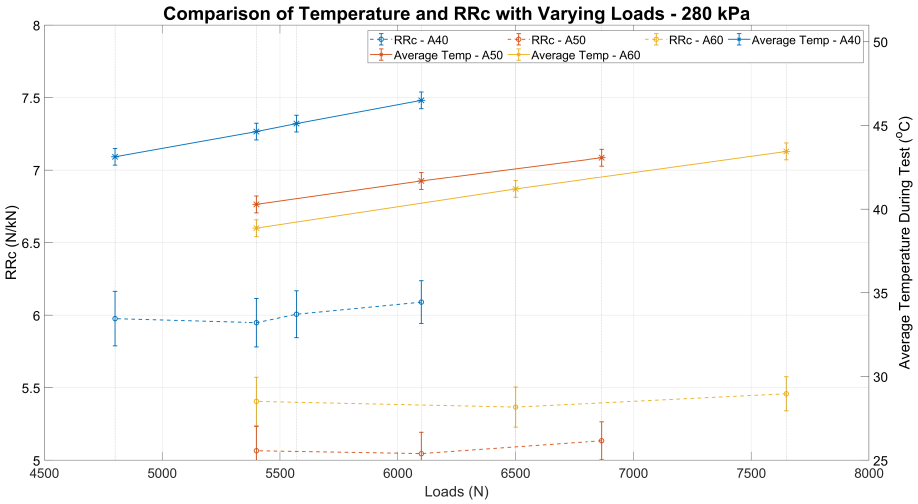

Figure A.1: Comparison of temperature and RRc for varying loads at 280 kPa inflation pressure

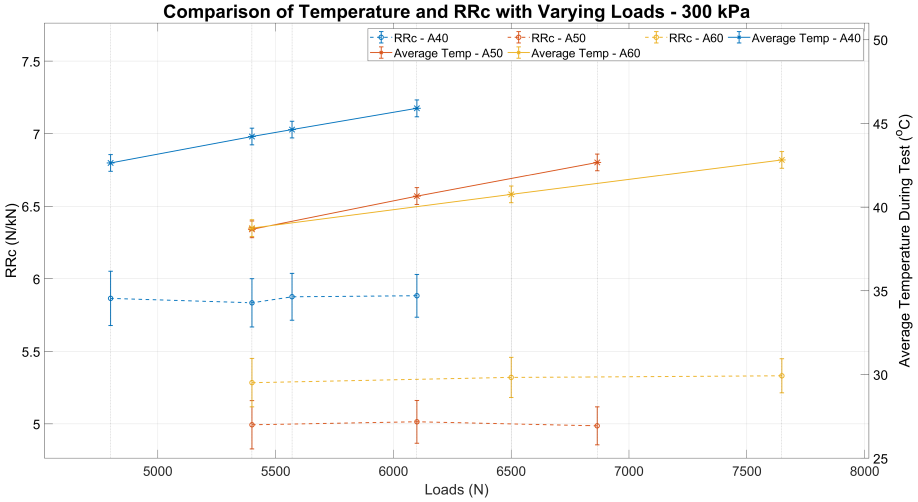

Figure A.2: Comparison of temperature and RRc for varying loads at 300 kPa inflation pressure

A.2 Results of the rolling resistance model for various inflation pressures, loads and speeds

This section has some figures of the results of the rolling resistance model along with the errors. The spikes in the predictions can be attributed to corresponding spikes in the measured temperature data.

A.2.1 Operating pressure lower than parameterization pressure

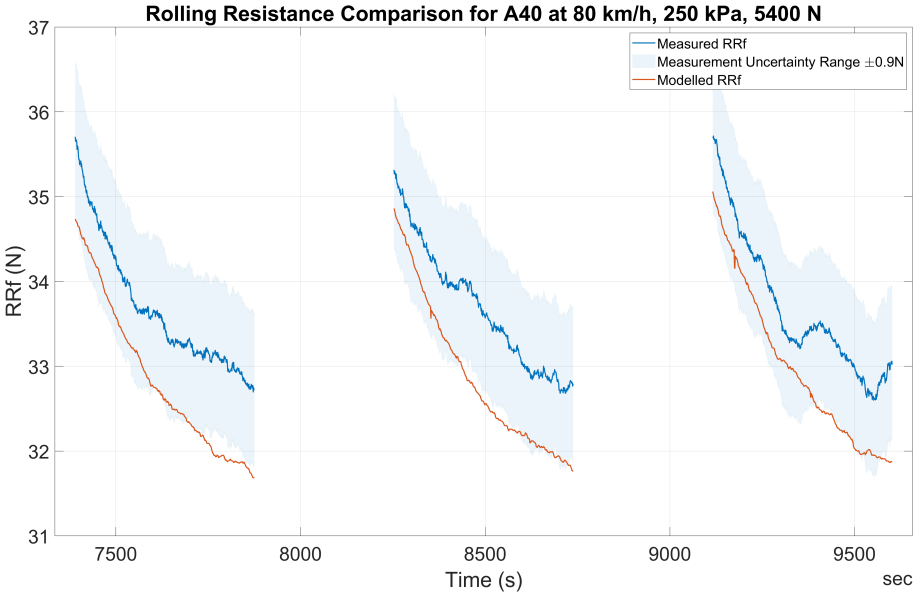

Figure A.3: Measured and modelled RRf at lower pressure than parametrization pressure

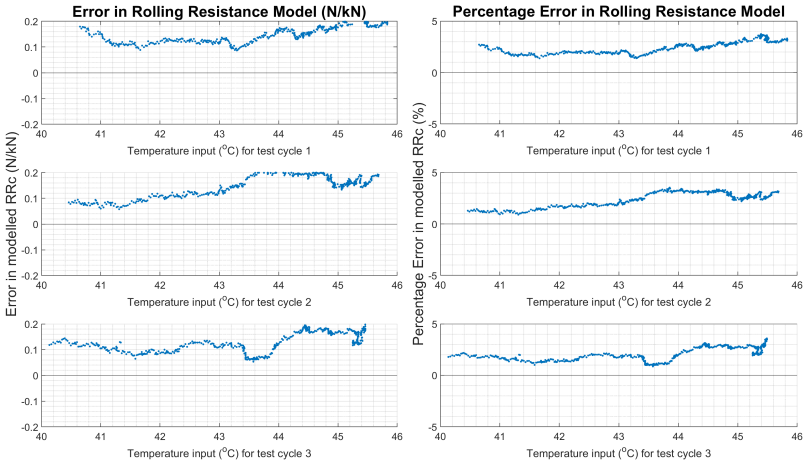

Figure A.4: (L) Error in Modelled RRf (N/kN); (R) Percentage Error in modelled RRf

A.2.2 Operating pressure higher than parametrization pressure

The following figure shows the modelled rolling resistance for an inflation pressure of 300 kPa which is the higher than the inflation pressure used in the parametrization.

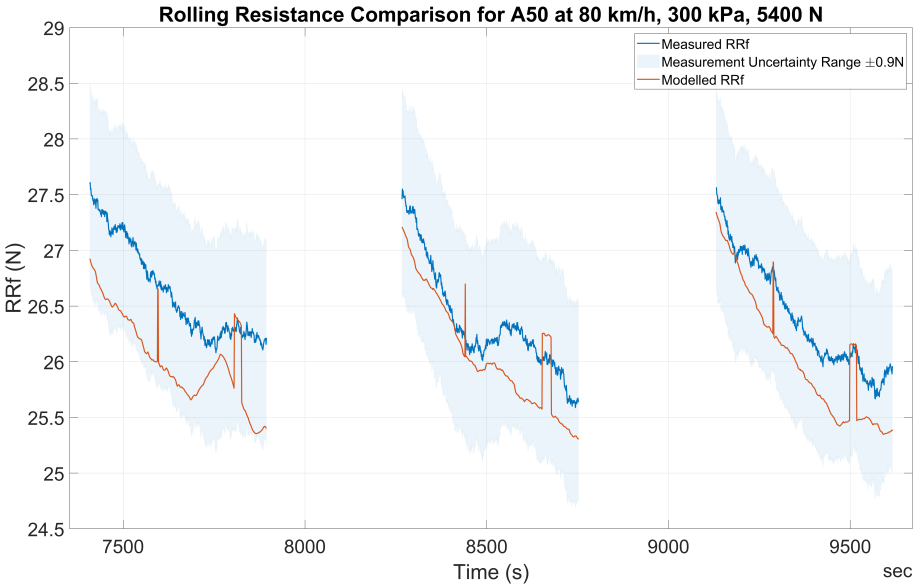

Figure A.5: Measured and modelled RRf at higher pressure than parametrization pressure

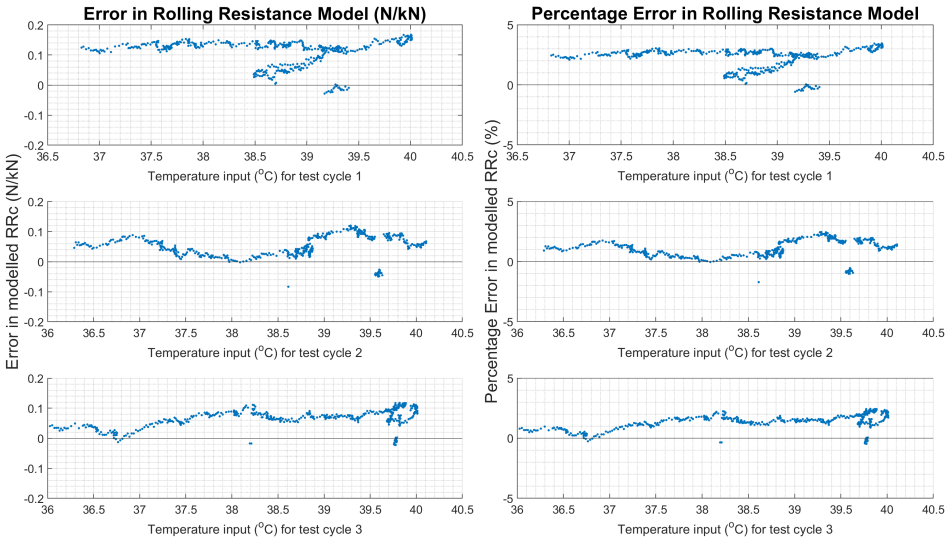

Figure A.6: (L) Error in Modelled RRf (N/kN); (R) Percentage Error in modelled RRf

A.2.3 Operating speed higher than parametrization speed

The following figure shows the modelled rolling resistance for a speed of 120km/h which is the higher speed used in the parametrization.

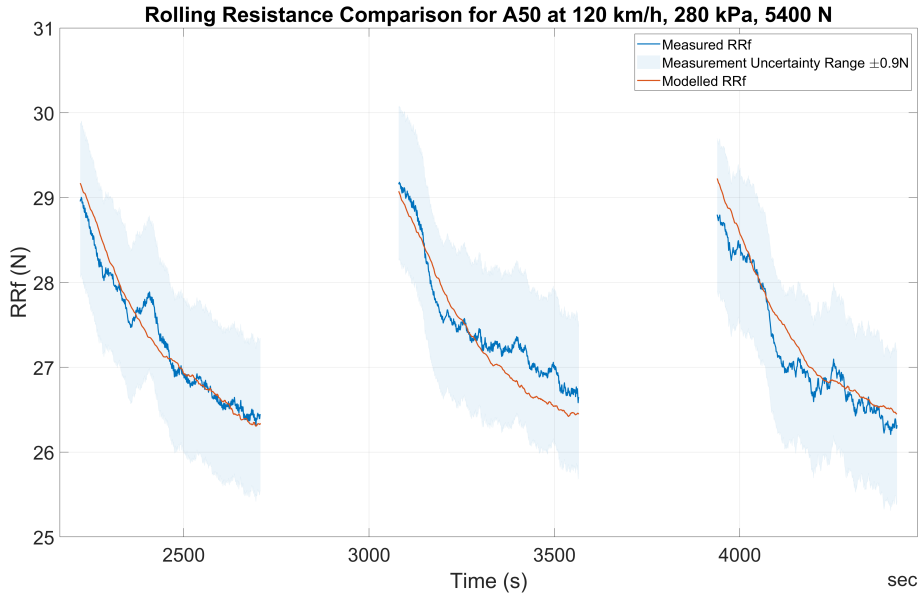

Figure A.7: Measured and modelled RRf at higher speed than parametrization speed

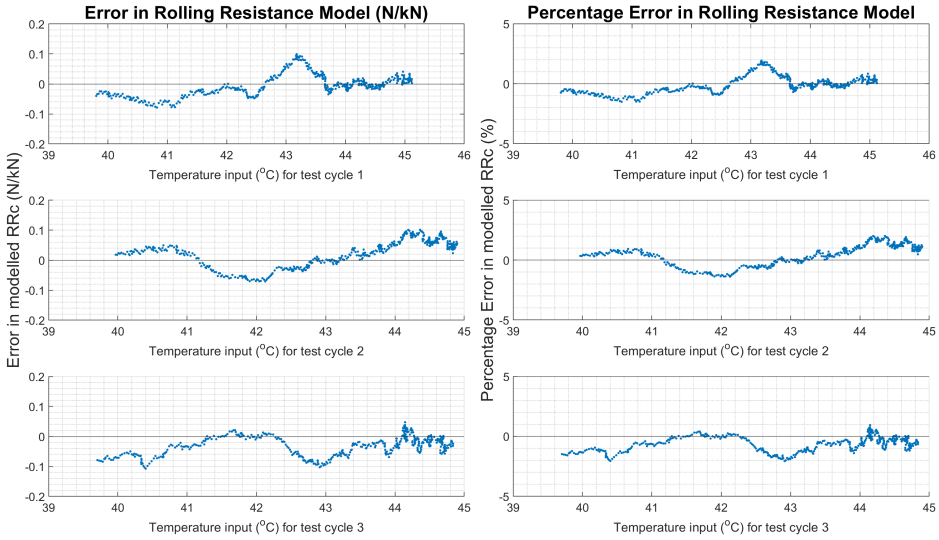

Figure A.8: (L) Error in Modelled RRf (N/kN); (R) Percentage Error in modelled RRf

A.2.4 Operating load higher than parametrized load

The following figure shows the predicted rolling resistance for an operating load of 6865N which is higher than the parameterization load of 5400N.

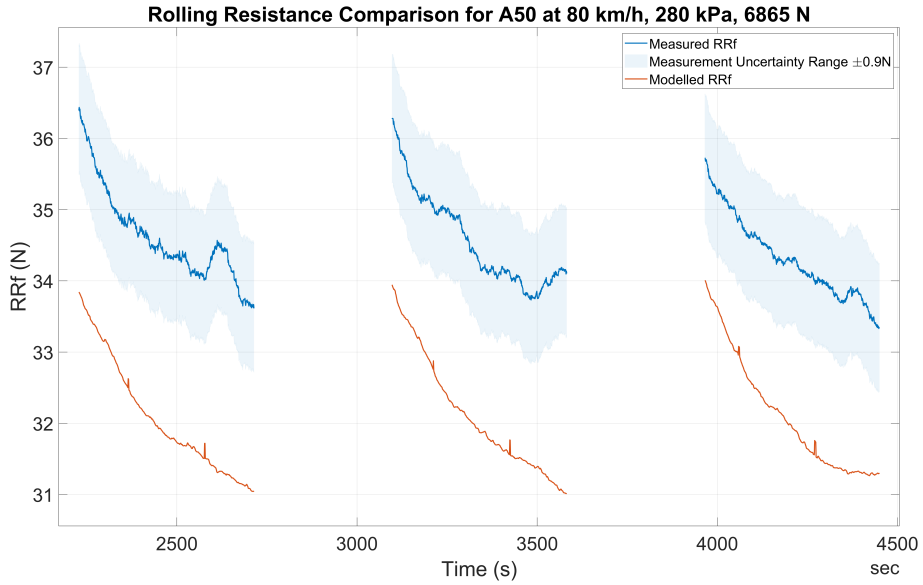

Figure A.9: Measured and modelled RRf at load higher than parametrization load

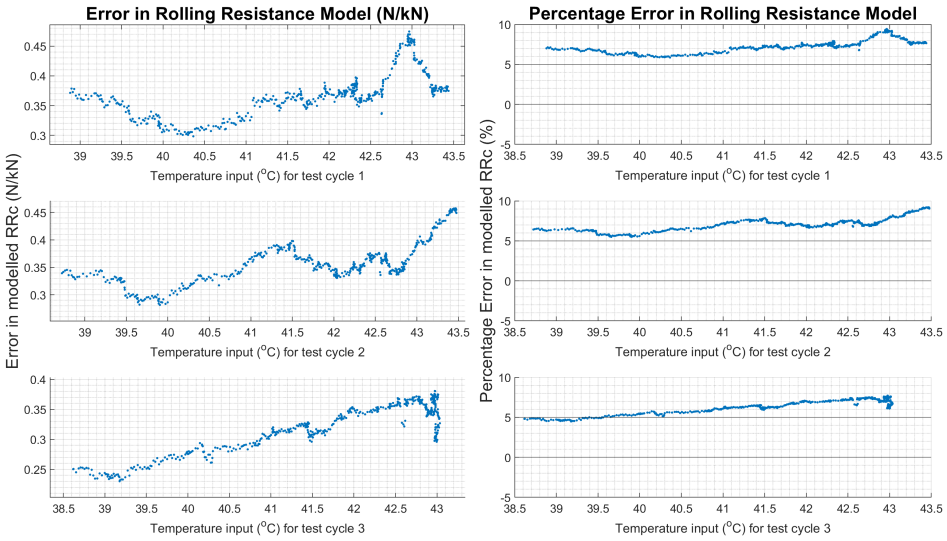

Figure A.10: (L) Error in Modelled RRf (N/kN); (R) Percentage Error in modelled RRf

B

Appendix B: Automation

B.1 Synchronizing torque and temperature signals

Since the temperature and drum torque data is logged by different sensors, each having their own logging frequency and format, the data needed to be synchronized, which is shown in the plot below.

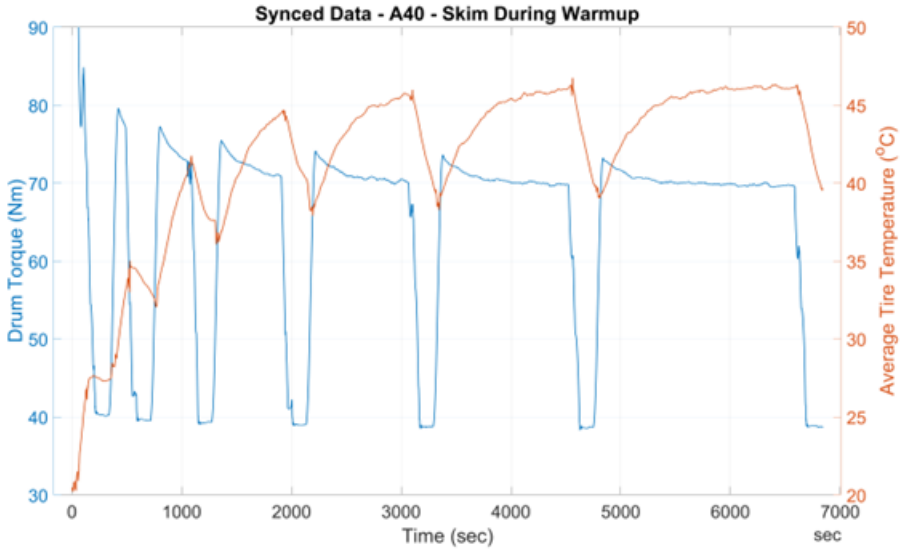

Figure B.1: Synchronized Data Results for A40 Tire for Transient Skim Test

The data synchronization and cleanup is done by importing the data into MATLAB and using the synchronize() function along with the timestamps recorded by the sensor. The data must be synchronized to match the trends in temperature and drum torque recorded.

B.2 Automating Finding Measurement Test and Skim Test Range

The ranges for the measurement and skim tests are automated using a signal from the ISO test measurement logs called 'LoadArrived'. This signal is binary, with 1 (true) indicating that a load is applied and 0 (false) indicating that the load is taken off. The magnitude of the load can change when the signal transitions from 0 to 1, which marks the start and end times of load applications.

The automation process identifies these transitions and adjusts the ranges by a few seconds around the starts and stops of the loading sections to meet specific data requirements. This ensures accurate and consistent range selection for measurement and skim tests.

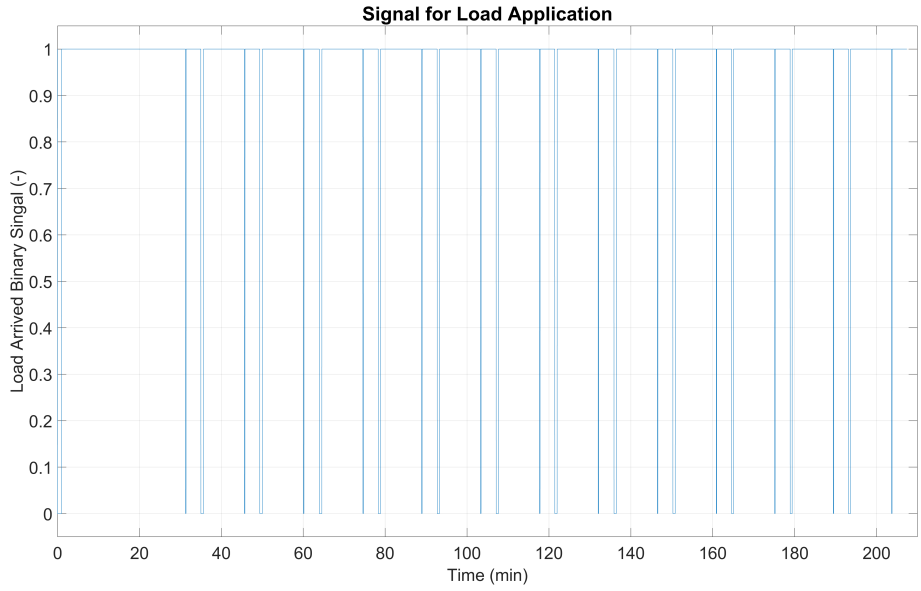

Figure B.2: Signal for Load Application

The range output by the function is shown in the figure below:

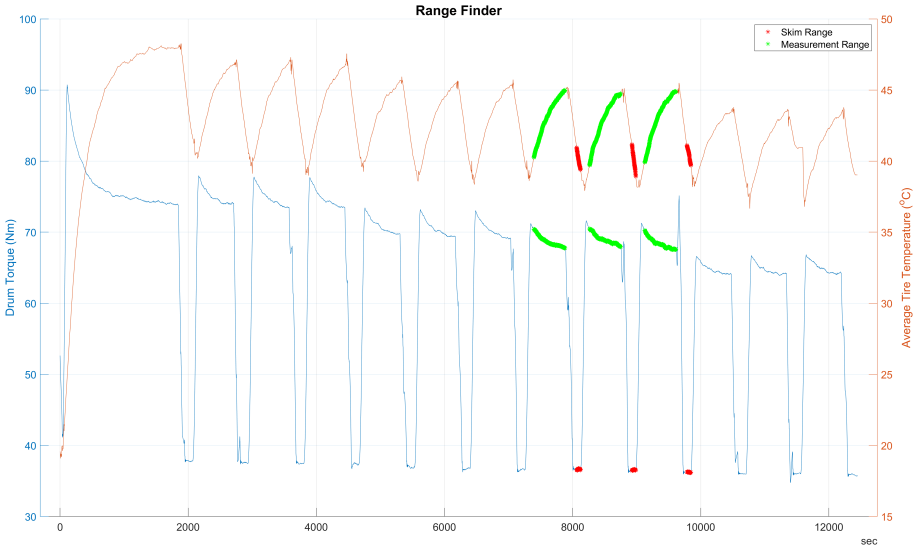

Figure B.3: Working of Range Finder

DEPARTMENT OF VEHICLE ENGINEERING AND AUTONOMOUS SYSTEMS
CHALMERS UNIVERSITY OF TECHNOLOGY
Gothenburg, Sweden
www.chalmers.se

CHALMERS
UNIVERSITY OF TECHNOLOGY